

## Development and Calibration of AASHTO LRFD Specifications for Structural Supports for Highway Signs, Luminaires, and Traffic Signals

### DETAILS

---

110 pages | 8.5 x 11 | PAPERBACK

ISBN 978-0-309-30818-2 | DOI 10.17226/22240

### AUTHORS

---

Jay A. Puckett, Michael G. Garlich, Andrzej (Andy) Nowak, and Michael Barker;  
National Cooperative Highway Research Program; Transportation Research Board;  
National Academies of Sciences, Engineering, and Medicine

BUY THIS BOOK

FIND RELATED TITLES

### Visit the National Academies Press at [NAP.edu](http://NAP.edu) and login or register to get:

---

- Access to free PDF downloads of thousands of scientific reports
- 10% off the price of print titles
- Email or social media notifications of new titles related to your interests
- Special offers and discounts



Distribution, posting, or copying of this PDF is strictly prohibited without written permission of the National Academies Press. (Request Permission) Unless otherwise indicated, all materials in this PDF are copyrighted by the National Academy of Sciences.

NATIONAL COOPERATIVE HIGHWAY RESEARCH PROGRAM

---

---

**NCHRP REPORT 796**

---

---

**Development and Calibration  
of AASHTO LRFD Specifications  
for Structural Supports  
for Highway Signs, Luminaires,  
and Traffic Signals**

**Jay A. Puckett**

BRIDGETECH, INC.

Laramie, WY

**Michael G. Garlich**

COLLINS ENGINEERS, INC.

Chicago, IL

**Andrzej (Andy) Nowak**

Auburn, AL

**Michael Barker**

Laramie, WY

*Subscriber Categories*

Bridges and Other Structures

---

Research sponsored by the American Association of State Highway and Transportation Officials  
in cooperation with the Federal Highway Administration

---

**TRANSPORTATION RESEARCH BOARD**

WASHINGTON, D.C.

2014

[www.TRB.org](http://www.TRB.org)

## **NATIONAL COOPERATIVE HIGHWAY RESEARCH PROGRAM**

Systematic, well-designed research provides the most effective approach to the solution of many problems facing highway administrators and engineers. Often, highway problems are of local interest and can best be studied by highway departments individually or in cooperation with their state universities and others. However, the accelerating growth of highway transportation develops increasingly complex problems of wide interest to highway authorities. These problems are best studied through a coordinated program of cooperative research.

In recognition of these needs, the highway administrators of the American Association of State Highway and Transportation Officials initiated in 1962 an objective national highway research program employing modern scientific techniques. This program is supported on a continuing basis by funds from participating member states of the Association and it receives the full cooperation and support of the Federal Highway Administration, United States Department of Transportation.

The Transportation Research Board of the National Academies was requested by the Association to administer the research program because of the Board's recognized objectivity and understanding of modern research practices. The Board is uniquely suited for this purpose as it maintains an extensive committee structure from which authorities on any highway transportation subject may be drawn; it possesses avenues of communications and cooperation with federal, state and local governmental agencies, universities, and industry; its relationship to the National Research Council is an insurance of objectivity; it maintains a full-time research correlation staff of specialists in highway transportation matters to bring the findings of research directly to those who are in a position to use them.

The program is developed on the basis of research needs identified by chief administrators of the highway and transportation departments and by committees of AASHTO. Each year, specific areas of research needs to be included in the program are proposed to the National Research Council and the Board by the American Association of State Highway and Transportation Officials. Research projects to fulfill these needs are defined by the Board, and qualified research agencies are selected from those that have submitted proposals. Administration and surveillance of research contracts are the responsibilities of the National Research Council and the Transportation Research Board.

The needs for highway research are many, and the National Cooperative Highway Research Program can make significant contributions to the solution of highway transportation problems of mutual concern to many responsible groups. The program, however, is intended to complement rather than to substitute for or duplicate other highway research programs.

## **NCHRP REPORT 796**

Project 10-80  
ISSN 0077-5614  
ISBN 978-0-309-30818-2  
Library of Congress Control Number 2014954483

© 2014 National Academy of Sciences. All rights reserved.

### **COPYRIGHT INFORMATION**

Authors herein are responsible for the authenticity of their materials and for obtaining written permissions from publishers or persons who own the copyright to any previously published or copyrighted material used herein.

Cooperative Research Programs (CRP) grants permission to reproduce material in this publication for classroom and not-for-profit purposes. Permission is given with the understanding that none of the material will be used to imply TRB, AASHTO, FAA, FHWA, FMCSA, FTA, or Transit Development Corporation endorsement of a particular product, method, or practice. It is expected that those reproducing the material in this document for educational and not-for-profit uses will give appropriate acknowledgment of the source of any reprinted or reproduced material. For other uses of the material, request permission from CRP.

### **NOTICE**

The project that is the subject of this report was a part of the National Cooperative Highway Research Program, conducted by the Transportation Research Board with the approval of the Governing Board of the National Research Council.

The members of the technical panel selected to monitor this project and to review this report were chosen for their special competencies and with regard for appropriate balance. The report was reviewed by the technical panel and accepted for publication according to procedures established and overseen by the Transportation Research Board and approved by the Governing Board of the National Research Council.

The opinions and conclusions expressed or implied in this report are those of the researchers who performed the research and are not necessarily those of the Transportation Research Board, the National Research Council, or the program sponsors.

The Transportation Research Board of the National Academies, the National Research Council, and the sponsors of the National Cooperative Highway Research Program do not endorse products or manufacturers. Trade or manufacturers' names appear herein solely because they are considered essential to the object of the report.

*Published reports of the*

### **NATIONAL COOPERATIVE HIGHWAY RESEARCH PROGRAM**

*are available from:*

Transportation Research Board  
Business Office  
500 Fifth Street, NW  
Washington, DC 20001

*and can be ordered through the Internet at:*

<http://www.national-academies.org/trb/bookstore>

Printed in the United States of America

# THE NATIONAL ACADEMIES

## *Advisers to the Nation on Science, Engineering, and Medicine*

The **National Academy of Sciences** is a private, nonprofit, self-perpetuating society of distinguished scholars engaged in scientific and engineering research, dedicated to the furtherance of science and technology and to their use for the general welfare. Upon the authority of the charter granted to it by the Congress in 1863, the Academy has a mandate that requires it to advise the federal government on scientific and technical matters. Dr. Ralph J. Cicerone is president of the National Academy of Sciences.

The **National Academy of Engineering** was established in 1964, under the charter of the National Academy of Sciences, as a parallel organization of outstanding engineers. It is autonomous in its administration and in the selection of its members, sharing with the National Academy of Sciences the responsibility for advising the federal government. The National Academy of Engineering also sponsors engineering programs aimed at meeting national needs, encourages education and research, and recognizes the superior achievements of engineers. Dr. C. D. Mote, Jr., is president of the National Academy of Engineering.

The **Institute of Medicine** was established in 1970 by the National Academy of Sciences to secure the services of eminent members of appropriate professions in the examination of policy matters pertaining to the health of the public. The Institute acts under the responsibility given to the National Academy of Sciences by its congressional charter to be an adviser to the federal government and, upon its own initiative, to identify issues of medical care, research, and education. Dr. Victor J. Dzau is president of the Institute of Medicine.

The **National Research Council** was organized by the National Academy of Sciences in 1916 to associate the broad community of science and technology with the Academy's purposes of furthering knowledge and advising the federal government. Functioning in accordance with general policies determined by the Academy, the Council has become the principal operating agency of both the National Academy of Sciences and the National Academy of Engineering in providing services to the government, the public, and the scientific and engineering communities. The Council is administered jointly by both Academies and the Institute of Medicine. Dr. Ralph J. Cicerone and Dr. C. D. Mote, Jr., are chair and vice chair, respectively, of the National Research Council.

The **Transportation Research Board** is one of six major divisions of the National Research Council. The mission of the Transportation Research Board is to provide leadership in transportation innovation and progress through research and information exchange, conducted within a setting that is objective, interdisciplinary, and multimodal. The Board's varied activities annually engage about 7,000 engineers, scientists, and other transportation researchers and practitioners from the public and private sectors and academia, all of whom contribute their expertise in the public interest. The program is supported by state transportation departments, federal agencies including the component administrations of the U.S. Department of Transportation, and other organizations and individuals interested in the development of transportation. **[www.TRB.org](http://www.TRB.org)**

**[www.national-academies.org](http://www.national-academies.org)**

# COOPERATIVE RESEARCH PROGRAMS

## **CRP STAFF FOR NCHRP REPORT 796**

**Christopher W. Jenks**, *Director, Cooperative Research Programs*  
**Christopher Hedges**, *Manager, National Cooperative Highway Research Program*  
**Waseem Dekelbab**, *Senior Program Officer*  
**Danna Powell**, *Senior Program Assistant*  
**Sheila A. Moore**, *Program Associate*  
**Eileen P. Delaney**, *Director of Publications*  
**Doug English**, *Editor*

## **NCHRP PROJECT 10-80 PANEL**

### **Area: Materials and Construction—Specifications, Procedures, and Practices**

**Loren R. Risch**, *Kansas DOT, Topeka, KS (Chair)*  
**Joseph M. Bowman**, *Hapco (retired), Abingdon, VA*  
**Timothy Bradberry**, *Texas DOT, Austin, TX*  
**Xiaohua Hannah Cheng**, *New Jersey DOT, Trenton, NJ*  
**Cabrina Marie Dieters**, *Tennessee DOT, Nashville, TN*  
**Carl J. Macchietto**, *Valmont Industries, Inc., Valley, NE*  
**Julius F. J. Volgyi, Jr.**, *(retired) Richmond, VA*  
**Justin M. Ocel**, *FHWA Liaison*  
**Stephen F. Maher**, *TRB Liaison*

## **AUTHOR ACKNOWLEDGMENTS**

NCHRP Project 10-80 is a diverse structural engineering project with topic areas ranging from aero-elastic vibrations, to steel and aluminum fatigue, to wide-ranging material types of steel, aluminum, concrete, wood, and fiber-reinforced plastics. The team wishes to thank the 36 DOT agencies who took time to complete its survey. Their input was very helpful.

The collaboration of the research team is especially noted, as without their specific expertise and years of practical knowledge, this project would not have been possible.

# FOREWORD

By **Waseem Dekelbab**

Staff Officer

Transportation Research Board

This report presents proposed AASHTO LRFD specifications for structural supports for highway signs, luminaires, and traffic signals. The proposed specifications are arranged in three divisions: (1) design according to LRFD methodology; (2) construction, including material specifications, fabrication, and installation; and (3) asset management, including inventory, inspection, and maintenance. In addition, the report provides details regarding the reliability calibration process and results. The material in this report will be of immediate interest to highway design engineers.

---

In June 2000, AASHTO and the Federal Highway Administration agreed on an implementation plan for the design of highway structures utilizing the load and resistance factor design (LRFD) methodology. As part of that agreement, all new culverts, retaining walls, and other standard structures on which states initiate preliminary engineering after October 1, 2010, shall be designed according to the LRFD specifications. The current edition of the *AASHTO Standard Specifications for Structural Supports for Highway Signs, Luminaires, and Traffic Signals* is generally based on the working stress design method. Also, the design, construction, and inspection languages are intertwined in the specifications and commentary, resulting in a document that is cumbersome and difficult to follow. The probability-based specification (i.e., LRFD) will result in structures that are based on a more uniform set of design criteria. The specifications will promote quality construction and fabrication practices and will address the current shortcomings of inspection and maintenance of these ancillary structures. The combination of these efforts will allow agencies to better design, manage, and maintain these transportation assets to improve the safety and reliability of structural supports nationwide. Agencies will be in a better position to meet the LRFD implementation plan, and the provisions will facilitate the design, construction, inspection, and maintenance of structural supports for highway signs, luminaires, and traffic signals.

Research was performed under NCHRP Project 10-80 by BridgeTech, Inc. The objective of this research was to develop proposed AASHTO LRFD specifications for structural supports for highway signs, luminaires, and traffic signals. Additionally, 16 comprehensive design examples were developed to illustrate the application of the new specifications.

The report includes the Research Report, which documents the entire research effort, and the Calibration Report (i.e., Appendix A). Appendix B: AASHTO LRFD Specifications will be published by AASHTO. Other appendices are not published but are available on the TRB website. These appendices are titled as follows:

- Appendix C: Design Examples,
- Appendix D: Survey Results, and
- Appendix E: Fatigue Resistance Comparisons.

# NOMENCLATURE AND DEFINITIONS

## **Nomenclature**

AA—Aluminum Association.

ACI—American Concrete Institute.

AISC—American Institute for Steel Construction.

Arm—A cantilevered member, either horizontal or sloped, which typically attaches to a pole.

ASD—Allowable stress design.

AWS—American Welding Society.

Bridge Support—Also known as span-type support; a horizontal or sloped member or truss supported by at least two vertical supports.

Cantilever—A member, either horizontal or vertical, supported at one end only.

CMS—Changeable message sign (also known as a dynamic message sign or a variable message sign).

Collapse—A major change in the geometry of the structure rendering it unfit for use.

Component—Either a discrete element of the structure or a combination of elements requiring individual design consideration.

Design Life—Period of time on which the statistical derivation of transient loads is based: 25 years for the specifications in this report.

Designer—The person responsible for design of the structural support.

Design—Proportioning and detailing the components and connections of a structure.

Ductility—Property of a component or connection that allows inelastic response.

Engineer—Person responsible for the design of the structure and/or review of design-related field submittals such as erection plans.

Evaluation—Determination of load-carrying capacity or remaining life of an existing structure.

Extreme Event Limit States—Limit states relating to events such as wind, earthquakes, and vehicle collisions, with return periods in excess of the design life of the structure.

Factored Load—Nominal loads multiplied by the appropriate load factors specified for the load combination under consideration.

Factored Resistance—Nominal resistance multiplied by a resistance factor.

Force Effect—A deformation, stress, or stress resultant (i.e., axial force, shear force, torsional, or flexural moment) caused by applied loads or imposed deformations.

FRC—Fiber-reinforced composite.

FRP—Fiber-reinforced polymer.

High-Level Lighting—Also known as high-mast lighting; lighting provided at heights greater than 55 ft., typically using four to 12 luminaires.

High-Mast High-Level Tower—Another description for a pole-type high-level luminaire support.

High-Mast Luminaire Tower—Truss-type or pole-type tower that provides lighting at heights greater than 55 ft., typically using four to 12 luminaires.

Limit State—A condition beyond which the structure or component ceases to satisfy the provisions for which it was designed.

Load and Resistance Factor Design (LRFD)—A reliability-based design methodology in which force effects caused by factored loads are not permitted to exceed the factored resistance of the components.

Load Effect—Same as force effect.

Load Factor—A statistically based multiplier applied to force effects accounting primarily for the variability of loads, the lack of accuracy in analysis, and the probability of simultaneous occurrence of different loads, but also related to the statistics of the resistance through the calibration process.

LRFD—Load and resistance factor design.

LRFD Bridge Construction Specifications—LRFD construction specifications for highway bridges.

LRFD Bridge Design Specifications (BDS)—LRFD specifications for design of highway bridges.

LRFD-LTS—New LRFD specifications for luminaires, traffic signals, and signs.

LTS—Luminaires, traffic signals, and signs.

Luminaire—A complete lighting unit consisting of a lamp or lamps together with the parts designed to provide the light, position and protect the lamps, and connect the lamps to an electric power supply.

Mast Arm—A member used to hold a sign, signal head, or luminaire in an approximately horizontal position.

Mean Recurrence Interval (MRI)—The expected time period for the return of a wind speed that exceeds the basic wind speed. The annual probability of exceeding the basic wind in any 1-year period is the reciprocal of this value.

Member—A component that is positioned between two physical joints of a structure (or LTS).

Model—An idealization of a structure for the purpose of analysis.

Monotube—A support that is composed of a single tube.

Multiple-Load-Path Structure—A structure capable of supporting the specified loads following loss of a main load-carrying component or connection.

NHI—National Highway Institute.

Nominal Resistance—The resistance of a component or connection to force effects, as indicated by the dimensions specified in the contract documents and by permissible stresses, deformations, or specified strength of materials.

Overhead Sign—A sign mounted over a roadway or near it, and elevated with respect to a travel way.

Owner—The person or agency having jurisdiction for the design, construction, and maintenance of the structural support.

Pole Top—A descriptive term indicating that an attachment is mounted at the top of a structural support, usually pertaining to one luminaire or traffic signal mounted at the top of a pole.

Pole—A vertical support that is often long, relatively slender, and generally rounded or multisided.

Rehabilitation—A process in which the resistance of the structure is either restored or increased.

Resistance Factor—A statistically based multiplier applied to nominal resistance accounting primarily for variability of material properties, structural dimensions and workmanship, and uncertainty in the prediction of resistance, but also related to the statistics of the loads through the calibration process.

Roadside Sign—A sign mounted beside the roadway on a single support or multiple supports.

SCOBs—AASHTO's Subcommittee on Bridges and Structures

SEI—Structural Engineering Institute (within ASCE).

Service Life—The period of time that the structure is expected to be in operation.

Service Limit States—Limit states relating to stress, deformation, and concrete cracking under regular operating conditions.

Sign—A device conveying a specific message by means of words or symbols, erected for the purpose of regulating, warning, or guiding traffic.

Span Wire—A steel cable or strand extended between two poles, commonly used as a horizontal support for signs and traffic signals.

STD—Standard specifications.

Strength Limit States—Limit states relating to strength and stability during the design life.  
 Structural Support—A system of members used to resist load effects associated with self-weight, attached signs, luminaires, traffic signals, and any other applicable loads.  
 Structure—The same as a structural support.  
 T-12—SCOBS technical committee for structural supports for signs, luminaires, and traffic signals.  
 Traffic Signal—An electrically operated traffic control device by which traffic is regulated, warned, or directed to take specific actions.  
 Truss—A structural system composed of a framework that is often arranged in triangles.  
 Variable Message Sign—A sign that illustrates a variable message (see CMS).  
 XML—Extensible markup language.

## Definitions

$R_n$  = nominal resistance  
 $V_{300}$  = 300-year design wind speed (ASCE/SEI 7-10)  
 $V_{700}$  = 700-year design wind speed (ASCE/SEI 7-10)  
 $V_{1700}$  = 1,700-year design wind speed (ASCE/SEI 7-10)  
 $V_{50}$  = 50-year design wind speed (ASCE/SEI 7-05)  
 $Q$  = random variable representing load  
 $R$  = random variable representing strength  
 $Cov_R$  = coefficient of variation for strength variable  $R$   
 $\lambda_R$  = bias factor for strength variable  $R$   
 $Cov_Q$  = coefficient of variation for load variable  $Q$   
 $\lambda_Q$  = bias factor for strength variable  $Q$   
 $Cov_{K_z}$  = coefficient of variation for design pressure variable  $K_z$   
 $\lambda_{K_z}$  = bias factor for press variable  $K_z$   
 $Cov_{C_d}$  = coefficient of variation for design pressure variable  $C_d$   
 $\lambda_{C_d}$  = bias factor for pressure variable  $C_d$   
 $Cov_G$  = coefficient of variation for design pressure variable  $G$   
 $\lambda_G$  = bias factor for pressure variable  $G$   
 $\phi$  = phi factor  
 $\gamma_{D1}$  = dead load design load factor (used in conjunction with dead + wind case)  
 $\gamma_{D2}$  = deal load design load factor (dead-load-only case)  
 $\gamma_W$  = wind load design load factor  
 OSF = (wind) overstress factor  
 Shape Factor =  $SF = \frac{Z}{S}$  (plastic moment/yield moment)  
 $I_{low}$  = importance factor (low)  
 $I_{med}$  = importance factor (med)  
 $I_{high}$  = importance factor (high)

# CONTENTS

1	<b>Summary</b>
3	<b>Chapter 1 Introduction and Research Approach</b>
3	Introduction
3	Organization
3	Contents of the LRFD-LTS Specifications
5	<b>Chapter 2 Findings</b>
5	Agency Survey
5	Literature
5	U.S. and International Specifications
5	Research Papers and Reports
5	Textbooks
5	Resistance Sections
5	Fabrication, Materials, and Detailing (Section 14)
8	Construction (Section 15)
8	Inspection and Reporting (Section 16)
8	Asset Management (Section 17)
12	<b>Chapter 3 Interpretation, Appraisal, and Application</b>
12	Load Models and Calibration
12	LRFD Limit-State Format
12	Dead Load Parameters
12	Wind Load Model
15	Wind Load Information from ASCE/SEI 7-10 and Available Literature
15	Statistical Parameters for Wind Load Variables
15	Statistical Parameters of Resistance
17	LRFD Reliability Analysis
17	Flexural Resistance
17	Load
19	Reliability Indices
19	Implementation
20	ASD Reliability Analysis
21	Resistance
22	Implementation
23	Calibration and Comparison
23	Implementation
23	Setting Target Reliability Indices
25	Implementation into Specifications

---

Appendices C through E are posted on the TRB website and can be found by searching for *NCHRP Report 796* at [www.TRB.org](http://www.TRB.org). Appendix B: AASHTO LRFD Specifications will be published by AASHTO.

25	Computed Reliability Indices
26	Sensitivities
26	Scope of Appendix A
26	Calibration Summary
28	Examples
<b>32</b>	<b>Chapter 4 Conclusions and Suggested Research</b>
32	Conclusions
32	Suggested Research
32	Follow-up Tasks
<b>34</b>	<b>Bibliography</b>
<b>A-1</b>	<b>Appendices</b>
A-1	Appendix A: Calibration Report

---

Note: Photographs, figures, and tables in this report may have been converted from color to grayscale for printing. The electronic version of the report (posted on the web at [www.trb.org](http://www.trb.org)) retains the color versions.

## S U M M A R Y

# Development and Calibration of AASHTO LRFD Specifications for Structural Supports for Highway Signs, Luminaires, and Traffic Signals

The objective of this research was to develop new specifications for structural supports for highway signs, luminaires, and traffic signals.

The AASHTO load and resistance factor design—luminaires, traffic signals, and signs (LRFD-LTS) specifications were written to incorporate an LRFD approach to design. Survey results indicated that present designs were performing well, with the exception of fatigue where winds are persistently active.

The LRFD-LTS specifications were calibrated using the AASHTO STD-LTS (standard LTS specifications) allowable stress design method as a baseline. The variabilities of the loads and resistances were considered in a rigorous manner. The wind loads have higher variabilities than the dead loads. Therefore, structures with a high wind-to-total-load ratio will require higher associated resistances compared to allowable stress design. This increase is on the order of 10% for high-mast structures. For structures with a wind-to-total-load ratio of approximately 0.5 (e.g., cantilever structures), the required resistance does not change significantly.

The reliability index for the LRFD-LTS specifications is more uniform over the range of load ratios of practical interest than the current allowable stress design–based specifications. This uniformity was one of the primary goals of this project.

Characteristics and outcomes of the LRFD-LTS specifications are:

1. The organization has been reformatted so that all sections are consistent,
2. Variable definitions and nomenclature are located in a consistent manner,
3. Improved text in the STD-LTS for editorial changes,
4. Updated references, including ASCE/SEI (Structural Engineering Institute) 07-10 wind hazard maps,
5. Latest fatigue research,
6. Most recent U.S. specifications for steel and aluminum,
7. Rigorous calibration,
8. Improved uniformity of reliability over typical wind load to total load ratios,
9. New sections on fabrication, materials, and detailing, construction, inspection, and asset management,
10. New appendix on an alternate method for fatigue design/evaluation,
11. Core element system is defined in a new appendix, and
12. Smart flags and environmental definitions are defined to support the core elements.

There are 16 example designs provided (in Appendix C, available on the TRB website by searching for *NCHRP Report 796* at [www.TRB.org](http://www.TRB.org)) to demonstrate the LRFD-LTS specifications. These examples address the typical systems in use today, and are included for all materials.

Finally, calibration is described in Appendix A. The interested reader and future specification committees should find this document to be of benefit.

---

## CHAPTER 1

# Introduction and Research Approach

### Introduction

The objective of this research was to develop new specifications for structural supports for luminaires, traffic signals, and signs (LTS). The resulting specifications are arranged in three divisions:

- Design, based on the load and resistance factor design (LRFD) methodology,
- Construction (e.g., material specifications, fabrication, installation), and
- Asset management (e.g., inventory, inspection, maintenance).

The research goal was to provide AASHTO the basis for forming a new edition of the AASHTO *Standard Specifications for Structural Supports for Highway Signs, Luminaires, and Traffic Signals* along with the necessary report that outlines reliability calibration and example problems. Herein the term *LRFD-LTS specifications* or *LRFD specifications* refers to the LRFD draft specifications developed as part of this project. Other AASHTO specifications titles are used with appropriate qualifiers (e.g., *STD-LTS* or *standard LTS specifications*).

### Organization

This project was divided into five phases that progressed sequentially. This final report is organized to document the deliverables listed in Table 1. The draft specifications are written in the AASHTO LRFD format and are ready for implementation after review, modification, and possible adoption by the Subcommittee for Bridges and Structures (SCOBs), and finally, approval by AASHTO. The Calibration Report in Appendix A documents many of the studies that were necessary to determine the load and resistance factors. It also addresses the simplification associated with ice loads.

The example problems are contained in Appendix C (available on the TRB website by searching for *NCHRP Report 796* at [www.TRB.org](http://www.TRB.org)); these will facilitate implementation and technology transfer.

This report will bring forward the highlights of the work for the purpose of a general overview. The reader is encouraged to review the LRFD specifications (a separate AASHTO publication), the example problems (Appendix C), and the Calibration Report (Appendix A).

### Contents of the LRFD-LTS Specifications

The LRFD-LTS specifications are organized in a similar manner to the STD-LTS for Division I—Design. There was serious consideration given to splitting Section 11: Fatigue Design, which contains both loads and resistance information, and placing this content in Section 3: Loads, Section 5: Steel Design, and Section 6: Aluminum Design. On discussion with the project team and panel, the decision was made to keep the fatigue information in the present section without splitting.

Division II: Fabrication and Construction contains two new sections for the LRFD-LTS specifications. Here, information associated with these topics available in the STD-LTS was extracted from the design sections and organized in Division II. Additional information was added based on research, observed problems in the field, and best practices.

Division III: Asset Management contains new information developed in this project as well as best practices regarding Section 16: Inspection and Reporting and Section 17: Asset Management.

All divisions are written for maintainability and expansion as research and practice guide the AASHTO LTS community and AASHTO T-12.

**Table 1. Project overview.**

<b>Phase</b>	<b>Description</b>	<b>Detailed Description</b>	<b>Deliverable</b>
<b>I</b>	Develop detailed outline for stand-alone specifications	The standard specifications will be converted to the LRFD approach and reorganized to provide design engineers with state-of-the-art specifications separating the design, construction, and asset management into three distinct divisions.	Typical initial activities were conducted, including: <ul style="list-style-type: none"> <li>a. Review of literature,</li> <li>b. Review of international specifications,</li> <li>c. Survey of AASHTO agencies,</li> <li>d. Development of detailed outline, and</li> <li>e. Recommend approach for developing the LRFD specifications.</li> </ul>
<b>II</b>	Develop LRFD design specifications division	Based on the approved work plan, develop the proposed design specifications. Prepare detailed design examples that fully illustrate the application of the new design methods.	The LRFD specifications (Division I) were written, calibrated, and documented with commentary and example problems. Three primary documents support this report: <ul style="list-style-type: none"> <li>a. Calibration Report (Appendix A),</li> <li>b. LRFD Specifications (AASHTO document), and</li> <li>c. Example Problems (Appendix C).</li> </ul>
<b>III</b>	Develop construction specifications division	Develop a construction division by extracting the current construction provisions from existing AASHTO specifications and incorporating updated material specifications, fabrication methods, and installation techniques supplemented by state-of-the-art practices.	The LRFD specifications (Division II) were written and organized into two new sections: <ul style="list-style-type: none"> <li>a. Fabrication, Materials, and Detailing; and</li> <li>b. Construction.</li> </ul> <p>These sections are contained in the LRFD specifications.</p>
<b>IV</b>	Develop asset management division specifications	Develop language outlining best practices for inventory, inspection, and maintenance. Additionally, develop metadata for inventory and commonly recognized element levels.	The LRFD specifications (Division III) were written and organized into two new sections: <ul style="list-style-type: none"> <li>a. Inspection, and</li> <li>b. Asset Management.</li> </ul>
<b>V</b>	Deliverables	Prepare and submit project deliverables, including a final report that documents the entire research effort and other items identified in the research plan.	This report and its appendices provide the final deliverables. There are four major documents: <ul style="list-style-type: none"> <li>a. The Final Report (this report),</li> <li>b. Calibration Report (appendix),</li> <li>c. Draft LRFD Specifications (AASHTO), and</li> <li>d. Example Problems (appendix).</li> </ul>

The contents of the LRFD-LTS specifications are as follows.

#### **Division I: Design**

- Section 1: Introduction
- Section 2: General Features of Design
- Section 3: Loads
- Section 4: Analysis and Design—General Considerations
- Section 5: Steel Design
- Section 6: Aluminum Design
- Section 7: Prestressed Concrete Design
- Section 8: Fiber-Reinforced Composite Design
- Section 9: Wood Design
- Section 10: Serviceability Requirements
- Section 11: Fatigue Design

- Section 12: Breakaway Supports
- Section 13: Foundation Design

#### **Division II: Fabrication and Construction**

- Section 14: Fabrication, Materials, and Detailing
- Section 15: Construction

#### **Division III: Asset Management**

- Section 16: Inspection and Reporting
- Section 17: Asset Management

#### **Appendices**

- Appendix A: Analysis of Span-Wire Structures
- Appendix B: Design Aids
- Appendix C: Alternative Fatigue Analysis/Evaluation
- Appendix D: Detailed Element Descriptions

## CHAPTER 2

# Findings

### Agency Survey

AASHTO member states were surveyed to obtain guidance regarding their practices related to design, fabrication, construction, and asset management. The questions and raw survey results are provided in Appendix D (available on the TRB website). The primary findings are provided in Table 2.

### Literature

#### U.S. and International Specifications

Domestic and selected international specifications were reviewed for application. Each is briefly discussed in Table 3.

#### Research Papers and Reports

Numerous research reports and papers were reviewed for an understanding of past, current, and new specification development. This project was not designed to create new work in the area of load or resistance but rather to incorporate existing work and to calibrate the specifications for load and resistance factor design.

Readers are led to work by Roy et al. (2011), Stam et al. (2011), and Connor et al. (2012) on fatigue resistance and loading. Kaczinski et al. (1998) and Dexter and Ricker (2002) form the basis of many articles on fatigue loading and resistance. The works of Roy et al. and Stam et al. were compared, and this comparison is summarized in Appendix E (on the TRB website). These projects were ongoing at the time of the present project.

*NCHRP Report 350: Recommended Procedures for the Safety Performance Evaluation of Highway Features* (Ross et al., 1993) has long been used for safety performance evaluation, and the *Manual for Assessing Safety Hardware (MASH)* (AASHTO, 2009) has replaced that document.

The researchers sought information from numerous reports upon which the new ASCE/SEI (Structural Engineering Insti-

tute) 7-10 was based (e.g., Vickery and Waldhera, 2008, Vickery et al., 2009a, 2009b, 2010).

### Textbooks

Some textbooks on structural reliability were helpful (e.g., Nowak and Collins, 2000, and a general chapter on the topic in Barker and Puckett, 2013).

### Resistance Sections

The steel and aluminum resistance sections were rewritten incorporating the latest standards and methods. Section 5: Steel Design employs methods from the American Institute of Steel Construction (AISC, 2010), and Section 6: Aluminum Design employs methods from the *Aluminum Design Manual* (Aluminum Association, 2010). Section 7: Prestressed Concrete Design, Section 8: Fiber-Reinforced Composite Design, Section 9: Wood Design, and Section 13: Foundation Design remain largely unchanged in concept but were recast into LRFD format and calibrated. Section 10: Serviceability Requirements was recast for LRFD; however, load and resistance factors were set to unity, resulting in no conceptual modifications from STD-LTS-5 (or 6).

Section 11: Fatigue Design was substantially modified from STD-LTS-5. However, work by Roy et al. (2011), Stam et al. (2011), and Connor et al. (2012) on fatigue resistance was extensively used in both the STD-LTS-6 and the LRFD-LTS specifications. These modifications were closely coordinated between AASHTO SCOBS T-12, the researchers noted here, and the present research team.

### Fabrication, Materials, and Detailing (Section 14)

The fabrication section is new for the LRFD-LTS specifications and contains information that was moved from the STD-LTS resistance sections. The AASHTO LRFD *Bridge*

**Table 2. Summary of survey findings.**

No.	Finding Summary	Relevance to the LRFD-LTS Specifications
1	Thirty-six agencies responded to the survey.	Reasonable sample of interested agencies.
2	When failures occur, typically they are due to fatigue-related issues.	Data are available for assessing fatigue-related failure. Changes in fatigue design could be justified.
3	The number of failures relative to the number of structures in the inventory is small.	The overall performance of existing structures (STD-LTS designs) is good and likely acceptable. Calibrating to existing designs appears to be reasonable.
4	About 76% of the respondents have used vibration mitigation devices.	Specification changes are needed for determining the performance of and/or designing using dampeners. This is beyond the research scope and could be a future research project to develop unified test methods.
5	Approximately 31% have special details for fatigue resistance designs.	These details have been surveyed in other work. NCHRP Project 10-80 relied on work by Roy et al. (2011), Stam et al. (2011), and Connor et al. (2012) for Section 11: Fatigue Design.
6	About 25% have specifications or practices for base-plate design.	LRFD-LTS specifications incorporate the latest research for sizing base plates (Roy et al., 2011).
7	Little interest was indicated for fiber-reinforced composite poles.	Section 8: Fiber-Reinforced Composite Design was given a lower priority (time and effort).
8	Anchor bolt failures have been observed for strength, fatigue, and corrosion.	Anchor bolts were addressed with respect to strength, fatigue, and construction.
9	Approximately 71% use ACI 318 Appendix D for design of anchorages.	ACI 318-11 Appendix D is suggested within the LRFD-LTS specifications [American Concrete Institute (ACI), 2011].
10	A325 bolts are most commonly used.	A325 bolts were used in all examples.
11	Hooks and straight anchor bars are used in about one-third and two-thirds of cases, respectively.	Both hook and straight anchor bars are considered.
12	About 38% of the respondents have observed foundation failures.	No specification action was taken in this regard. Section 13: Foundation Design provides guidance. Most departments of transportation (DOTs) use standards for drilled shafts, etc.
13	Approximately 35% used AASHTO LRFD for design, and 52% used Brom's method.	AASHTO LRFD is commonly used; appropriate references or repeated provisions are appropriate. Brom's method was kept in the LRFD-LTS specifications.
14	Nearly 90% of respondents are satisfied with the approach of the STD-LTS, with the following notable exceptions:  20% indicated a need for change in Section 3: Loads [ASCE/SEI (Structural Engineering Institute) 7-10 update].  28% indicated a need for change in Section 11: Fatigue Design. (Several suggestions were made; the most important is incorporation of the latest research.)  There were not many comments about aluminum.	The LRFD-LTS specifications use the new ASCE/SEI 7-10 wind loads.  Section 11 was extensively modified to include the most recent fatigue research. This work was adopted in the LTS-6.  Section 6: Aluminum Design was updated to be consistent with the <i>Aluminum Design Manual</i> (Aluminum Association, 2010).

**Table 3. Specifications reviewed.**

<b>Specification</b>	<b>Comments</b>
<b>AASHTO STD-LTS-5 (5<sup>th</sup> edition)</b>	This was the allowable stress (standard) specification when the project started.
<b>AASHTO STD-LTS-6 (6<sup>th</sup> edition)</b>	This is the current STD-LTS (2013). These specifications incorporate recent work on fatigue resistance and fatigue loading for high-mast towers. Section 11 in STD-LTS-6 is conceptually identical to the LRFD-LTS specifications.
<b>AASHTO Bridge Construction Specifications (AASHTO LRFD, 2013)</b>	The bridge construction document was reviewed for application to LTS. It is cited in the LRFD-LTS specifications with application to fabrication and construction.
<b>AASHTO LRFD Bridge Design Specifications (BDS) (2009-2013)</b>	The LRFD-BDS were used where possible to avoid duplication and parallel maintenance in the future. There was some consideration of merging the LRFD-LTS specifications with the LRFD-BDS; however, the LRFD-LTS specifications are distinct, and users of LRFD-LTS specifications are often different from LRFD-BDS users.
<b>ACI 318-2011</b>	Appendix D from this document is cited for use for anchorages. Again, this information is not repeated and will likely be kept current by the ACI.
<b>Precast/Prestressed Concrete Institute (PCI), 2010</b>	Reference was reviewed for information on poles.
<b>Aluminum Association, 2010</b>	The LRFD-LTS specifications, Section 6, parallel the aluminum design specification. This incorporates the most recent design procedures into the LTS.
<b>ASCE, 2010</b>	The LRFD-LTS specifications directly employed the new wind hazard maps and the research on which they are based. This keeps the wind loading unified with the most used U.S. standards.
<b>AASHTO, 2009</b>	The <i>Manual for Assessing Safety Hardware (MASH)</i> was reviewed for roadside safety, breakaway components, etc. MASH is cited where appropriate as it is the standard that AASHTO and FHWA are using moving forward.
<b>National Design Specification (AWC, 2012)</b>	The National Design Specification was reviewed for the LRFD approach for wood design. The LRFD-LTS specifications parallel this specification.
<b>Canadian Standards Association (CSA), 2006</b>	The Canadian specifications were reviewed for wind load provision for the strength and fatigue limit states. The CSA uses a rigorous and theoretically based approach to luminaire poles. This is based on a generalized stiffness and mass approach to model vortex-induced vibration. This was not employed since NCHRP was engaged in research for a high-mast tower to establish the fatigue loading that accounts for transverse- and along-wind effects. The research was implemented into the LRFD-LTS specifications, Section 11: Fatigue Design.
<b>Eurocode 1: Actions on Structures – Part 1-4: General Actions – Wind Actions</b>	There was nothing that was compelling enough to change the researchers approach of being consistent with ASCE/SEI 7-10.
<b>Eurocode 3: Design of Steel Structures – Part 3-1: Towers, Masts, and Chimneys – Towers and Masts</b>	The Eurocode employs methods that are similar to CSA for mast and towers. This might be an alternate approach for AASHTO in order to address smaller luminaire poles.
<b>ASTM Standards</b>	ASTM standards are cited throughout the LRFD-LTS specifications.

*Construction Specifications* were employed where applicable, in addition to the American Welding Association guidelines for steel and aluminum. Various ASTM standards were reviewed for their applicability to the fabrication process.

Specific articles are:

- 14.1 Scope,
- 14.2 Working Drawings,
- 14.3 Steel Structures,
- 14.4 Aluminum Structures,
- 14.5 Prestressed Concrete Structures,
- 14.6 Composite (Fiber-Reinforced Polymer) Structures,
- 14.7 Wood Structures, and
- 14.8 References.

These articles address:

- Materials,
- Bolted connections,
- Welded connections,
- Castings, and
- Fabrication (tolerances).

Since this is the first edition for this section, it is expected that the community will continue to offer T-12 ideas for improvement based on best practices and new research.

## Construction (Section 15)

The construction section is new for the LRFD-LTS and contains information that was moved from the STD-LTS resistance sections. The AASHTO LRFD *Bridge Construction Specifications* were employed where applicable, in addition to the American Welding Association guidelines for steel and aluminum.

Specific articles are:

- 15.1 General
- 15.2 Erection
- 15.3 Anchor Bolts
- 15.4 Bolted Connections
- 15.5 Steel Structures
- 15.6 Aluminum Structures
- 15.7 Prestressed Concrete Structures
- 15.8 Composite (Fiber-Reinforced Polymer) Structures
- 15.9 Wood Structures
- 15.10 Foundations
- 15.11 References

In part, the following items are addressed:

- Primarily reference-applicable portions of the AASHTO LRFD *Bridge Construction Specifications*,

- Current state of practice and provisions,
- Proper fastener tightening and connection fit-up of end plates, and
- Information to achieve a structural grout pad, if desired.

## Inspection and Reporting (Section 16)

Section 16 was written more toward an advisory perspective because current regulation does not mandate inspections of ancillary structures. Currently, FHWA has a document on the inspection of ancillary structures with a more general treatment to ensure that a consistent and proper inspection is performed. Section 16 is also new to the LRFD-LTS specifications.

The articles are:

- 16.1 Scope
- 16.2 Types of Inspections
- 16.3 Inspection Frequency
- 16.4 Qualifications and Responsibilities of Inspection Personnel
- 16.5 Safety
- 16.6 Planning, Scheduling, and Equipment
- 16.7 Inspection Forms and Reports
- 16.8 Elements and Element System
- 16.9 Procedures
- 16.10 References

An important part of this report is the new article 16.8: Elements and Element Systems.

The element set presented within includes two element types, identified as national ancillary structure elements (NASE) and ancillary structure management elements (ASME). The combination of these two element types makes up the AASHTO element set. All elements, whether they are NASE or ASME, have the same general requirements:

- Standard number of condition states, and
- Standard number of comprised condition states, such as good, fair, poor, and severe general descriptions.

A detailed description of each element is located in Appendix D of the LRFD-LTS specifications. Table 4 illustrates one element description (steel anchor rods).

Element titles and brief descriptions for NASE, ASME, and protective coatings are provided in Table 5, Table 6, and Table 8, respectively. Table 7 provides smart flags (defects), and Table 9 describes environmental factors (states).

## Asset Management (Section 17)

Section 17 was written in an advisory manner because current regulations do not mandate management of ancillary structures. However, the trend is toward more formal

**Table 4. Element description.**

<b>Element #702</b> <b>Steel Anchor Rods</b> <b>Count</b> <b>National Ancillary Structure Elements</b>		<b>Description</b> Element defines all steel anchor rods extending from the foundation, and includes all washers and nuts. Inclusive of weathering steel.		
<b>Quantity Calculation</b> The quantity is the sum of the number of exposed steel anchor rods.				
<b>Condition State Definitions</b>				
<b>Defect</b>	<b>Condition State 1</b>	<b>Condition State 2</b>	<b>Condition State 3</b>	<b>Condition State 4</b>
Corrosion	None	Freckled rust	Section loss	The condition is beyond the limits established in condition state three (3), warrants a structural review to determine the strength or serviceability of the element or ancillary structure, or both.
Connections	Sound	Sound	Isolated failures	
Misalignment	None	Present, but less than 1:20	Greater than 1:20	
Cracking/Fatigue	None	None	Cracks exist	
<b>Feasible Actions</b>				
	<b>Condition State 1</b>	<b>Condition State 2</b>	<b>Condition State 3</b>	<b>Condition State 4</b>
	Do Nothing Protect	Do Nothing Protect	Do Nothing Protect Repair Rehab	Do Nothing Replace Rehab
<b>Elemental Commentary</b> None				

**Table 5. National ancillary structure elements.**

<b>Element No.</b>	<b>Title</b>	<b>Description</b>
<b>701</b>	Concrete Foundation	Element defines all reinforced concrete foundations. Grout pads are not included.
<b>702</b>	Steel Anchor Rods	Element defines all steel anchor rods extending from the foundation, and includes all washers and nuts. Inclusive of weathering steel.
<b>703</b>	Aluminum Anchor Rods	Element defines all aluminum anchor rods extending from the foundation, and includes all washers and nuts.
<b>704</b>	Steel Base Plate	Element defines all steel base plates connecting the columns to the anchor rods, and includes all gusset plates, their welds, and the weld from the column to the base plate. Inclusive of weathering steel.
<b>705</b>	Aluminum Base Plate	Element defines all aluminum base plates connecting the columns to the anchor rods, and includes all gusset plates, their welds, and the weld from the column to the base plate.
<b>706</b>	Steel End Support Column	Element defines all steel end support columns. Inclusive of weathering steel.
<b>707</b>	Aluminum End Support Column	Element defines all aluminum end support columns.
<b>708</b>	Concrete End Support Column	Element defines all concrete end support columns.
<b>709</b>	Timber End Support Column	Element defines all timber end support columns.
<b>710</b>	Steel End Support Frame	Element defines all steel end support frames, including the uprights, horizontals, and diagonals. Inclusive of weathering steel.

*(continued on next page)*

**Table 5. (Continued).**

<b>Element No.</b>	<b>Title</b>	<b>Description</b>
711	Aluminum End Support Frame	Element defines all aluminum end support frames, including the uprights, horizontals, and diagonals.
712	Steel High-Mast Light or Luminaire Support Column	Element defines all steel high-mast light or luminaire support columns. Inclusive of weathering steel.
713	Aluminum High-Mast Light or Luminaire Support Column	Element defines all aluminum high-mast light or luminaire support columns.
714	Concrete High-Mast Light or Luminaire Support Column	Element defines all concrete high-mast light or luminaire support columns.
715	Fiberglass High-Mast Light or Luminaire Support	Element defines all fiberglass high-mast light or luminaire supports.
716	Bolted, Welded, or Slip Joint Splice Connection for Steel End Support or High-Mast Luminaire (HML)	Element defines all steel base plates (and bolts), welds, or slip-fit connections for splices located in steel end supports (or frames) or high-mast light or luminaire supports. Inclusive of weathering steel.
717	Bolted, Welded, or Slip Joint Splice Connection for Aluminum End Support or HML	Element defines all aluminum base plates (and bolts), welds, or slip-fit connections for splices located in aluminum end supports (or frames) or high-mast light or luminaire supports.
718	End Support-to-Chord Connection	Element defines all plates, bolts, and welds connecting support columns to chords. Inclusive of weathering steel.
719	Steel Single Chord Span	Element defines all steel spans composed of single chords (mast arm). Inclusive of weathering steel.
720	Aluminum Single Chord Span	Element defines all aluminum spans composed of single chords (mast arm) or braced cantilever (trombone-type) luminaire or signal support arms.
721	Steel Truss Span	Element defines all steel spans composed of multiple chords with or without trussing. Inclusive of weathering steel.
722	Aluminum Truss Span	Element defines all aluminum spans composed of multiple chords with or without trussing.
723	Span-Wire Assembly	Element defines all span wires and connections to other span wires and to supports.
724	Steel Bridge Mount Assembly	Element defines all steel assemblies mounted to bridge fascias, including all connections. Inclusive of weathering steel.
725	Aluminum Bridge Mount Assembly	Element defines all aluminum assemblies mounted to bridge fascias, including all connections.
726	Bolted, Welded, or Slip Joint Splice Connection for Steel Span	Element defines all steel base plates (and bolts), welds, or slip-fit connections for splices located in steel spans or luminaire arms. Inclusive of weathering steel.
727	Bolted, Welded, or Slip Joint Splice Connection for Aluminum Span	Element defines all aluminum base plates (and bolts), welds, or slip-fit connections for splices located in aluminum spans or luminaire arms.

**Table 6. Ancillary structural management elements.**

<b>Element No.</b>	<b>Title</b>	<b>Description</b>
801	Sign Panel	This element defines all sign panels.
802	Sign Panel Face Material	Element defines the face material of all sign panels.
803	Catwalk	This element defines all catwalks.
804	Handrails	This element defines all catwalk handrails.
805	Luminaires/Signal Heads	This element defines all luminaires and/or signal heads.
806	Electrical/Mechanical System	This element defines the mechanical/electrical system.
807	Dampeners	This element defines all visible dampeners.
808	Miscellaneous Attachments	This element defines all equipment or devices mounted to the structure that are not covered under other elements.

**Table 7. Smart flags (defect flags).**

Element No.	Title
900	Steel Cracking/Fatigue
901	Aluminum Cracking/Fatigue
902	Anchor Rod Standoff
903	Impact Damage
904	Undersized Components/Elements
905	Grout Pads
906	Guardrail/Protection
907	Distortion
908	Non-Foundation Concrete Cracking
909	Non-Foundation Concrete Efflorescence
910	Settlement
911	Misalignment
912	Steel Section Loss
913	Steel Out-of-Place Bending
914	Erosion

management programs to all assets: bridges, pavements, tunnels, and now ancillary structures. Several departments of transportation (DOTs) have existing inventory systems to log their inspection data, and these are beginning to be used for asset management.

Section 17 articles are:

- 17.1 Scope
- 17.2 Notation
- 17.3 Management Organization
- 17.4 Components of an Ancillary Structure File
- 17.5 Replacement Considerations
- 17.6 Maintenance Program
- 17.7 References

A similar format to that of the AASHTO *Manual for Bridge Evaluation* (AASHTO, 2010) was used. Article 17.5 contains a host of considerations for replacement, such as:

- Structural condition,
- Functionality,
- Roadway improvements, and
- Aesthetics.

It also contains new information on estimated remaining fatigue life, assessment of dents, and unreinforced holes.

Section 17 should be a reasonable beginning to the subject of asset management and should provide a basis for expansion and enhancement as methods and best practices evolve.

**Table 8. Protective coatings.**

Element No.	Title	Description
950	Steel Protective Coating	The element is for steel elements that have a protective coating such as paint, galvanization, or another top coat steel corrosion inhibitor.
951	Concrete Protective Coating	This element is for concrete elements that have a protective coating applied to them. These coatings include silane/siloxane waterproofers, crack sealers such as high molecular weight methacrylate, or any top coat barrier that protects concrete from deterioration and reinforcing steel from corrosion.

**Table 9. Environmental factors (states).**

Environment	Description
1—Benign	Neither environmental factors nor operating practices are likely to significantly change the condition of the element over time, or their effects have been mitigated by the presence of highly effective protective systems.
2—Low	Environmental factors, operating practices, or both either do not adversely influence the condition of the element or their effects are substantially lessened by the application of effective protective systems.
3—Moderate	Any change in the condition of the element is likely to be quite normal as measured against those environmental factors, operating practices, or both that are considered typical by the agency.
4—Severe	Environmental factors, operating practices, or both contribute to the rapid decline in the condition of the element. Protective systems are not in place or are ineffective.

## CHAPTER 3

## Interpretation, Appraisal, and Application

**Load Models and Calibration****LRFD Limit-State Format**

The LRFD format is widely used for structural design of buildings, bridges, and other structures. In 1994, the *AASHTO LRFD Bridge Design Specifications* (LRFD-BDS) was published in its first edition for bridge design and is now in its sixth edition. The limit-state format is:

$$\sum \gamma_i Q_i \leq \phi R_n = R_r$$

where:

- $\gamma_i$  = load factors,
- $Q_i$  = load effects,
- $\phi$  = resistance factors,
- $R_n$  = resistance, and
- $R_r$  = factored resistance.

The researchers considered the loads for design that are presented in Table 10.

**Dead Load Parameters**

Dead load is the weight of structural and permanently attached nonstructural components. Variation in the dead load, which affects statistical parameters of resistance, is caused by variation of gravity weight of materials (concrete and steel), variation of dimensions (tolerances in design dimensions), and idealization of analytical models. The bias factor (ratio of mean to nominal) value of dead load is  $\lambda = 1.05$ , with a coefficient of variation ( $Cov$ ) = 0.10 for cast-in-place elements, and  $\lambda = 1.03$  and  $Cov = 0.08$  for factory-made members. The assumed statistical parameters for dead load are based on the data available in the literature (e.g., Ellingwood et al., 1980; Nowak, 1999).

**Wind Load Model**

Note that wind is now an extreme limit state. In ASCE/SEI 7-10, the wind speeds are increased significantly in the new wind hazard maps. The load factor, however, is decreased from 1.6 to 1.0, which is the same as seismic events in the document. Because a seismic event is considered an extreme event within the LRFD-BDS, within the LRFD-LTS specifications, so is wind. The increases in wind speeds are nominally balanced in most locations of the country with the decreased load factors that result in nominally the same wind pressures.

Figure 1 illustrates a typical wind hazard map for the western half of the United States for the most common structures. These winds have a mean recurrence interval (MRI) of 700 years, with a 7% exceedance probability of 50 years.

Figure 2 illustrates a typical wind hazard map for the eastern half of the United States. For this level of wind, ASCE assigns an importance level of II; the number of people considered at risk (for buildings) is between two and 200 people (see the small figure inserts along the right side). This level of risk was aligned with LTS structures of a typical nature where they could fall on a roadway. Note that in the Midwest, the wind speed was 90 mph in ASCE/SEI 7-05 and was 90 mph in STD-LTS-6. In this region, it is now 115 mph.

Because the wind pressure is proportional to the square of speed, the increase in pressure is  $(115/90)^2 = 1.632$ , which is close to the value of the wind load factor of 1.6 in ASCE/SEI 7-05. The wind load factor is now 1.0; therefore, for much of the United States, the wind pressures did not change. However, in coastal regions, the new maps incorporate better data, and the wind maps in some areas have changed. This is automatically included in LRFD-LTS specifications as the ASCE/SEI 7-10 maps are used directly.

Table 11 is the load combination table for the LRFD-LTS specifications. The abbreviations provided in Table 10 are used in this table.

**Table 10. LTS loads.**

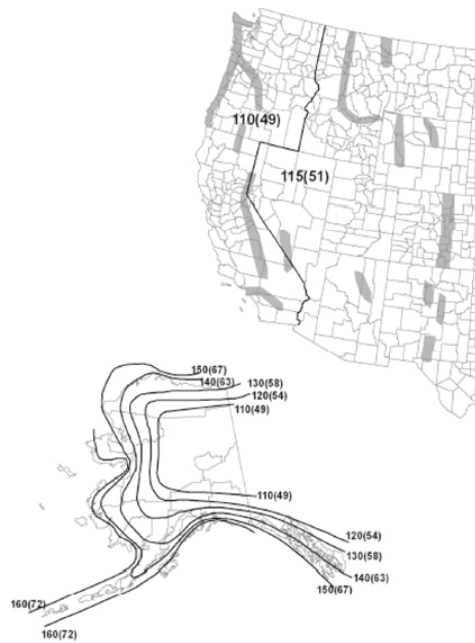
Load	Abbrev.	Description	Limit State
Dead load components	DC	Gravity	Strength
Live load	LL	Gravity (typically service personnel)	Strength
Wind	W	Lateral load	Extreme
Ice	IC	Gravity	Strength
Wind on ice	WI	Lateral	Extreme
Truck gust	TrG	Vibration	Fatigue
Natural wind gust	NWG	Vibration	Fatigue
Vortex-induced vibration	VIV	Vibration	Fatigue
Combined wind on high-mast towers	HMT	Vibration	Fatigue
Galloping-induced vibration	GIV	Vibration	Fatigue

The Strength I limit state for dead load only (Comb. 1) was calibrated. The Strength I limit state for dead load and live load was considered a minor case and may control only for components that support personnel servicing the traffic devices (Comb. 2). A live load factor based on ASCE/SEI 7-10 was used directly.

The Extreme I limit state combines dead loads with wind loads (Comb. 4). This is an important limit state. This combination was a strength limit in the allowable stress design (ASD)

LTS specification. The combination is termed “extreme” because ASCE/SEI 7-10 uses new wind speed maps that are associated with a unit load factor. (Note that a unit load factor is also used for seismic events, which are definitely considered extreme events.) Therefore, in the LRFD-LTS specifications, the term “extreme” is used.

The Extreme I limit state that combines dead load, wind, and ice (Comb. 5) was studied in detail, and it was determined that it will not be critical in the vast majority of cases, and in



**Notes:**

1. Values are nominal design 3-s gust wind speeds in m/s (mph) at 10 m (33 ft) above ground for Exposure C category,
2. Linear interpolation between wind contours is permitted.
3. Islands and coastal areas outside the last contour shall use the last wind speed contour of the coastal area.
4. Mountainous terrain, gorges, ocean promontories, and special wind regions shall be examined for unusual wind conditions.
5. Wind speeds correspond to approximately a 7% probability of exceedance in 50 years (Annual Exceedance Probability = 0.00143, MRI = 700 Years)

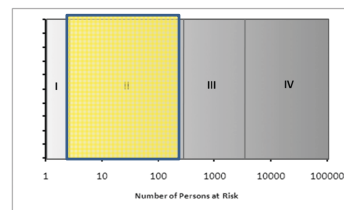


**Figure 1. Typical ASCE/SEI wind hazard map for the western United States.**

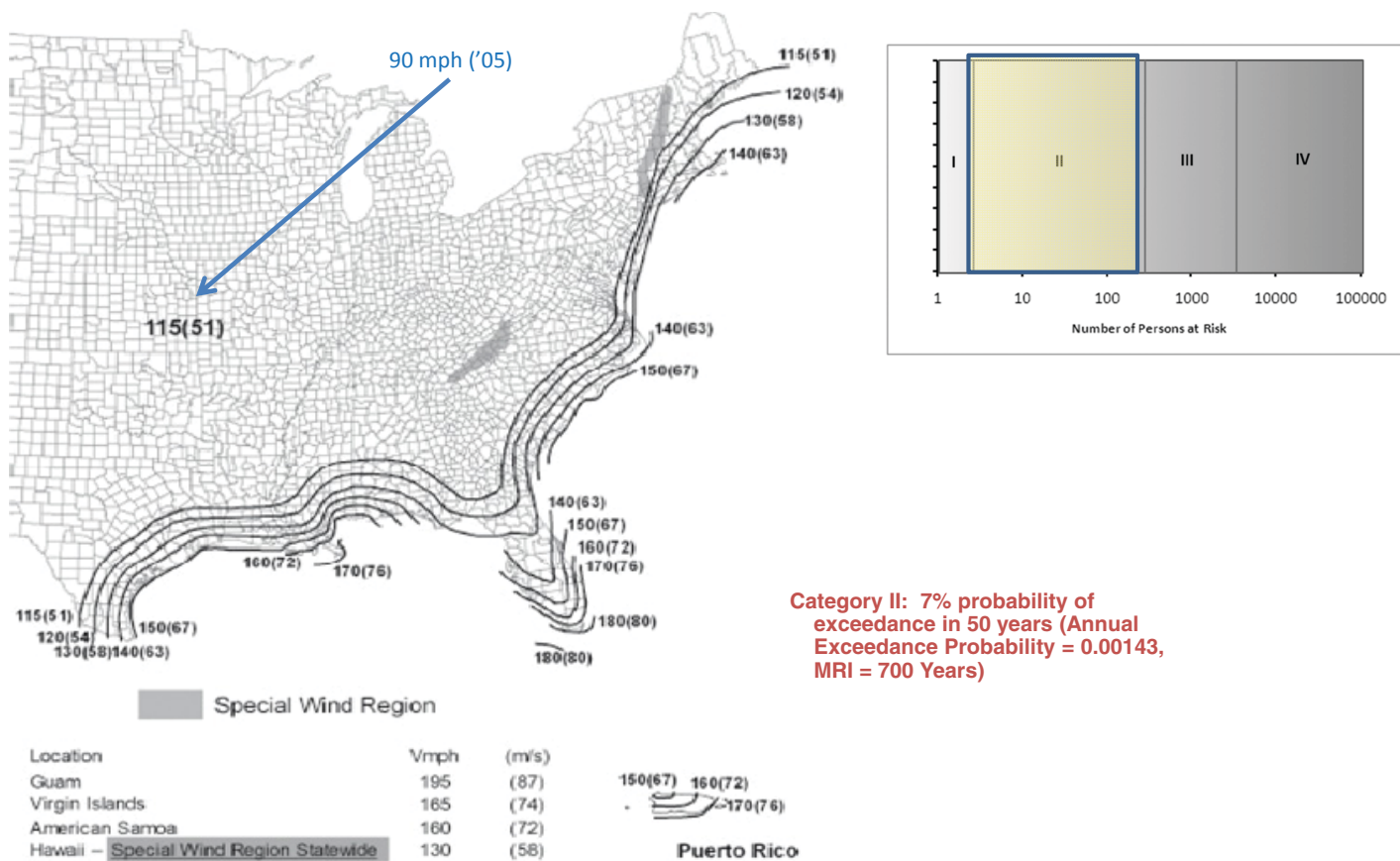


Figure 26.5-1A (Continued)

Figure 2. Typical ASCE/SEI wind hazard map for the eastern United States.

Table 11. Limit states considered in the LRFD-LTS specifications.

Comb. No.	Limit State	Calibrated?	Permanent	Transient			Fatigue (loads applied separately)				
				LL	W	IC	TrG	NWG	VIV	HMT	GIV
1	Strength I	Yes	1.25								
2	Strength I	No	1.25	1.6							
3	Strength I	Yes	1.1/0.9								
4	Extreme I	Yes	1.1/0.9		1.0						
5	Extreme I	Studied in detail	X		X	X					
6	Service I	No	1.0		1.0						
7	Service III	No	1.0		1.0						
8	Fatigue I	No, except for HMT					1.0	1.0	1.0	1.0	1.0
9	Fatigue II	No	1.0				1.0	1.0	1.0	1.0	1.0

the few cases where it will be critical, it is close to the dead load combined with wind (Comb. 4). Details are presented in Appendix A.

The Service I and III limit states were not calibrated, and the same factors that were used in the previous ASD-based specifications were used.

The Fatigue I limit is often critical, depending on the connection details. Significant work has been conducted on the fatigue performance of LTS connections (Connor et al., 2012, and Roy et al., 2011). The recommendations of the researchers of those projects were used without further calibration. The Fatigue II limit is for the finite-life approach used to determine remaining service life for an in-service structure.

## Wind Load Information from ASCE/SEI 7-10 and Available Literature

According to ASCE/SEI 7-10, the basic wind speed,  $V$ , used in the determination of design wind load on buildings and other structures should be determined from maps included in ASCE/SEI 7-10 (Fig. 26.5-1), depending on the risk category, with exceptions as provided in Section 26.5.2 (special wind regions) and 26.5.3 (estimation of basic speeds from regional climatic data).

For Risk Category II, it is required to use the map of wind speed  $V_{700}$  (Fig. 26.5-1A), corresponding to an approximately 7% probability of exceedance in 50 years (annual exceedance probability = 0.00143, MRI = 700 years) (see Figure 1 and Figure 2).

For Risk Categories III and IV, it is required to use the map of wind speed  $V_{1700}$  (Fig. 26.5-1B), corresponding to an approximately 3% probability of exceedance in 50 years (annual exceedance probability = 0.000588, MRI = 1,700 years) (not shown in this report; reference ASCE/SEI 7-10).

For Risk Category I, it is required to use the map of wind speed  $V_{300}$  (Fig. 26.5-1C), corresponding to an approximately 15% probability of exceedance in 50 years (annual exceedance probability = 0.00333, MRI = 300 years) (not shown in this report; see ASCE/SEI 7-10).

The basic wind speeds in ASCE/SEI 7-10 (Fig. 26.5-1) are based on the 3-s gust wind speed map. The non-hurricane wind speed is based on peak gust data collected at 485 weather stations where at least 5 years of data were available (Peterka, 1992; Peterka and Shahid, 1998). For non-hurricane regions,

measured gust data were assembled from a number of stations in state-sized areas to decrease sampling error, and the assembled data were fit using a Fisher-Tippett Type I extreme value distribution. The hurricane wind speeds on the United States Gulf and Atlantic coasts are based on the results of a Monte Carlo simulation model described in Vickery and Waldhera (2008) and Vickery et al. (2009a, 2009b, and 2010).

## Statistical Parameters for Wind Load Variables

The wind pressure is computed using the following formula:

$$P_z = 0.0256 \cdot K_z \cdot K_d \cdot G \cdot V^2 \cdot C_d \text{ (psf)}$$

where:

- $V$  = basic wind speed (mph),
- $K_z$  = height and exposure factor,
- $K_d$  = directionality factor,
- $G$  = gust effect factor, and
- $C_d$  = drag coefficient.

The parameters  $V$ ,  $K_z$ ,  $K_d$ ,  $G$ , and  $C_d$  are random variables, and the distribution function of wind pressure and the wind load statistics are required to determine appropriate probability-based load and load combination factors. The cumulative distribution function (CDF) of wind speed is particularly significant because  $V$  is squared. However, the uncertainties in the other variables also contribute to the uncertainty in  $P_z$ .

The CDFs for the random variables used to derive the wind load criteria that appear in ASCE/SEI 7-10 are summarized in Table 12 (Ellingwood, 1981).

## Statistical Parameters of Resistance

Load-carrying capacity is a function of the nominal value of resistance ( $R_n$ ) and three factors: material factor ( $m$ ), representing material properties, fabrication factor ( $f$ ), representing the dimensions and geometry, and professional factor ( $p$ ), representing uncertainty in the analytical model:

$$R = R_n \cdot m \cdot f \cdot p$$

**Table 12. Wind load statistics (Ellingwood, 1981).**

Parameter	Mean/Nominal	Cov	CDF
Exposure factor, $K_z$	1.0	0.16	Normal
Gust factor, $G$	1.0	0.11	Normal
Pressure coefficient, $C_p$	1.0	0.12	Normal

**Table 13. Statistical parameters for material and dimensions (Ellingwood et al., 1980).**

Parameters	$\lambda$	Cov
Static yield strength, flanges	1.05	0.10
Static yield strength, webs	1.10	0.11
Young's modulus	1.00	0.06
Static yield strength in shear	1.11	0.10
Tensile strength of steel	1.10	0.11
Dimensions, $f$	1.00	0.05

The statistical parameters for  $m$ ,  $f$ , and  $p$  were considered by various researchers, and the results were summarized by Ellingwood et al. (1980) based on material test data available in the 1970s.

The actual strength in the structure can differ from structure to structure, but these differences are included in the fabrication and professional bias factors ( $\lambda_f$  and  $\lambda_p$ ). Material parameters for steel were established based on the yield strength data.

The typical parameters are listed in Table 13 to Table 16.

The resistance (load-carrying capacity) is formulated for each of the considered limit states and structural components:

$$\text{Bending resistance, elastic state: } M = f_y \cdot S$$

$$\text{Bending resistance, plastic state: } M = f_y \cdot Z$$

$$\text{Shear resistance: } V = A_{\text{shear}} \cdot 0.57 \cdot f_y$$

$$\text{Torsion capacity: } T = \frac{J}{0.5 \cdot d} \cdot 0.57 \cdot f_y$$

$$\text{Axial capacity: } P = A \cdot f_y$$

**Table 15. Resistance statistics for cold-formed steel members (Ellingwood et al., 1980).**

Limit State	Resistance	
	$\lambda$	Cov
Tension member	1.10	0.11
Braced beams in flexure, flange stiffened	1.17	0.17
Braced beams in flexure, flange unstiffened	1.60	0.28
Laterally unbraced beams	1.15	0.17
Columns, flexural buckling, elastic	0.97	0.09
Columns, flexural buckling, inelastic, compact	1.20	0.13
Columns, flexural buckling, inelastic, stiffened	1.07	0.20
Columns, flexural buckling, inelastic, unstiffened	1.68	0.26
Columns, flexural buckling, inelastic, cold work	1.21	0.14
Columns, torsional-flexural buckling, elastic	1.11	0.13
Columns, torsional-flexural buckling, inelastic	1.32	0.18

Generally, the limit state that controls the design of luminaires is calculated using an interaction equation for load combination that produces torsion, shear, flexure, and axial force [Section C-H3-8, AISC *Steel Construction Manual* (AISC, 2010)].

$$\left( \frac{P_r}{P_c} + \frac{M_r}{M_c} \right) + \left( \frac{V_r}{V_c} + \frac{T_r}{T_c} \right)^2 \leq 1.0$$

where:

- $P$  = axial force,
- $M$  = bending moment,
- $V$  = shear, and
- $T$  = torsion.

The terms with the subscript  $r$  represent the required strength (load effect), and those with the subscript  $c$  represent the corresponding available strengths (load-carrying capacity).

**Table 14. Resistance statistics for hot-rolled steel elements (Ellingwood et al., 1980).**

Limit State	Professional		Material		Fabrication		Resistance	
	$\lambda$	Cov	$\lambda$	Cov	$\lambda$	Cov	$\lambda$	Cov
Tension member, yield	1.00	0	1.05	0.10	1.00	0.05	<b>1.05</b>	<b>0.11</b>
Tension member, ultimate	1.00	0	1.10	0.10	1.00	0.05	<b>1.10</b>	<b>0.11</b>
Elastic beam, LTB	1.03	0.09	1.00	0.06	1.00	0.05	<b>1.03</b>	<b>0.12</b>
Inelastic beam, LTB	1.06	0.09	1.05	0.10	1.00	0.05	<b>1.11</b>	<b>0.14</b>
Plate girders in flexure	1.03	0.05	1.05	0.10	1.00	0.05	<b>1.08</b>	<b>0.12</b>
Plate girders in shear	1.03	0.11	1.11	0.10	1.00	0.05	<b>1.14</b>	<b>0.16</b>
Beam – columns	1.02	0.10	1.05	0.10	1.00	0.05	<b>1.07</b>	<b>0.15</b>

Note: LTB = lateral-torsional buckling.

**Table 16. Resistance statistics for aluminum structures (Ellingwood et al., 1980).**

Limit State	Resistance	
	$\lambda$	Cov
Tension member, limit-state yield	1.10	0.08
Tension member, limit-state ultimate	1.10	0.08
Beams, limit-state yield	1.10	0.08
Beams, limit-state lateral buckling	1.03	0.13
Beams, limit-state inelastic local buckling	1.00	0.09
Columns, limit-state yield	1.10	0.08
Columns, limit-state local buckling	1.00	0.09

The limit-state function can be written:

$$g(Q_i, R_i) = 1.0 - \left( \frac{Q_1}{R_1} + \frac{Q_2}{R_2} \right) - \left( \frac{Q_3}{R_3} + \frac{Q_4}{R_4} \right)^2$$

The interaction equation is a nonlinear function; therefore, to calculate combined load-carrying capacity, Monte Carlo simulation was used for each random variable. This procedure allows for finding function  $g$  and calculating reliability index  $\beta$ . For calibration purposes, using a first-order second-moment approach, the resistance parameters were assumed to have a bias factor of 1.05 and a coefficient of variation of 10%. The details are provided in Appendix A.

## LRFD Reliability Analysis

The calibration between ASD and LRFD is based on the calibration of ASCE/SEI 7-05 50-year  $V_{50}$  wind speed and ASCE/SEI 7-10 700-year  $V_{700}$  wind speed. The ASCE/SEI 7-10 wind speed maps for a 700-year wind are calibrated to the ASCE/SEI 7-05 50-year wind speed, where the difference between LRFD design wind load factors (ASCE/SEI 7-05  $\gamma_W = 1.6$  vs. ASCE/SEI 7-10  $\gamma_W = 1.0$ ) is  $(V_{700}/V_{50})^2 = 1.6$ . Thus, the LRFD ASCE/SEI 7-05  $V_{50}$  wind speed is equivalent (for pressures that are proportional to  $V^2$ ) to the ASCE/SEI 7-10  $V_{700}$  wind speed. Likewise, the ASCE/SEI 7-10  $V_{300}$  and  $V_{1700}$  winds speeds are equivalent to ASCE/SEI 7-05  $V_{50}$  wind speeds adjusted for importance [low  $I_{low} = 0.87 = (V_{300}/V_{700})^2$  and high  $I_{high} = 1.15 = (V_{1700}/V_{700})^2$ ]. The ASCE/SEI 7-05  $V_{50}$  wind speed is used as the mean wind speed (adjusted for design map values compared to statistical means) for the reliability analyses.

## Flexural Resistance

The flexural resistance is discussed here, and other actions and combinations of actions are provided in detail in Appendix A.

The LRFD design requirement for a structure at the optimal design limit is:

$$\phi R_n = \max \begin{cases} \gamma_{D2} M_D \\ \gamma_{D1} M_D + \gamma_W M_W \end{cases}$$

where:

- $R_n$  = nominal resistance,
- $M_D$  = nominal dead load (DL) moment,
- $M_W$  = nominal wind load (WL) moment,
- $\gamma_{D1}$  = dead load design load factor (used in conjunction with dead + wind case),
- $\gamma_{D2}$  = dead load design load factor (dead load only case),
- $\gamma_W$  = wind load design load factor, and
- $\phi$  = resistance factor.

To meet the design limit, the nominal resistance is:

$$R_n = \max \begin{cases} \frac{1}{\phi} \gamma_{D2} M_D \\ \frac{1}{\phi} [\gamma_{D1} M_D + \gamma_W M_W] \end{cases}$$

The mean resistance is:

$$\bar{R} = \lambda_R R_n$$

where:

- $\lambda_R$  = bias factor for strength variable  $R$ , and
- $\bar{R}$  = statistical mean of variable  $R$ .

At the optimal design limit, the mean of  $R$  becomes:

$$\bar{R} = \max \begin{cases} \frac{\lambda_R}{\phi} \gamma_{D2} M_D \\ \frac{\lambda_R}{\phi} [\gamma_{D1} M_D + \gamma_W M_W] \end{cases}$$

The coefficient of variation for the strength is  $Cov_R$ .

## Load

The total applied nominal moment at the ASCE/SEI 7-10 700-year wind speed is:

$$M_{T1} = M_D + M_{700}$$

where:

- $M_{T1}$  = total nominal moment at ASCE/SEI 7-10 700-year wind speed,
- $M_D$  = dead load moment, and
- $M_{700}$  = nominal moment from wind at ASCE/SEI 7-10 700-year wind speed.

To standardize the comparisons between ASD and LRFD, and for any specified-year wind, all analyses and comparisons are based on the total nominal moment for the LRFD 700-year total applied moment equal to 1.0:

$$M_{T_1} = M_D + M_{700} = 1.0$$

and, the dead load moment can be represented by:

$$M_D = 1 - M_{700}$$

The calibration and comparisons vary the  $M_{700}$  wind load effect from 1.0 to 0.0, while  $M_D$  varies from 0.0 to 1.0 so that the total applied nominal moment at the ASCE/SEI 7-10 700-year load remains 1.0. The total applied nominal moments for ASD and other LRFD year wind speeds is adjusted to be equivalent to the ASCE/SEI 7-10 700-year wind speed load case.

Given that the nominal moment from wind for any year wind can be determined by:

$$M_{WT} = \left( \frac{V_T}{V_{700}} \right)^2 M_{700}$$

where:

$V_T$  = wind speed for any year  $T$  wind speed, and

$M_{WT}$  = nominal wind moment at any year  $T$ .

and the total applied nominal moment becomes:

$$M_{T_2} = M_D + M_{WT} = (1 - M_{700}) + \left( \frac{V_T}{V_{700}} \right)^2 M_{700}$$

where:

$M_{T_2}$  = total applied nominal moment at any year  $T$  wind speed.

To determine the mean wind moment for the reliability analyses, the mean moment at the 50-year wind speed is determined from the ASCE/SEI 7-10 wind speed relation:

$$V_T = [0.36 + 0.10 \ln(12T)] V_{50}$$

or:

$$V_{50} = \frac{V_T}{0.36 + 0.10 \ln(T)} = \lambda_V V_T$$

where:

$\lambda_V$  = bias factor for wind speed at year  $T$ ,

and the nominal wind moment at the 50-year wind speed becomes:

$$M_{50} = \lambda_V^2 M_{700}$$

The nominal moment at the 50-year wind speed is proportional to  $V^2$  by:

$$M_{50} \propto K_d K_z G C_d V_{50}^2$$

where:

$K_d$  = directionality coefficient,

$K_z$  = elevation coefficient,

$G$  = gust effect factor, and

$C_d$  = drag coefficient.

The mean wind moment for the reliability analyses is:

$$\bar{M}_{50} \propto \bar{K}_d \bar{K}_z \bar{G} \bar{C}_d \bar{V}_{50}^2$$

where the variables are the means. Assuming that  $K_d$  does not vary, the other non-wind-speed variables' nominal values are related to the means by the bias factors. Combining them into a single bias factor  $\lambda_p$  gives:

$$\bar{K}_z \bar{G} \bar{C}_d = \lambda_{K_z} \lambda_G \lambda_{C_d} K_z G C_d = \lambda_p K_z G C_d$$

where:

$$\lambda_p = \lambda_{K_z} \lambda_G \lambda_{C_d}$$

and:

$K_d$  does not vary.

Considering that the map design values may differ from the statistical mean of the 50-year wind speed, the mean 50-year wind speed can be represented by:

$$\bar{V}_{50} = \lambda_X V_{50} = \lambda_X \lambda_V V_{700}$$

where:

$\lambda_X = \frac{\mu_{50}}{V_{50}}$  = bias for the 50-year wind speed,

$\mu_{50}$  = mean 50-year wind speed, and

$V_{50}$  = map design 50-year wind speed.

The mean wind moment for the reliability analyses becomes:

$$\bar{M}_{50} = \lambda_p \lambda_V^2 \lambda_X^2 M_{700}$$

where:

$$M_{700} \propto K_d K_z G C_d V_{700}^2$$

Referring back to the basis that all comparisons are equated with a total ASCE/SEI 7-10 applied nominal moment of:

$$M_D + M_{700} = 1$$

**Table 17. Regional wind statistics.**

	V <sub>50</sub>	μ <sub>50</sub>	COV <sub>μ50</sub>	V <sub>300</sub>	V <sub>700</sub>	V <sub>1700</sub>
Florida Coastal	150	130	0.14	170	180	200
Midwest & West	90	75	0.1	105	115	120
West Coast	85	67	0.095	100	110	115
Southern Alaska	130	110	0.105	150	160	165

and using that the nominal dead load moment and mean dead load moment are:

$$M_D = 1 - M_{700}$$

$$\bar{M}_D = \lambda_D (1 - M_{700})$$

where:

$\lambda_D$  = bias factor for dead load moment,

The mean load effect on the structure becomes:

$$Q = \bar{M}_D + \bar{M}_{50} = \lambda_D (1 - M_{700}) + \lambda_P \lambda_V^2 \lambda_X^2 M_{700}$$

where  $Q$  = the mean moment.

To find the coefficient of variation for  $Q$ , first the coefficient of variation for the mean wind moment is determined from:

$$Cov_{M_{50}} = \sqrt{(2Cov_V)^2 + Cov_{K_z}^2 + Cov_G^2 + Cov_{Cd}^2}$$

noting that  $V$  in the  $V^2$  term is 100% correlated, and the coefficient of  $V^2$  ( $Cov_{V^2}$ ) is two times the coefficient of variation of  $V$  ( $Cov_V$ ).

Combining the statistical properties for the dead and wind moments to determine the coefficient of variation for the total mean moment  $Q$  results in

$$Cov_Q = \frac{\sigma_Q}{Q} = \frac{\sqrt{[Cov_D \lambda_D (1 - M_{700})]^2 + [Cov_{M_{50}} \lambda_P \lambda_V^2 \lambda_X^2 M_{700}]^2}}{\bar{Q}}$$

## Reliability Indices

$Q$  and  $R$  are assumed to be lognormal and independent:

$$\mu_{\ln R} = \ln \bar{R} - \frac{1}{2} \sigma_{\ln R}^2$$

$$\sigma_{\ln R}^2 = \sqrt{\ln(1 + Cov_R^2)}$$

$$\mu_{\ln Q} = \ln \bar{Q} - \frac{1}{2} \sigma_{\ln Q}^2$$

$$\sigma_{\ln Q}^2 = \sqrt{\ln(1 + Cov_Q^2)}$$

where  $\sigma$  is the standard deviation of the variable indicated.

The reliability index  $\beta$  is:

$$\beta = \frac{\mu_{\ln R} - \mu_{\ln Q}}{\sqrt{\sigma_{\ln R}^2 + \sigma_{\ln Q}^2}} = \frac{\ln\left(\frac{\bar{R}}{\bar{Q}}\right) - \frac{1}{2}(\sigma_{\ln R}^2 + \sigma_{\ln Q}^2)}{\sqrt{\sigma_{\ln R}^2 + \sigma_{\ln Q}^2}}$$

## Implementation

The LRFD reliability analysis was coded into a spreadsheet to study four regions in the United States:

- Florida Coastal Region,
- Midwest and Western Region,
- Western Coastal Region, and
- Southern Alaska Region.

Inputs for LRFD reliability analyses spreadsheet:

$V_{300}$ ,  $V_{700}$ ,  $V_{1700}$  per ASCE/SEI 7-10 design wind speeds

$\mu_{50}$ ,  $V_{\mu 50}$ ,  $V_{50}$  per ASCE/SEI 7-05 design wind speeds

Regional wind statistics are provided in Table 17.

Global inputs (same for all regions) are:

$\lambda_D$ ,  $\lambda_R$ ,  $Cov_D$ ,  $Cov_R$

$\lambda_{K_z}$ ,  $\lambda_G$ ,  $\lambda_{Cd}$ ,  $Cov_{K_z}$ ,  $Cov_G$ ,  $Cov_{Cd}$

$\phi$ ,  $\gamma_{D1}$ ,  $\gamma_{D2}$ ,  $\gamma_W$

Table 18 provides global inputs (inputs are highlighted).

**Table 18. Input to reliability calibration (all regions).**

			COV	BIAS
BIAS <sub>D</sub>	1.03	COV <sub>Kz</sub>	0.16	1.00
COV <sub>D</sub>	0.08	COV <sub>G</sub>	0.11	1.00
BIAS <sub>R</sub>	1.05	COV <sub>Cd</sub>	0.12	1.00
COV <sub>R</sub>	0.10		Total Bias <sub>p</sub>	1.00
	D+W	D Only		
φ	0.90			
γ <sub>D</sub>	1.10	1.25		
γ <sub>W</sub>	1.00			

**Table 19. Reliability indices for Midwest and Western Region (MRI = 700 yrs).**

				700 Year Wind		$V_{700}$	115				
				T	700	$V_{50}$	91.00991	Theory			
				$BIAS_x$	0.8241	$V_{700}/V_{700}$	1.00	$(V_{700}/V_{700})^2$			
				$COV_V$	0.100	$(V_{300}/V_{700})^2$	1.00	1.00			
Equiv				$BIAS_V$	0.79						
$M_{700}$	$M_{T2}$	$M_{700}/M_{T2}$	$R_n$	R	$\sigma_{lnR}$	Q	$COV_{M50}$	$COV_Q$	$\sigma_{lnQ}$	LRFD $\beta$	
1.00	1.00	1.00	1.11	1.17	0.10	0.43	0.30	0.30	0.30	3.35	
0.90	1.00	0.90	1.12	1.18	0.10	0.49	0.30	0.24	0.24	3.54	
0.80	1.00	0.80	1.13	1.19	0.10	0.55	0.30	0.19	0.19	3.69	
0.70	1.00	0.70	1.14	1.20	0.10	0.61	0.30	0.15	0.15	3.77	
0.60	1.00	0.60	1.16	1.21	0.10	0.67	0.30	0.13	0.13	3.75	
0.50	1.00	0.50	1.17	1.23	0.10	0.73	0.30	0.11	0.10	3.60	
0.40	1.00	0.40	1.18	1.24	0.10	0.79	0.30	0.09	0.09	3.34	
0.30	1.00	0.30	1.19	1.25	0.10	0.85	0.30	0.08	0.08	2.98	
0.20	1.00	0.20	1.20	1.26	0.10	0.91	0.30	0.08	0.08	2.57	
0.10	1.00	0.10	1.25	1.31	0.10	0.97	0.30	0.08	0.08	2.38	
0.00	1.00	0.00	1.39	1.46	0.10	1.03	0.30	0.08	0.08	2.71	

The results for the Midwest and Western Region ASCE/SEI 7-10 700-year wind speed are shown in Table 19 (other regions are similar). For the 300-year wind speed, the results are shown in Table 20. Notice that the total nominal moment,  $M_{T2}$ , is less than 1.0 because the wind moment,  $M_{300}$ , is less than  $M_{700}$ . Likewise, for the 1,700-year wind speed,  $M_{T2}$  is larger than 1.0 since  $M_{1700}$  is greater than  $M_{700}$ , as shown in Table 21.

Using the 300-year wind speed requires less nominal resistance; conversely, using the 1,700-year wind speed increases the

required nominal resistance. Because the mean load Q and its variation do not change, this difference in required nominal resistance changes the reliability indices  $\beta$  accordingly.

### ASD Reliability Analysis

Because the LRFD reliability analyses are based on the total nominal moment  $M_D + M_{700} = 1.0$ , the ASD analyses must adjust the moments for a consistent comparison.

**Table 20. Reliability indices for Midwest and Western Region (MRI = 300 yrs).**

				300 Year Wind		$V_{300}$	105				
				T	300	$V_{50}$	91.00991	Theory			
				$BIAS_x$	0.8241	$V_{700}/V_{700}$	1.00	$(V_{700}/V_{700})^2$			
				$COV_V$	0.100	$(V_{300}/V_{700})^2$	0.83	0.87			
Equiv				$BIAS_V$	0.79						
$M_{300}$	$M_{T2}$	$M_{300}/M_{T2}$	$R_n$	R	$\sigma_{lnR}$	Q	$COV_{M50}$	$COV_Q$	$\sigma_{lnQ}$	LRFD $\beta$	
0.83	0.83	1.00	0.93	0.97	0.10	0.43	0.30	0.30	0.30	2.77	
0.75	0.85	0.88	0.96	1.00	0.10	0.49	0.30	0.24	0.24	2.92	
0.67	0.87	0.77	0.99	1.03	0.10	0.55	0.30	0.19	0.19	3.04	
0.58	0.88	0.66	1.02	1.07	0.10	0.61	0.30	0.15	0.15	3.11	
0.50	0.90	0.56	1.04	1.10	0.10	0.67	0.30	0.13	0.13	3.12	
0.42	0.92	0.45	1.07	1.13	0.10	0.73	0.30	0.11	0.10	3.03	
0.33	0.93	0.36	1.10	1.16	0.10	0.79	0.30	0.09	0.09	2.86	
0.25	0.95	0.26	1.13	1.19	0.10	0.85	0.30	0.08	0.08	2.61	
0.17	0.97	0.17	1.16	1.22	0.10	0.91	0.30	0.08	0.08	2.32	
0.08	0.98	0.08	1.25	1.31	0.10	0.97	0.30	0.08	0.08	2.38	
0.00	1.00	0.00	1.39	1.46	0.10	1.03	0.30	0.08	0.08	2.71	

**Table 21. Reliability indices for Midwest and Western Region (MRI = 1,700 yrs).**

				1700 Year Wind		$V_{1700}$	120				
				T	1700			Theory			
						$V_{1700}/V_{700}$	1.04	$(V_{1700}/V_{700})^2$			
						$(V_{1700}/V_{700})^2$	1.09	1.15			
Equiv											
$M_{1700}$	$M_{T2}$	$M_{1700}/M_{T2}$	$R_n$	R	$\sigma_{lnR}$	Q	$COV_{M50}$	$COV_Q$	$\sigma_{lnQ}$	LRFD $\beta$	
1.09	1.09	1.00	1.21	1.27	0.10	0.43	0.30	0.30	0.30	3.62	
0.98	1.08	0.91	1.21	1.27	0.10	0.49	0.30	0.24	0.24	3.84	
0.87	1.07	0.81	1.21	1.27	0.10	0.55	0.30	0.19	0.19	4.01	
0.76	1.06	0.72	1.21	1.27	0.10	0.61	0.30	0.15	0.15	4.09	
0.65	1.05	0.62	1.21	1.28	0.10	0.67	0.30	0.13	0.13	4.06	
0.54	1.04	0.52	1.22	1.28	0.10	0.73	0.30	0.11	0.10	3.89	
0.44	1.04	0.42	1.22	1.28	0.10	0.79	0.30	0.09	0.09	3.58	
0.33	1.03	0.32	1.22	1.28	0.10	0.85	0.30	0.08	0.08	3.17	
0.22	1.02	0.21	1.22	1.28	0.10	0.91	0.30	0.08	0.08	2.69	
0.11	1.01	0.11	1.25	1.31	0.10	0.97	0.30	0.08	0.08	2.38	
0.00	1.00	0.00	1.39	1.46	0.10	1.03	0.30	0.08	0.08	2.71	

Using the ASCE/SEI 7-05 criteria for the ASD design, the wind moment for a 50-year wind speed is:

$$Design M_{50} = M_{700} \left( \frac{Design V_{50}}{V_{700}} \right)^2$$

Considering that the Design  $V_{50}$  may differ from  $V_{50} = (\lambda_V)^2 V_{700}$ , a bias factor,  $\lambda_{Design}$ , is introduced, and:

$$Design M_{50} = \lambda_{Design}^2 \left( \frac{V_{50}}{V_{700}} \right)^2 M_{700} = \lambda_{Design}^2 \lambda_V^2 M_{700}$$

$$\lambda_{Design} = \frac{Design V_{50}}{V_{50}}$$

The total ASD design moment,  $M_{T3}$ , consistent with  $M_D + M_{700} = 1.0$ , becomes:

$$M_{T3} = M_D + Design M_{50} = (1 - M_{700}) + \lambda_{Design}^2 \lambda_V^2 M_{700}$$

## Resistance

The LRFD nominal resistance is assumed to be the plastic moment capacity. To directly compare resistances between LRFD and ASD sections, the nominal resistance for the ASD design is increased by the section shape factor for a compact section:

$$R_n = SF M_y$$

where  $SF$  is the shape factor.

The allowable stress for a compact section using the allowed overstress factor (OSF) of 4/3 for wind loads is:

$$F_{allow} = \frac{4}{3} (0.66) F_y = (OSF)(0.66) F_y$$

Using moments instead of stresses, the allowable moment is  $OSF (0.66) M_y$ , and the design requirement for an optimal design is:

$$(OSF)(0.66) M_y = M_D + Design M_{50} I$$

where:

$I = I_{low} = 0.87$  (low importance) comparable to ASCE/SEI 7-10 300-year wind speed,

$I = I_{med} = 1.00$  (medium importance) comparable to ASCE/SEI 7-10 700-year wind speed, and

$I = I_{high} = 1.15$  (high importance) comparable to ASCE/SEI 7-10 1,700-year wind speed.

The nominal resistance (to directly compare to the LRFD design) is determined by increasing the design strength by the shape factor as:

$$R_n = SF M_y = \frac{SF}{OSF} \frac{1}{0.66} [(1 - M_{700}) + \lambda_{Design}^2 \lambda_V^2 M_{700} I]$$

For the ASD reliability analyses, the statistical properties are:

$$\bar{R} = \lambda_R R_n$$

**Table 22. Midwest and Western Region reliability indices ( $I = 1.00$ ).**

LRFD				ASD		Strength	
				Total Design		Ratio	
Equiv				Moment		$R_{nLRFD}$	
$R_{nLRFD}$	$M_{50}$	$M_{T3}$	$M_{50}/M_{T3}$	$M_D+M_{50I}$	$R_{nASD}$	$R_{nASD}$	ASD $\beta$
1.11	0.61	0.61	1.00	0.61	0.90	1.23	2.69
1.12	0.55	0.65	0.85	0.65	0.96	1.17	2.94
1.13	0.49	0.69	0.71	0.69	1.02	1.11	3.20
1.14	0.43	0.73	0.59	0.73	1.08	1.06	3.44
1.16	0.37	0.77	0.48	0.77	1.13	1.02	3.63
1.17	0.31	0.81	0.38	0.81	1.19	0.98	3.74
1.18	0.24	0.84	0.29	0.84	1.25	0.94	3.77
1.19	0.18	0.88	0.21	0.88	1.31	0.91	3.71
1.20	0.12	0.92	0.13	0.92	1.36	0.88	3.57
1.25	0.06	0.96	0.06	0.96	1.42	0.88	3.39
1.39	0.00	1.00	0.00	1.00	1.48	0.94	3.19

and:

$Q$ ,  $Cov_Q$ , and  $\sigma_{\ln Q}$  are unchanged.

The coefficient of variation for the strength (resistance) is  $Cov_R$ .

The equations for determining the reliability indices are identical to those used for the LRFD cases.

### Implementation

For the four regions, the ASD reliability analyses require additional inputs.

Inputs for ASD are:

- Importance factors  $I_{low} = 0.87$ ,  $I_{med} = 1.00$ , and  $I_{high} = 1.15$ ;
- Shape factor  $SF = Z_x/S_x = 1.30$  for a circular section; and
- Wind overstress factor  $OSF = 4/3 = 1.333$ .

The results for the Midwest and Western Region ASCE/SEI 7-05, medium importance  $I_{med} = 1.00$  are shown in Table 22.

The LRFD required nominal strength is shown for direct comparison. For the Midwest and Western Region for a low importance  $I_{low} = 0.87$ , the results are shown in Table 23. Table 24 provides results for a high importance  $I_{high} = 1.15$ .

**Table 23. Midwest and Western Region reliability indices ( $I = 0.87$ ).**

LRFD				ASD		Strength	
				Total Design		Ratio	
Equiv				Moment		$R_{nLRFD}$	
$R_{nLRFD}$	$M_{50}$	$M_{T3}$	$M_{50}/M_{T3}$	$M_D+M_{50I}$	$R_{nASD}$	$R_{nASD}$	ASD $\beta$
0.93	0.61	0.61	1.00	0.53	0.79	1.18	2.25
0.96	0.55	0.65	0.85	0.58	0.86	1.12	2.49
0.99	0.49	0.69	0.71	0.63	0.93	1.07	2.75
1.02	0.43	0.73	0.59	0.67	0.99	1.02	3.00
1.04	0.37	0.77	0.48	0.72	1.06	0.98	3.23
1.07	0.31	0.81	0.38	0.77	1.13	0.95	3.39
1.10	0.24	0.84	0.29	0.81	1.20	0.92	3.48
1.13	0.18	0.88	0.21	0.86	1.27	0.89	3.49
1.16	0.12	0.92	0.13	0.91	1.34	0.87	3.43
1.25	0.06	0.96	0.06	0.95	1.41	0.89	3.33
1.39	0.00	1.00	0.00	1.00	1.48	0.94	3.19

**Table 24. Midwest and Western Region reliability indices ( $I = 1.15$ ).**

LRFD				ASD		Strength	
Equiv				Total Design		Ratio	
				Moment		$R_{nLRFD}$	
$R_{nLRFD}$	$M_{50}$	$M_{T3}$	$M_{50}/M_{T3}$	$M_D + M_{50}I$	$R_{nASD}$	$R_{nASD}$	ASD $\beta$
1.21	0.61	0.61	1.00	0.70	1.04	1.16	3.14
1.21	0.55	0.65	0.85	0.73	1.08	1.12	3.41
1.21	0.49	0.69	0.71	0.76	1.13	1.07	3.67
1.21	0.43	0.73	0.59	0.79	1.17	1.04	3.90
1.21	0.37	0.77	0.48	0.82	1.22	1.00	4.06
1.22	0.31	0.81	0.38	0.85	1.26	0.97	4.13
1.22	0.24	0.84	0.29	0.88	1.30	0.93	4.09
1.22	0.18	0.88	0.21	0.91	1.35	0.91	3.94
1.22	0.12	0.92	0.13	0.94	1.39	0.88	3.73
1.25	0.06	0.96	0.06	0.97	1.43	0.87	3.47
1.39	0.00	1.00	0.00	1.00	1.48	0.94	3.19

Notice that the total nominal moment,  $M_{T3}$ , does not change, but the total design moment  $M_D + M_{50}I$  changes with the importance factor, resulting in different required nominal strength  $R_n$ . Similarly, for high importance, the required nominal strength  $R_n$  increases as shown in the following for the Midwest and Western Region.

The importance factors directly change the required nominal resistances. Because the mean load  $Q$  and its variation do not change (not shown in these tables but the same as in the LRFD tables), this difference in required nominal resistances changes the reliability indices  $\beta$  accordingly.

## Calibration and Comparison

Using the proposed flexure load and resistance factors, and with the statistical properties incorporated into the reliability analyses, the plots in Table 25 compare the reliability indices for the four regions between current ASD design procedures and the proposed LRFD procedures. The *Minimum Beta* plots represent the minimum indices over the four regions. Similarly, the *Average Beta* plots show the averages over the four regions. For the LRFD 300-year, 700-year, and 1,700-year wind speed cases, the equivalent ASD designs use  $I_{low} = 0.87$ ,  $I_{med} = 1.00$ , and  $I_{high} = 1.15$  importance factors, respectively.

The proposed LRFD procedures result in comparable but more consistent reliability over the range of designs. For low-importance structures (using 300-year wind speeds), the reliability indices are lower, as intended. Likewise, for higher-importance structures (1,700-year wind speeds), the reliability indices are higher. This is shown in Figure 3 for the LRFD procedures. The ratios are the averages over the four regions.

At low wind moments ( $\gamma_{D2}M_D$  controls the design), there is no difference. However, for higher wind moments, the required strength increases for high-importance structures and decreases for lower-importance structures.

As expected, the LRFD-required strength at a higher percentage of wind load ( $M_{Wind}/M_{Total}$  high) is greater than that required for ASD. This behavior is demonstrated in Figure 4, where the ratios are the average for the four regions.

At a total moment where the wind is responsible for approximately 60% or more of the total, the proposed LRFD-LTS procedures will require more section capacity than the current ASD procedures. Below 60%, the LRFD-LTS procedures will require less section capacity than ASD.

## Implementation

### Setting Target Reliability Indices

The statistical characterization of the limit-state equation and the associated inputs are presented in the preceding sections. The reliability indices are computed based on the current ASD practice and the LRFD-LTS specifications. Comparisons made and presented previously are based on the recommended load and resistance factors. These factors are illustrated for the 700-year wind speeds (MRI = 700 yrs). This MRI is for the typical structure; however, some consideration is warranted for structures that are located on routes with low average daily traffic (ADT) or that are located away from the travelway, whereby failure is unlikely to be a safety issue. Similarly, consideration is also warranted for structures located on heavily traveled roads, where a failure has a significant chance of harming travelers or suddenly stopping traffic, possibly creating a

Table 25. Minimum and average reliability indices (all regions).

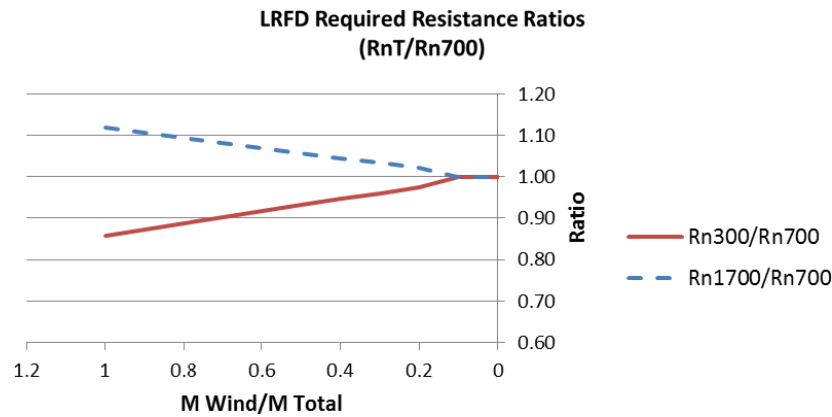
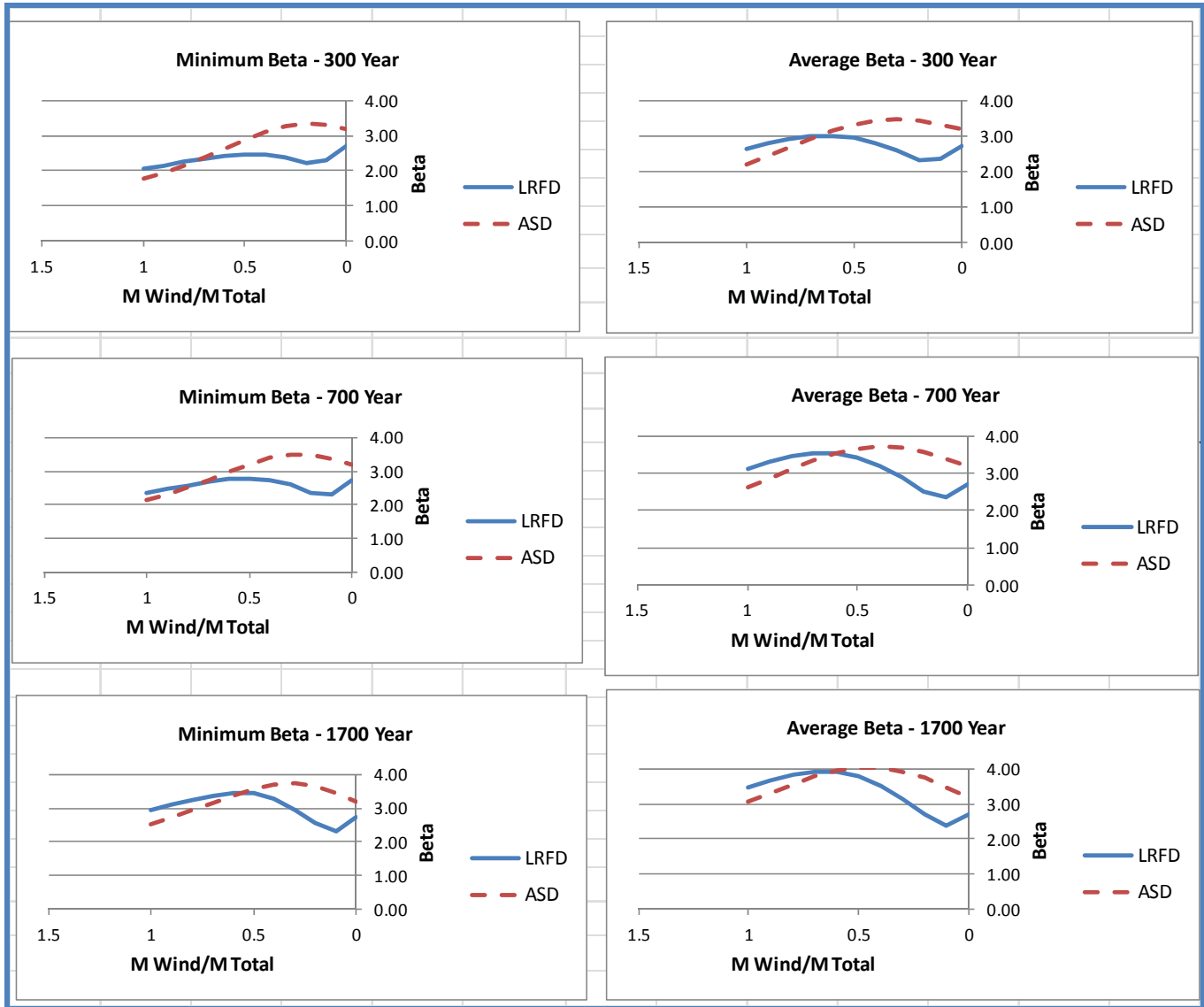


Figure 3. Resistance ratios for different return periods.

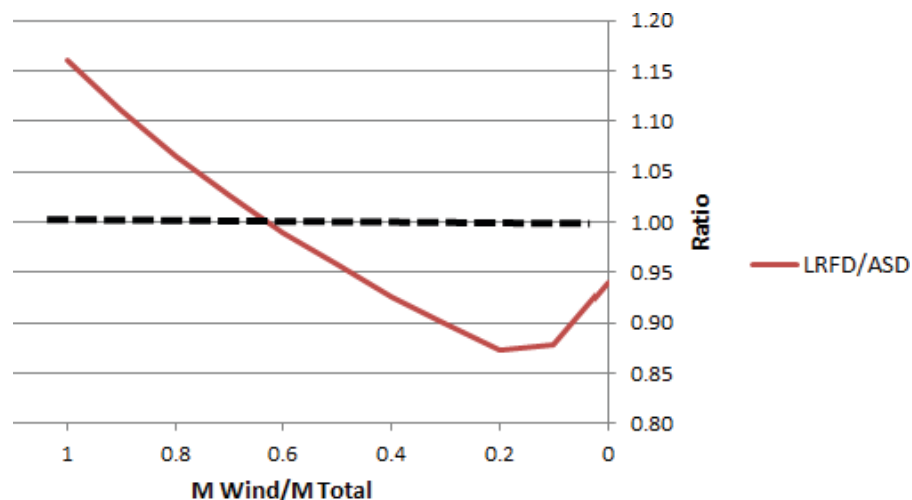


Figure 4. Resistance ratios LRFD versus ASD.

situation conducive to a traffic collision with the structure or a chain-reaction impact of vehicles.

Ultimately, judgment is used to set the target reliability indices for the different applications. The target reliability index ( $\beta$ ) is often based on typical average performance under the previous design specifications (i.e., ASD). However, even in the ASD methods, an importance factor was considered: 0.87 and 1.15 for less important and more important applications, respectively. Some variations were also considered for hurricane versus non-hurricane regions.

There were similar concerns for the LRFD-LTS specifications' assignment of the MRI considered for design. Less important structures are assigned an MRI of 300 years, while an important structure uses an MRI of 1,700 years. Typical structures are assigned an MRI of 700 years.

The description of this implementation is provided next with the resulting reliability indices for each region.

### Implementation into Specifications

The possible structure locations were divided into two primary categories:

1. Failures where a structure is likely to cross the travelway and, within those structures, those that are located on a typical travelway versus a lifeline travelway, which are those that are critical for emergency use/egress; and
2. Failures where a structure cannot cross the travelway and that, consequently, are of lesser importance.

Within these categories, the ADT is used to further distinguish the consequence of failure. The traffic speed was initially considered in the research but was not used in the final report based on simplicity and judgment. Table 26 summarizes this approach.

From this design approach, Table 26 establishes the MRI and directs the user to the appropriate wind hazard map, which provides the design wind speed.

### Computed Reliability Indices

Based on the load and resistance statistical characteristics, the reliability indices  $\beta$  are computed for the four regions for a wind-to-total-load ratio of 0.5 and 1.0. The 0.5 ratio is typical of a traffic signal pole, and the 1.0 ratio is typical of a high-mast pole. Other ratios were computed; however, for brevity, only these two are illustrated.

Table 27 illustrates the relationship between Table 26 and the computed values. For example, assume that a structure is located on a travelway with ADT of between 1,000 and 10,000, and a failure could result in a structure crossing the roadway. From Table 26, the MRI is 700. The statistical properties for the 700-year wind in the region of interest (Midwest and Western in this case) are then used to compute  $\beta$ . The computed value of  $\beta = 3.60$  for  $WL/(DL + WL) = 0.5$  is shown in Table 27. Similarly,  $\beta = 3.35$  for the  $WL/(DL + WL) = 1.0$ .

Table 26. MRI related to structure location and consequence of failure.

	Risk Category		
	Typical	High	Low
Traffic Volume	<35	N/A	N/A
ADT < 100	300	1,700	300
100 < ADT ≤ 1,000	700	1,700	300
1,000 < ADT ≤ 10,000	700	1,700	300
ADT > 10,000	1,700	1,700	300
Typical: Support failure could cross travelway.			
High: Support failure could stop a lifeline travelway.			
Low: Support failure could not cross travelway.			
Roadside sign supports: use 10-year MRI.			

**Table 27. Relationship between MRI and computed reliability indices (Midwest and Western Region load ratio = 0.5 and 1.0).**

(Midwest and West) Load Ratio [WL/(DL+WL) = 0.5]			
	Importance		
Traffic Volume	Typical	High	Low
ADT<100	3.03	3.89	3.03
100<ADT≤1000	3.60	3.89	3.03
1000<ADT≤10000	3.60	3.89	3.03
ADT>10000	3.89	3.89	3.03
Typical: Failure could cross travelway			
High: Support failure could stop a life-line travelway			
Low: Support failure could not cross travelway			
Roadway sign supports: use 300 years (Low)			

	Importance		
	Typical	High	Low
Traffic Volume	<35	n/a	n/a
ADT<100	300	1700	300
100<ADT≤1000	700	1700	300
1000<ADT≤10000	700	1700	300
ADT>10000	1700	1700	300
Typical: Failure could cross travelway			
High: Support failure could stop a life-line travelway			
Low: Support failure could not cross travelway			
Roadway sign supports: use 300 years			

(Midwest and West) Load Ratio [WL/(DL+WL) = 1.0]			
	Importance		
Traffic Volume	Typical	High	Low
ADT<100	2.77	3.62	2.77
100<ADT≤1000	3.35	3.62	2.77
1000<ADT≤10000	3.35	3.62	2.77
ADT>10000	3.62	3.62	2.77
Typical: Failure could cross travelway			
High: Support failure could stop a life-line travelway			
Low: Support failure could not cross travelway			
Roadway sign supports: use 300 years (Low)			

Other indices were computed for load ratios in each region. The results are illustrated in Appendix A.

Note that for the same region and location, the load ratio of 0.5 has a higher  $\beta$  than does the ratio of 1.0. This is because the wind-dominated structure will experience a higher load variability (all wind) than one that is 50% dead load. Comparing the same application (cell) across regions, the region with the lower wind variability will have a higher  $\beta$ .

The resulting indices are reasonable for the various applications, and the load and resistance factors were accordingly set. The load factors are summarized in Table 11.

**Sensitivities**

The previous discussion outlined the results of assignment of load and resistance factors and the resulting reliability indices. It is useful to illustrate the sensitivities of these assignments to the resulting reliability indices. The minimum and average values for all regions are used as a demonstration by varying the dead load, wind load, and resistance factors for steel flexure strength and extreme limit states (see Table 28).

Note that an increase in resistance factor  $\phi$  decreases the reliability index  $\beta$ . An increase in load factor  $\gamma$  increases  $\beta$ .

Typical traffic signal structures have load ratios in the region of one-half, while the high-mast poles have very little dead load effect, and ratios are nearer to unity. In Table 28, the area contained within the dotted line indicates the region that is of typical interest.

**Scope of Appendix A**

Appendix A outlines the complex calibration process and includes more detail than the brief description in the main body of the report. Appendix A includes:

- Wind statistic quantification,
- Resistance quantifications,
- Calibration for different actions and interactions, and
- Monte Carlo simulations.

**Calibration Summary**

Judgment must be employed in the calibration regarding the performance of existing structures under the current specifications and setting the target reliability index  $\beta$  for the LRFD-LTS specifications.

Table 28. Sensitivity of the reliability index to load and resistance factors.

Parameters	Minimum $\beta$	Average $\beta$	Resistance Ratio
<b>Baseline</b> $\phi = 0.9$ $\gamma_{\text{dead-only}} = 1.25$ $\gamma_{\text{dead}} = 1.1$ $\gamma_{\text{wind}} = 1.0$	<b>Minimum Beta - 700 Year</b> 	<b>Average Beta - 700 Year</b> 	<b>Required Resistance Ratios (LRFD/ASD)</b> 
$\phi = 0.9$ $\gamma_{\text{dead-only}} = 1.35$ $\gamma_{\text{dead}} = 1.1$ $\gamma_{\text{wind}} = 1.0$	<b>Minimum Beta - 700 Year</b> 	<b>Average Beta - 700 Year</b> 	<b>Required Resistance Ratios (LRFD/ASD)</b> 
$\phi = 0.9$ $\gamma_{\text{dead-only}} = 1.25$ $\gamma_{\text{dead}} = 1.2$ $\gamma_{\text{wind}} = 1.0$	<b>Minimum Beta - 700 Year</b> 	<b>Average Beta - 700 Year</b> 	<b>Required Resistance Ratios (LRFD/ASD)</b> 
$\phi = 0.95$ $\gamma_{\text{dead-only}} = 1.25$ $\gamma_{\text{dead}} = 1.1$ $\gamma_{\text{wind}} = 1.0$	<b>Minimum Beta - 700 Year</b> 	<b>Average Beta - 700 Year</b> 	<b>Required Resistance Ratios (LRFD/ASD)</b> 
$\phi = 1.0$ $\gamma_{\text{dead-only}} = 1.25$ $\gamma_{\text{dead}} = 1.1$ $\gamma_{\text{wind}} = 1.0$	<b>Minimum Beta - 700 Year</b> 	<b>Average Beta - 700 Year</b> 	<b>Required Resistance Ratios (LRFD/ASD)</b> 
$\phi = 0.85$ $\gamma_{\text{dead-only}} = 1.25$ $\gamma_{\text{dead}} = 1.1$ $\gamma_{\text{wind}} = 1.0$	<b>Minimum Beta - 700 Year</b> 	<b>Average Beta - 700 Year</b> 	<b>Required Resistance Ratios (LRFD/ASD)</b> 

The LRFD-LTS specifications were calibrated using the standard ASD-based specifications as a baseline. The variabilities of the loads and resistances were considered in a rigorous manner. The wind loads have higher variabilities than the dead loads. Therefore, a structure with a high wind-to-total-load ratio will require higher resistance and associated resistances compared to ASD. This increase is on the order of 10% for high-mast structures. For structures with a wind-to-total-load ratio of approximately 0.5 to 0.6 (e.g., cantilever structures), the required resistance will not change significantly.

It is important to note that resistance is proportional to section thickness and proportional to the square of the diameter [i.e., a 10% resistance increase may be associated with a 10% increase in thickness (area) or a 5% increase in diameter or area].

The reliability index for the LRFD-LTS specifications is more uniform over the range of load ratios of practical interest than are the current ASD-based specifications.

### Examples

Table 29 illustrates 15 example designs that were used to demonstrate the LRFD-LTS specifications. These problems were solved with the support of Mathcad (Version 15), a popular computer utility program for engineering computations, and are available as a PDF in Appendix C.

Figure 5 provides a typical first page as an example. The problem description is followed by a table of contents showing that section of the report.

**Table 29. Example designs.**

Example No.	Title	Graphic
1	Cantilevered Overhead Sign Support – Truss with Post	
2	Traffic Sign Support Structure	
3	High Mast	
4	Monotube Overhead Traffic Signal and Sign Support Bridge	



Table 29. (Continued).

Example No.	Title	Graphic
10	Aluminum Pole Design	
11	Span Wire with Prestressed Concrete Poles	
12	Prestressed Concrete Light Pole	
13	Luminaire Support – Fiber-Reinforced Polymer (FRP)	
14	Street Light Pole – Timber	
15	Road Sign – Timber	

Example 2 Design Review  
**Title:** Traffic Sign Support Structure  
**Location:** Chicago, Illinois  
**Project:** NCHRP 10-80  
**AASHTO Specification:** LTS 2009  
**Initial Date:** October 15, 2010  
**Engineers:** Puckett and Jablin  
**Revision Dates:** n/a                      **Revision abstract:** n/a

**Problem Statement:** A traffic signal pole is located in Chicago, IL. The pole has three signals and adjoining signs. The geometry, signal and sign locations, and weights are provided in the figure below. The pole location is windy and fatigue limit state must be checked. The structure is located on a busy roadway where typical traffic speed limit is 45 mph and the ADT is 5000. The roadway is not a lifeline roadway. Material properties, section data, and geometry are defined below.

---

Contents

**Specification Checks In This Sheet:**

- [Interaction Check at Arm Base](#)
- [Arm Base Weld Check](#)
- [Shear Strength Check at Pole Base](#)
- [Pole Base Plate Check](#)
- [Galloping Fatigue Stress at the Arm Base Weld](#)
- [Natural Wind Fatigue Stress at the Arm Base Weld](#)
- [Truck Gust Fatigue Stress at the Arm Base Weld](#)
- [Galloping Fatigue Stress at the Arm Base Bolts](#)

*Figure 5. Typical problem statement.*

## CHAPTER 4

# Conclusions and Suggested Research

## Conclusions

The AASHTO LRFD-LTS specifications have been written to incorporate:

1. An LRFD approach to design;
2. Improved uniformity of reliability over typical wind load to total load ratios;
3. An organization that has been reformatted so that all sections are consistent;
4. Variable definitions and nomenclature that are located in a consistent manner;
5. Improved-text STD-LTS for possible editorial changes;
6. Updated references, including ASCE/SEI 07-10 wind hazard maps;
7. The latest fatigue research;
8. Inclusion of the most recent U.S. specifications for steel and aluminum;
9. Rigorous calibration;
10. New sections on fabrication, construction, inspection, and asset management;
11. A new appendix on an alternate method for fatigue design;
12. A core element system defined in a new appendix; and
13. Smart flags and environmental definitions that are defined to support the core elements.

Sixteen example designs were developed to demonstrate the LRFD-LTS specifications. These examples address many of the typical systems in use today. Examples are included for all materials.

Finally, calibration is described in a comprehensive appendix. The interested reader or specification committee may find this document of benefit.

## Suggested Research

During the course of the project, the team identified several issues that could use the most attention via research studies. These topics are described in Table 30.

In summary, the LTS community has made significant investment in research over the past decade. Many of the problems that were not well understood just 5 years ago are now much better understood. The LRFD-LTS specifications incorporate much of this work.

## Follow-up Tasks

More work may be required that is not necessarily research. Possible follow-up tasks are:

1. Revise the example problems to illustrate the STD-LTS results for comparison.
2. Perform analysis to determine the cost implications for the transition to LRFD-LTS.
3. Work with T-12 on revisions of the NCHRP work for implementation into agenda items.
4. Review the fatigue resistance differences with T-12, and determine if these need to be addressed in the future (see Appendix E).
5. Develop agenda items to support adoption.
6. Develop presentation materials to support adoption.
7. Answer detailed questions from DOTs after their review of the LRFD-LTS specifications.
8. Support T-12 in maintaining the LRFD-LTS specifications, at least for during initial implementation.
9. Continue support for core element development.
10. Develop short courses or webinars to introduce the LRFD-LTS specifications.

**Table 30. Suggested research.**

<b>Topic/Issue</b>	<b>Description</b>
<b>Fatigue design for luminaire poles less than 55 ft tall</b>	Work by Connor et al. (2012) was focused on high-mast poles. The specifications do not require a fatigue design for poles less than 55 ft tall. There is evidence that fatigue problems persist for shorter poles. Methods are available to address this in a rational manner. CAN/CSA 6 provides a good start in this area.
<b>Dampener testing standard/method</b>	Dampeners have been shown to be effective for several LTS structures. However, there are currently no standardized test procedures to determine whether dampeners work or the degree to which they will decrease stress cycles. Such testing will likely involve using multiple frequencies to establish a response curve to harmonic excitation.
<b>Calibrate fatigue limit state</b>	Connor et al. (2012) suggested wind pressures above average values to be conservative. However, this was not a formal calibration. Similarly, other fatigue loads and resistances have not been calibrated. In Appendix A: Calibration Report, initial work was conducted to combine work by Roy et al. (2011) and high-mast work by Connor et al. (2012) to compute reliability factors. This work should be further extended for all structure types.
<b>Modification of stress concentration factor equation for fatigue</b>	Work by Roy et al. (2011) was comprehensive and provided a host of improved details and assessment methods for determining fatigue resistance. Equation 11.9.3.1-1 and associated $K_F$ are based on empirical curve fits of the data. An approach using a nondimensional parametric approach could be used. This has the advantage that the user can readily observe the behavior associated with the geometry and design decisions.
<b>Aluminum fatigue</b>	Recent work on fatigue resistance [e.g., Roy et al. (2011)] focused on steel connections. Aluminum connections are assigned a reduction of $1/2.6 = 38\%$ . There are some standard pole connections that might benefit from work to determine if this factor is appropriate. If the 55-ft limit is addressed (see top of table), then aluminum poles will be affected. With low fatigue resistance, this might affect the economic viability of those products.
<b>Sign plate removal</b>	With the recent advancement of light-emitting diode (LED) signal lights that have brighter illumination, are sign plates necessary? The removal of the sign plate might be the first step in addressing poles that are expressing dynamic excitation due to wind.
<b>Improving inspection and asset management</b>	The core elements outlined in this report are a start. Continued work will be needed. Software could be developed to support LTS asset management.

# Bibliography

This bibliography also includes all references cited in this report.

- AASHTO. 2002. *Standard Specifications for Highway Bridges*, 17th Edition, HB-17. American Association of State Highway and Transportation Officials, Washington, D.C.
- AASHTO. 2007. *AASHTO Maintenance Manual for Roadways and Bridges*, Fourth Edition, MM-4. American Association of State Highway and Transportation Officials, Washington, D.C.
- AASHTO. 2009. *Standard Specifications for Structural Supports for Highway Signs, Luminaires, and Traffic Signals*, 5th Edition, with 2010 and 2011 Interim Revisions
- AASHTO. 2009. *Manual for Assessing Safety Hardware (MASH)*, First Edition. American Association of State Highway and Transportation Officials, Washington, D.C.
- AASHTO. 2009. *A Policy on Geometric Design of Highways and Streets*, Fifth Edition, GDHS-5. American Association of State Highway and Transportation Officials, Washington, D.C.
- AASHTO. 2010. *Highway Safety Manual*, 1st Edition, HSM-1. American Association of State Highway and Transportation Officials, Washington, D.C.
- AASHTO. 2010. *Roadway Lighting Design Guide*, Sixth Edition, GL-6. American Association of State Highway and Transportation Officials, Washington, D.C.
- AASHTO. 2010. *Manual for Bridge Evaluation*, 2nd Edition with 2013 Interim Revisions. American Association of State Highway and Transportation Officials, Washington, D.C.
- AASHTO. 2011. *Roadside Design Guide*, Fourth Edition, RSDG-3-M. American Association of State Highway and Transportation Officials, Washington, D.C.
- AASHTO. 2011. *AASHTO Guide Manual for Bridge Element Inspection*, 1st Edition. American Association of State Highway and Transportation Officials, Washington, D.C.
- AASHTO. 2012. *Standard Specification for Castings, Iron-Chromium-Nickel, Corrosion Resistant, for General Applications*, M 163. American Association of State Highway and Transportation Officials, Washington, D.C. Available individually in downloadable form; also in *Standard Specifications for Transportation Materials and Methods of Sampling and Testing*, 32nd Edition, HM-32.
- AASHTO. 2012. *Standard Specification for Steel Castings, Carbon, For General Applications*, M 103. American Association of State Highway and Transportation Officials, Washington, D.C. Available individually in downloadable form; also in *Standard Specifications for Transportation Materials and Methods of Sampling and Testing*, 32nd Edition, HM-32.
- AASHTO. 2013. *AASHTO LRFD Bridge Design Specifications*, Sixth Edition. American Association of State Highway and Transportation Officials, Washington, D.C.
- AASHTO. 2013. *Standard Specifications for Transportation Materials and Methods of Sampling and Testing*, 33rd Edition, HM-28. American Association of State Highway and Transportation Officials, Washington, D.C.
- AASHTO-AGC-ARTBA Joint Committee. 1998. *Guide to Small Sign Support Hardware*, Task Force 13 Report, Subcommittee on New Highway Materials, GSSSH-1. American Association of State Highway and Transportation Officials, Association of General Contractor, and American Road and Transportation Builders Association Joint Committee, Washington, D.C.
- AASHTO/FHWA. 2009. *Joint Implementation Plan for the AASHTO Manual for Assessing Hardware*. American Association of State Highway and Transportation Officials, Washington, D.C. (<https://bookstore.transportation.org/imageview.aspx?id=709&DB=3>).
- AASHTO LRFD. 2013. *Bridge Construction Specifications*, Third Edition. American Association of State Highway and Transportation Officials, Washington, D.C.
- ACI. 1995. "Code Requirements for Nuclear Safety Related Concrete Structures," Appendix B, Steel Embedments, ACI 349-90. American Concrete Institute, Farmington Hills, MI.
- ACI. 2011. *Building Code Requirements for Structural Concrete*, ACI 318-2011. American Concrete Institute, Farmington Hills, MI.
- AF & PA. 2012. *National Design Specification for Wood Construction*. American Forest & Paper Products Association, Washington, D.C.
- Ahearn, E. B., and J. A. Puckett. 2010. *Reduction of Wind-Induced Vibrations in High-Mast Light Poles*, Report No. FHWA-WY-10/02F. University of Wyoming, Laramie, WY.
- AISC. 2010. *Steel Construction Manual*, 14th Edition. American Institute of Steel Construction Inc.
- Albert M. N., L. Manuel, K. H. Frank, and S. L. Wood. 2007. *Field Testing of Cantilevered Traffic Signal Structures under Truck-Induced Gust Loads*, Report No. FHWA/TX-07/4586-2. Center for Transportation Research, Texas Department of Transportation, Austin, Texas.
- Aluminum Association. 2009. *Aluminum Standards and Data*. Aluminum Association, Washington, D.C.
- Aluminum Association. 2010. *Aluminum Design Manual 2010*. Aluminum Association, Washington, D.C.

- Amir, G., and A. Whittaker. 2000. "Fatigue-Life Evaluation of Steel Post Structures II: Experimentation," *Journal of Structural Engineering*. American Society of Civil Engineers, Vol. 126, No. 3, Vol. 2 (March 2000), pp. 331–340.
- ASCE. 1985. *Structural Plastics Design Manual*, ASCE Manuals and Reports on Engineering Practice No. 63. American Society of Civil Engineers, New York, NY.
- ASCE. 2010. *Minimum Design Loads for Buildings and Other Structures*, Report no. ASCE/SEI 7-10. American Society of Civil Engineers, Reston, VA.
- ASCE/PCI Joint Committee on Concrete Poles. 1997. "Guide for the Design of Prestressed Concrete Poles—Final Draft," *PCI Journal*. American Society of Civil Engineers and Precast/Prestressed Concrete Institute, Chicago, IL.
- ASCE/SEI Standard 7-10. 2010. "Minimum Design Loads for Buildings and Other Structures." American Society of Civil Engineers, Reston, VA.
- ASM International. 1995. *Engineered Materials Handbook*. ASM International, Materials Park, OH.
- ASTM. 1995. "Standard Specification for General Requirements for Prestressed Concrete Poles Statically Cast," ASTM C 935-80. In *Annual Book of ASTM Standards*. American Society for Testing and Materials, West Conshohocken, PA (withdrawn 2011).
- ASTM. 2001. "Standard Specification for Reinforced Thermosetting Plastic Poles," ASTM D 4923-01. In *Annual Book of ASTM Standards*. American Society for Testing and Materials, West Conshohocken, PA. (withdrawn 2010, no replacement).
- ASTM. 2002. "Standard Practice for Establishing Allowable Properties for Visually Graded Dimension Lumber from In-Grade Test of Full-Size Specimens," ASTM D 1990-00e1. In *Annual Book of ASTM Standards*. American Society for Testing and Materials, West Conshohocken, PA.
- ASTM. 2006. "Standard Practice for Operating Light and Water Exposure Apparatus (Fluorescent UV-Condensation Type) for Exposure of Non-Metallic Materials," ASTM G154-06. In *Annual Book of ASTM Standards*. American Society for Testing and Materials, West Conshohocken, PA.
- ASTM. 2006. "Standard Specification for Spun Cast Prestressed Concrete Poles," ASTM C 1089-98. In *Annual Book of ASTM Standards*. American Society for Testing and Materials, West Conshohocken, PA.
- ASTM. 2007. "Standard Specification for Anchor Bolts, Steel, 36, 55, and 105-kis Yield Strength," ASTM F 1554-07ae1. In *Annual Book of ASTM Standards*. American Society for Testing Materials, West Conshohocken, PA.
- ASTM. 2008. "Standard Test Method for Tensile Properties of Polymer Matrix Composite Materials," ASTM D 3039-08. In *Annual Book of ASTM Standards*. American Society for Testing and Materials, West Conshohocken, PA.
- ASTM. 2009. "Standard Specification for Ductile Iron Castings," ASTM A 536-84(2009). In *Annual Book of ASTM Standards*. American Society for Testing Materials, West Conshohocken, PA.
- ASTM. 2009. "Standard Specification for Ferritic Malleable Iron Castings," ASTM A 47/A 47M-99(2009). In *Annual Book of ASTM Standards*. American Society for Testing Materials, West Conshohocken, PA.
- ASTM. 2009. "Standard Specification for Low-Alloy Steel Deformed and Plain Bars for Concrete Reinforcement," ASTM A 706/A 706M-09b, In *Annual Book of ASTM Standards*. American Society for Testing Materials, West Conshohocken, PA.
- ASTM. 2010. "Standard Test Method for Compressive Properties of Rigid Plastics," ASTM D 695-10. In *Annual Book of ASTM Standards*. American Society for Testing and Materials, West Conshohocken, PA.
- ASTM. 2010. "Standard Test Method for Flexural Properties of Unreinforced and Reinforced Plastics and Electrical Insulating Materials," ASTM D 790-10. In *Annual Book of ASTM Standards*. American Society for Testing and Materials, West Conshohocken, PA.
- ASTM. 2010. "Standard Test Method for Shear Strength of Plastics by Punch Tool," ASTM D 732-10. In *Annual Book of ASTM Standards*. American Society for Testing and Materials, West Conshohocken, PA.
- ASTM. 2010. "Standard Test Method for Tensile Properties of Plastics," ASTM D 638-10. In *Annual Book of ASTM Standards*. American Society for Testing and Materials, West Conshohocken, PA.
- ASTM. 2011. "Standard Practice for Establishing Structural Grades and Related Allowable Properties for Visually Graded Lumber," ASTM D 245-06. In *Annual Book of ASTM Standards*. American Society for Testing and Materials, West Conshohocken, PA.
- ASTM. 2011. "Standard Test Methods for Establishing Clear Wood Strength Values," ASTM D 2555-06. In *Annual Book of ASTM Standards*. American Society for Testing and Materials, West Conshohocken, PA.
- ASTM. 2012. "Standard Specification for Castings, Iron-Chromium, Iron-Chromium-Nickel Corrosion Resistant, for General Industrial Use," ASTM A 743/A 743M-12. In *Annual Book of ASTM Standards*. American Society for Testing Materials, West Conshohocken, PA.
- ASTM. 2012. "Standard Specification for Castings, Steel and Alloy, Common Requirements, for General Industrial Use," ASTM A 781/A 781M-12b. In *Annual Book of ASTM Standards*. American Society for Testing Materials, West Conshohocken, PA.
- ASTM. 2012. "Standard Specification for Deformed and Plain Carbon-Steel Bars for Concrete Reinforcement," ASTM A 615/A 615M-12. In *Annual Book of ASTM Standards*. American Society for Testing Materials, West Conshohocken, PA.
- ASTM. 2012. "Standard Specification for Gray Iron Castings," ASTM A 48/A 48M-03(2012). In *Annual Book of ASTM Standards*. American Society for Testing Materials, West Conshohocken, PA.
- ASTM. 2012. "Standard Methods for Establishing Design Stresses for Round Timber Piles," ASTM D 2899-12. In *Annual Book of ASTM Standards*. American Society for Testing and Materials, West Conshohocken, PA.
- ASTM. 2012. "Standard Specification and Test Method for Establishing Recommended Design Stresses for Round Timber Construction Poles," ASTM D 3200-74. In *Annual Book of ASTM Standards*. American Society for Testing and Materials, West Conshohocken, PA.
- ASTM. 2012. "Standard Specifications for Round Timber Piles," ASTM D 2899-12. In *Annual Book of ASTM Standards*. American Society for Testing and Materials, West Conshohocken, PA.
- AWPA. 2003. *Book of Standards 2003*. American Wood Protection Association (formerly the American Wood Preservers' Association), Birmingham, AL.
- AWC. 2012. National Design Specification (NDS) for Wood Construction, American Wood Council, Leesburg, VA.
- AWS. 1996. *Structural Welding Code-Steel*, ANSI/AWS D1.1-96. American Welding Society, Miami, FL.
- AWS. 2008. *Structural Welding Code-Aluminum*, ANSI/AWS D1.2/D1.2M:2008. American Welding Society, Miami, FL.
- Barker, M., and J. A. Puckett. 2013. *Design of Highway Bridges—An LRFD Approach*, Third Edition. Wiley, New York, NY.
- Barbero, E. J., and I. G. Raftoyiannis. 1993. "Local Buckling of FRP Beams and Columns," *Journal of Materials in Civil Engineering*.

- American Society of Civil Engineers, New York, NY, Vol. 5, No. 3 (August 1993).
- Barbero, E. J., and R. A. Ritchey. 1993. "A Universal Design Equation for FRP Columns." Paper presented at the 48th Annual Conference, Composites Institute, Cincinnati, OH, February 8–11, 1993. The Society of the Plastics Industry, Inc., Washington, D.C.
- Bronstad, M. E., and J. D. Michie. 1974. *NCHRP Report 153: Recommended Procedures for Vehicle Crash Testing of Highway Appurtenances*. TRB, National Research Council, Washington, D.C.
- Changery M. J., E. Simiu, and J. J. Filliben. 1979. "Extreme Wind Speeds at 129 Stations in the Contiguous United States," Building Science Series, Vol. 118.
- Connor, R. J., S. H. Collicott, A. M. DeSchepper, R. J. Sherman, and J. A. Ocampo. 2012. *NCHRP Report 718: Fatigue Loading and Design Methodology for High-Mast Lighting Towers*, Transportation Research Board of the National Academies, Washington, D.C.
- Cook, R. A., D. Bloomquist, A. M. Agosta, and K. F. Taylor. 1996. *Wind Load Data for Variable Message Signs*, Report No. FL/DOT/RMC/0728-9488. University of Florida, Gainesville, FL. Report prepared for Florida Department of Transportation.
- Creamer, B. M., K. G. Frank, and R. E. Klingner. 1979. *Fatigue Loading of Cantilever Sign Structures from Truck Wind Gusts*, Report No. FHWA/TX-79/10+209-1F. Center for Highway Research, Texas State Department of Highways and Public Transportation, Austin, TX.
- CSA. 2006. *Canadian Highway Bridge Design Code*, CAN/CSA S6-06, A National Standard of Canada, Canadian Standards Association and Standards Council of Canada, Mississauga, Ontario, Canada.
- Dexter, R. J., and K. W. Johns. 1998. *Fatigue-Related Wind Loads on Highway Support Structures: Advanced Technology for Large Structural Systems*, Report No. 98-03. Lehigh University, Bethlehem, PA.
- Dexter, R., and M. Ricker. 2002. *NCHRP Report 469: Fatigue-Resistant Design of Cantilever Signal, Sign, and Light Supports*. TRB, National Research Council, Washington, D.C.
- Ellingwood, B. 1981. "Wind and Snow Load Statistics for Probabilistic Design." *J. Struct. Div.*, ASCE, 107(7), 1345–1349.
- Ellingwood, B., T. V. Galambos, J. G. McGregor, and C. A. Cornell. 1980. "Development of a Probability Based Load Criterion for American National Standard A58," NBS Special Report 577, U.S. Department of Commerce, National Bureau of Standards.
- FHWA. 2009. *Manual on Uniform Traffic Control Devices*, 2009 Edition of MUTCD, Revision 3. Federal Highway Administration, U.S. Department of Transportation, Washington, D.C.
- Fisher, J. W., A. Nussbaumer, P. B. Keating, and B. T. Yen. 1993. *NCHRP Report 354: Resistance of Welded Details Under Variable Amplitude Long-Life Fatigue Loading*. TRB, National Research Council, Washington, D.C.
- Florea M. J., L. Manuel, K. H. Frank, and S. L. Wood. 2007. *Field Tests and Analytical Studies of the Dynamic Behavior and the Onset of Galloping in Traffic Signal Structures*, Report No. FHWA/TX-07/4586-1. Center for Transportation Research, Texas Department of Transportation, Austin, Texas.
- Fouad, F., J. S. Davidson, N. Delatte, E. A. Calvert, S.-E. Chen, E. Nunez, and R. Abdalla. 2003. *NCHRP Report 494: Structural Supports for Highway Signs, Luminaires, and Traffic Signals*. Transportation Research Board of the National Academies, Washington, D.C.
- Hosking, J. R. M. and J. R. Wallis 1987. "Parameter and Quantile Estimation for the Generalized Pareto Distribution," *Technometrics*, Vol. 29, No. 3, pp. 339–349.
- Jirsa, et al. 1984. Strength and Behavior of Bolt Installations Anchored in Concrete Piers, Report No. FHWA/TX-85/51+305-1F. Texas State Department of Highways and Public Transportation, Austin, TX.
- Johnson, A. F. 1985. "Design of RP Cylinders under Buckling Loads." Paper presented at the 40th Annual Conference, Reinforced Plastics/Composites Institute, Atlanta, GA, January 28–February 1, 1985, the Society of the Plastics Industry, Inc., Washington, D.C.
- Jones, K. F. 1996. *Ice Accretion in Freezing Rain*, CRREL Report 96-2. [http://www.crrel.usace.army.mil/techpub/CRREL\\_Reports/reports/CR96\\_02.pdf](http://www.crrel.usace.army.mil/techpub/CRREL_Reports/reports/CR96_02.pdf).
- Jones, K. F. 1998. "A Simple Model for Freezing Rain Ice Loads," Atmospheric Research, Elsevier, Hanover, USA, Vol. 46, pp. 87–97, <ftp://ftp.crrel.usace.army.mil/pub/outgoing/kjones/SimpleModel.pdf>.
- Jones, K. F. and H. B. White. 2004. "The Estimation and Application of Extremes," Electrical Transmission in a New Age, Omaha, ASCE, Reston, Virginia, pp. 32–47, <ftp://ftp.crrel.usace.army.mil/pub/outgoing/kjones/ETNAJonesandWhite.pdf>.
- Jones, K. F., R. Thorkildson, and N. Lott. 2002. "The Development of a U.S. Climatology of Extreme Ice Loads," National Climatic Data Center Technical Report No. 2002-01.
- Jones, K. F., R. Thorkildson, and N. Lott. 2002. "The Development of the Map of Extreme Ice Loads for ASCE Manual 74," Electrical Transmission in a New Age, Omaha, ASCE, Reston, Virginia, pp. 9–31, <ftp://ftp.ncdc.noaa.gov/pub/data/techrpts/tr200201/tr2002-01.pdf>.
- Kaczinski, M. R., R. J. Dexter, and J. P. Van Dien. 1998. *NCHRP Report 412: Fatigue Resistant Design of Cantilevered Signal, Sign and Light Supports*. TRB, National Research Council, Washington, D.C.
- Koenigs, M. T., T. A. Botros, D. Freytag, and K. H. Frank. 2003. *Fatigue Strength of Signal Mast Arm Connections*, Report No. FHWA/TX-04/4178-2. Center for Transportation Research, Texas Department of Transportation, Austin, TX.
- Lott, N. and K. F. Jones. 1998. "Using U.S. Weather Data for Modeling Ice Loads from Freezing Rain," Proceedings of the 8th International Workshop on Atmospheric Icing of Structures, Iceland.
- McDonald, J. R., et al. 1995. *Wind Load Effects on Signals, Luminaires and Traffic Signal Structures*, Report No. 1303-1F. Wind Engineering Research Center, Texas Tech University, Lubbock, TX.
- Michie, J. D. 1981. *NCHRP Report 230: Recommended Procedures for the Safety Performance Evaluation of Highway Appurtenances*. TRB, National Research Council, Washington, D.C.
- Miner, M. A. 1945. "Cumulative Damage in Fatigue," *J. Appl. Mech.*, 12. NOAA. 2010. *Comparative Climatic Data for the United States Through 2010*, National Climatic Data Center, Asheville, NC.
- Nowak, A. S. 1999. "Calibration of LRFD Bridge Design Code," NCHRP Report 368, Transportation Research Board, National Academy Press, Washington D.C.
- Nowak, A. S. and K. R. Collins. 2000. "Reliability of Structures," McGraw-Hill International Editions, Civil Engineering Series, Singapore.
- PCI. 2010. *PCI Design Handbook—Precast and Prestressed Concrete*, Seventh Edition. Precast/Prestressed Concrete Institute, Chicago, IL.
- Peterka, J. A. 1992. "Improved Extreme Wind Prediction for the United States," *Journal of Wind Engineering and Industrial Aerodynamics*, Elsevier, Amsterdam, the Netherlands, Vol. 41, pp. 533–541.
- Peterka, J. A. and S. Shahid. 1998. "Design Gust Wind Speeds in the United States," *Journal of Structural Engineering*, Vol. 124, pp. 207–214.
- RCSC. 2004. Specification for Structural Joints Using ASTM A325 or A490 Bolts. Research Council on Structural Connections, Chicago, IL.

- Ross, H. E. 1995. "Evolution of Roadside Safety." In *Transportation Research Circular 435: Roadside Safety Issues*. TRB, National Research Council, Washington, D.C.
- Ross, H. E., D. L. Sicking, R. A. Zimmer, and J. D. Michie. 1993. *NCHRP Report 350: Recommended Procedures for the Safety Performance Evaluation of Highway Features*. TRB, National Research Council, Washington, D.C.
- Roy, S., Y. C. Park, R. Sause, J. W. Fisher, and E. K. Kaufmann. 2011. *NCHRP Web Only Document 176: Cost-Effective Connection Details for Highway Sign, Luminaire, and Traffic Signal Structures*. Final Report for NCHRP Project 10-70. Transportation Research Board of the National Academies, Washington, D.C.
- Stam, A., N. Richman, C. Pool, C. Rios, T. Anderson, and K. Frank. 2011. *Investigation of the Fatigue Life of Steel Base Plate to Pole Connections for Traffic Structures*. Center for Transportation Research Technical Report 9-1526-1 Austin, TX.
- Slaughter, W. S., N. A. Fleck, and B. Budiansky. 1993. "Compressive Failure of Fiber Composites: The Roles of Multiaxial Loading and Creep," *Journal of Engineering Materials and Technology*. American Society of Mechanical Engineers, New York, NY, Vol. 115.
- Vickery, P. J., and Waldhera, D. 2008. "Development of design wind speed maps for the Caribbean for application with the wind load provisions of ASCE 7," ARA Rep. No. 18108-1. Pan American Health Organization, Regional Office for The Americas World Health Organization, Disaster Management Programme, 525 23rd Street NW, Washington, D.C.
- Vickery, P. J., Wadhera, D., Galsworthy, J., Peterka, J. A., Irwin, P. A., and Griffis, L. A. 2010. "Ultimate Wind Load Design Gust Wind Speeds in the United States for Use in ASCE-7," *Journal of Structural Engineering*, Vol. 136, pp. 613–625.
- Vickery, P. J., Wadhera, D., Powell, M. D., Chen, Y. 2009a. "A Hurricane Boundary Layer and Wind Field Model for Use in Engineering Applications," *Journal of Applied Meteorology and Climatology*, Vol. 48, Issue 2, p. 381.
- Vickery, P. J., Wadhera, D., Twisdale, L. A., Lavelle, F. M. 2009b. "U.S. Hurricane Wind Speed Risk and Uncertainty," *Journal of Structural Engineering*, Vol. 135, pp. 301–320.
- Wang, Q. J. 1991. "The POT Model Described by the Generalized Pareto Distribution with Poisson Arrival Rate," *Journal of Hydrology*, Vol. 129, pp. 263–280.
-

## APPENDIX A

## Calibration Report

## CONTENTS

<b>Section 1. Introduction.....</b>	<b>A-3</b>
Appendix Context.....	A-3
Scope .....	A-3
Appendix Organization.....	A-3
<b>Section 2. Load Model .....</b>	<b>A-5</b>
Dead Load Parameters.....	A-5
Wind Speed Statistical Parameters.....	A-5
Information from ASCE/SEI 7-10 and Available Literature.....	A-5
Statistical Parameters for Wind Load Variables .....	A-5
Development of Statistical Parameters for Wind Speed.....	A-6
Conclusions.....	A-9
<b>Section 3. Ice Load Parameters.....</b>	<b>A-10</b>
Information from ASCE/SEI 7-10 and Available Literature.....	A-10
Development of Statistical Parameters for Uniform Radial Ice Thickness....	A-10
Conclusions.....	A-12
<b>Section 4. Correlation Between Ice Thickness and Concurrent 3-s Gust Wind.....</b>	<b>A-19</b>
Information from ASCE/SEI 7-10 and Available Literature.....	A-19
Possible Combination of Uniform Radial Ice Thickness and Concurrent 3-s Gust Speeds .....	A-19
Conclusions.....	A-19
Secondary Analysis for Wind on Ice .....	A-20
Conclusion .....	A-20
<b>Section 5. Resistance Model .....</b>	<b>A-26</b>
Statistical Parameters of Resistance .....	A-26
Conclusion .....	A-26
<b>Section 6. Fatigue Resistance for High-Mast Luminaires .....</b>	<b>A-28</b>
Background.....	A-28
Stress Range Versus Number of Cycles Relationship from Test Results.....	A-28
Stress Range Versus Number of Cycles Relationship for Infinite Life .....	A-28
Statistical Parameters for Resistance.....	A-29
Reliability Analysis for Fatigue Limit State.....	A-29
Conclusions.....	A-40

<b>Section 7. Reliability Analysis</b> .....	<b>A-45</b>
LRFD Reliability Analysis—Flexure .....	A-45
Flexural Resistance .....	A-45
Load.....	A-45
Reliability Indices .....	A-47
Implementation.....	A-47
ASD Reliability Analysis—Flexure.....	A-48
Resistance.....	A-49
Implementation.....	A-50
Calibration and Comparison .....	A-51
LRFD Reliability Analysis—Torsion .....	A-51
Strength.....	A-51
Load.....	A-53
Implementation.....	A-53
ASD Reliability Analysis—Torsion .....	A-53
Strength.....	A-53
Implementation.....	A-54
Calibration and Comparison .....	A-54
LRFD Flexure-Shear Interaction.....	A-55
Monte Carlo Moment/Shear Interaction Simulation.....	A-56
<b>Section 8. Implementation</b> .....	<b>A-58</b>
Setting Target Reliability Indices.....	A-58
Implementation into Specifications .....	A-58
Computed Reliability Indices.....	A-58
Sensitivities .....	A-59
<b>Section 9. Summary</b> .....	<b>A-64</b>
<b>Annex A</b> .....	<b>A-65</b>
<b>Annex B</b> .....	<b>A-69</b>

## SECTION 1

# Introduction

### Appendix Context

The research for NCHRP Project 10-80 required several integrally linked activities:

- Assessment of existing literature and specifications,
- Organization and rewriting the LRFD-LTS specifications,
- Calibration of the load and resistance factors, and
- Development of comprehensive examples illustrating the application of LRFD-LTS specifications.

The purpose of this appendix is to provide the details regarding the calibration process and results. This appendix is intended for those who are especially interested in the details of the process.

The draft LRFD-LTS specifications are being published by AASHTO. In addition, Appendix C provides a series of example problems that illustrate the application of the LRFD-LTS specifications.

### Scope

The LRFD-LTS specifications consider the loads for design presented in Table 1-1.

The combinations considered are based on either judgment or experience and are illustrated in Table 1-2. The proposed load factors are shown.

The Strength I limit state for dead load only (Comb. 1) was calibrated. The Strength I limit state for dead load and live load was considered a minor case and may control only for components that support personnel servicing the traffic devices (Comb. 2). The live load factor based on ASCE/SEI 7-10 was used directly and not studied within the present calibration.

The Extreme I limit state combines dead loads with wind loads (Comb. 4). This is an important limit state. This combination was a strength limit in the ASD LTS specification. The combination is termed “extreme” because ASCE/SEI 7-10 uses

new wind hazard maps that are associated with a unit load factor. (Note that a unit load factor is also used for seismic events, which are definitely considered extreme events.) Therefore, in the LRFD-LTS specifications, the term “extreme” is used.

The Extreme I limit state that combines dead load, wind, and ice (Comb. 5) was studied in detail, and it was determined that it will not be critical in the vast majority of cases, and in the few cases where it will be critical, it is close to the dead load combined with wind (Comb. 4).

The Service I and III limit states were not calibrated, and the same factors that were used in the previous ASD-based specifications were used.

The Fatigue I limit is often critical depending on the connection details. Significant work has been conducted on the fatigue performance of LTS connections (Connor et al., 2012, and Roy et al., 2011). The recommendations of the researchers of those projects were used without further calibration.

In the case of high-mast towers, recent research for connection resistance (Roy et al., 2011) and load effects for vortex shedding and along wind vibrations combined (Connor et al., 2012) was used to determine reliability indices for those structures. These data might be used in the future to change load or resistance factors for high-mast towers. In the meantime, this new methodology provides a roadmap for the fatigue limit-state calibration. Also note that improved detailing for new designs is considered economical, and therefore, any savings associated with decreasing loads might be considered minimal in these cases.

### Appendix Organization

This appendix begins by characterizing the dead and wind loads in Section 2. Here, the mean, bias, and variances are established. The ice load parameters are examined in Section 3.

Information from the previous sections is used to examine the wind-on-ice combination in Section 4. The resistance

**Table 1-1. LRFD-LTS loads.**

Load	Abbrev.	Description	Limit State
Dead load components	DC	Gravity	Strength
Live load	LL	Gravity (typically service personnel)	Strength
Wind	W	Lateral load	Extreme
Ice	IC	Gravity	Strength
Wind on ice	WI	Lateral	Extreme
Truck gust	TrG	Vibration	Fatigue
Natural wind gust	NWG	Vibration	Fatigue
Vortex-induced vibration	VIV	Vibration	Fatigue
Combined wind on high-mast towers	HMT	Vibration	Fatigue
Galloping-induced vibration	GIV	Vibration	Fatigue

**Table 1-2. Limit states considered in the LRFD-LTS specifications.**

Comb. No.	Limit State	Calibrated?	Permanant	Transient			Fatigue (loads applied separately)				
				LL	W	IC	TrG	NWG	VIV	HMT	GIV
			DC								
1	Strength I	Yes	1.25								
2	Strength I	No	1.25	1.6							
3	Strength I	Yes	1.1/0.9								
4	Extreme I	Yes	1.1/0.9		1.0						
5	Extreme I	Studied in detail	X		X	X					
6	Service I	No	1.0		1.0						
7	Service III	No	1.0		1.0						
8	Fatigue I	No, except for HMT					1.0	1.0	1.0	1.0	1.0
9	Fatigue II	No					1.0	1.0	1.0	1.0	1.0

model is provided in Section 5. Sections 2 to 5 provide the necessary prerequisite information for conducting the reliability analysis in Section 7 and calibrating the strength limit state. Section 8 illustrates the implementation of the reliability analysis for the specifications.

Section 6 addresses the reliability analysis for the fatigue limit state for high-mast luminaires. This section may be skipped if the reader is only interested in the strength limit state.

Finally, the calibration is summarized in Section 9.

Annexes are provided for a variety of data used in this study.

## SECTION 2

## Load Model

**Dead Load Parameters**

Dead load (DC) is the weight of structural and permanently attached nonstructural components. Variation in the dead load, which affects statistical parameters of resistance, is caused by variation of the gravity weight of materials (concrete and steel), variation of dimensions (tolerances in design dimensions), and idealization of analytical models. The bias factor (ratio of mean to nominal) value of dead load is  $\lambda = 1.05$ , with a coefficient of variation (Cov) = 0.10 for cast-in-place elements, and  $\lambda = 1.03$  and Cov = 0.08 for factory-made members. The assumed statistical parameters for dead load are based on the data available in the literature (Ellingwood, 1981 and Nowak, 1999).

**Wind Speed Statistical Parameters****Information from ASCE/SEI 7-10 and Available Literature**

According to the ASCE/SEI 7-10, the basic wind speed ( $V$ ) used in the determination of design wind load on buildings and other structures should be determined from maps included in the ASCE/SEI 7-10 (Fig. 26.5-1), depending on the risk category, with exceptions as provided in Section 26.5.2 (special wind regions) and 26.5.3 (estimation of basic speeds from regional climatic data).

For Risk Category II, it is required to use the map of wind speed  $V_{700}$  (Fig. 26.5-1A), corresponding to an approximately 7% probability of exceedance in 50 years (annual exceedance probability = 0.00143, MRI = 700 years).

For Risk Categories III and IV, it is required to use the map of wind speed  $V_{1700}$  (Fig. 26.5-1B), corresponding to an approximately 3% probability of exceedance in 50 years (annual exceedance probability = 0.000588, MRI = 1,700 years).

For Risk Category I, it is required to use the map of wind speed  $V_{300}$  (Fig. 26.5-1C), corresponding to an approximately

15% probability of exceedance in 50 years (annual exceedance probability = 0.00333, MRI = 300 years).

The basic wind speeds in ASCE/SEI 7-10 (Fig. 26.5-1) are based on the 3-s gust wind speed map. The non-hurricane wind speed is based on peak gust data collected at 485 weather stations where at least 5 years of data were available (Peterka, 1992; Peterka and Shahid, 1998). For non-hurricane regions, measured gust data were assembled from a number of stations in state-sized areas to decrease sampling error, and the assembled data were fit using a Fisher-Tippett Type I extreme value distribution. The hurricane wind speeds on the United States Gulf and Atlantic coasts are based on the results of a Monte Carlo simulation model described in Applied Research Associates (2001), Vickery and Waldhera (2008), and Vickery et al. (2009a, 2009b, and 2010).

The map presents the variation of 3-s wind speeds associated with a height of 33 ft (10 m) for open terrain (Exposure C). Three-second gust wind speeds are used because most National Weather Service stations currently record and archive peak gust wind (see Table 2-1).

**Statistical Parameters for Wind Load Variables**

The wind pressure is computed using the following formula:

$$P_z = 0.0256 \cdot K_z \cdot K_d \cdot G \cdot V^2 \cdot C_d \text{ (psf)}$$

where:

- $V$  = basic wind speed, mph,
- $K_z$  = height and exposure factor,
- $K_d$  = directionality factor,
- $G$  = gust effect factor, and
- $C_d$  = drag coefficient.

The parameters  $V$ ,  $K_z$ ,  $K_d$ ,  $G$ , and  $C_d$  are random variables, and the distribution function of wind pressure and the wind load

**Table 2-1. Summary of the wind speeds from the maps in ASCE/SEI 7-10 (Fig. 26.5-1).**

Location	V <sub>10</sub> (mph)	V <sub>50</sub> (mph)	V <sub>300</sub> (mph)	V <sub>700</sub> (mph)	V <sub>1700</sub> (mph)
Alaska 1	78	90	105	110	115
Alaska 2	78	100	110	120	120
Alaska 3	90	110	120	130	130
Alaska 4	100	120	130	140	150
Alaska 5	100	120	140	150	160
Alaska 6	113	130	150	160	165
Central USA	76	90	105	115	120
West Coast	72	85	100	110	115
Coastal Segment 1	76	90	105	115	120
Coastal Segment 2	76	100	110	120	130
Coastal Segment 3	76	110	120	130	140
Coastal Segment 4	80	120	130	140	150
Coastal Segment 5	80	130	140	150	160
Coastal Segment 6	90	140	150	160	170
Coastal Segment 7	90	140	150	170	180
Coastal Segment 8	90	150	160	170	190
Coastal Segment 9	90	150	170	180	200

statistics are required to determine appropriate probability-based load and load combination factors. The cumulative distribution function of wind speed is particularly significant because  $V$  is squared. However, the uncertainties in the other variables also contribute to the uncertainty in  $P_z$ .

The CDFs for the random variables used to derive the wind load criteria that appear in ASCE/SEI 7-10 are summarized in Table 2-2 (Ellingwood, 1981).

### Development of Statistical Parameters for Wind Speed

The statistical parameters of load components are necessary to develop load factors and conduct reliability analysis. The shape of the CDF is an indication of the type of distribution. For non-hurricane regions, measured gust data were fit using a Fisher-Tippett Type I extreme value distribution (Peterka and Shahid, 1998).

The CDF for the extreme Type I random variable is defined by:

$$F(x) = \exp(-\exp[-\alpha(x-u)])$$

where  $u$  and  $\alpha$  are distribution parameters:

$$\alpha \approx \frac{1.282}{\sigma_x}$$

$$u \approx \mu_x - 0.45\sigma_x$$

and  $\mu_x$  and  $\sigma_x$  are mean value and standard deviation, respectively.

Based on the type of distribution and statistical parameters for annual wind in specific locations, a Monte Carlo simulation was used to determine the statistical parameters of wind speed (Nowak and Collins, 2000). The annual statistical parameters are available from the Building Science Series (Changery et al., 1979). The data set includes 129 locations; 100 locations are from Central United States, and the remaining 29 locations are from other regions. The data set does not include regions of Alaska; however, based on the other locations, analogs are used.

Examples of Monte Carlo simulation are presented on Figures 2-1 to 2-6, with corresponding tables of statistical parameters (see Tables 2-3 to 2-10). Developed parameters for all locations are listed in Annex A.

**Table 2-2. Wind load statistics (Ellingwood, 1981).**

Parameter	Mean/Nominal	Cov	CDF
Exposure factor, $K_z$	1.0	0.16	Normal
Gust factor, $G$	1.0	0.11	Normal
Pressure coefficient, $C_p$	1.0	0.12	Normal

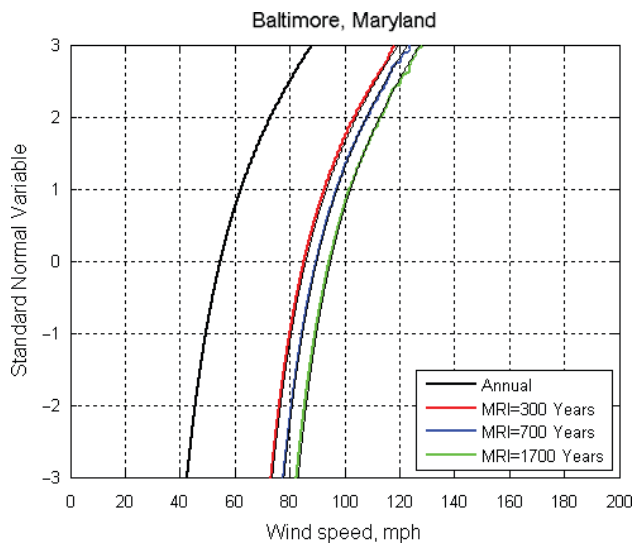


**Figure 2-1.** CDFs for annual and MRI 300, 700, and 1,700 years, for Baltimore, Maryland. (Note: Lines top to bottom in key are left to right in figure.)

**Table 2-3.** Statistical parameters of wind speed for Baltimore, Maryland.

Baltimore, MD	Mean	Cov
Annual	55.9	0.123
300 Years	87	0.080
700 Years	91	0.075
1,700 Years	96	0.070

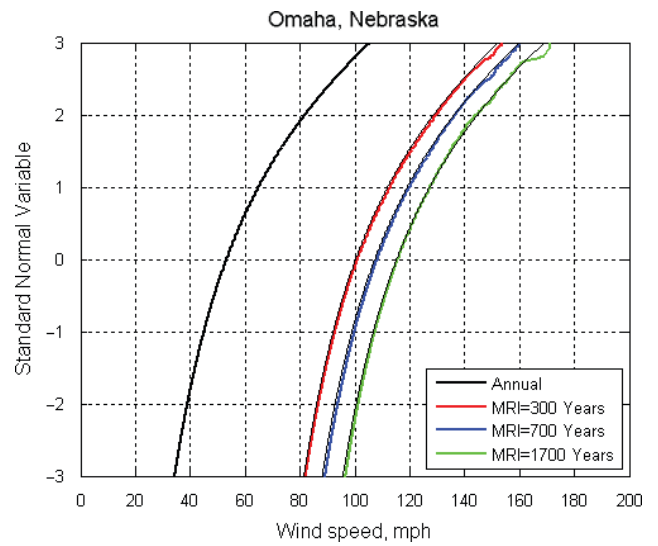


**Figure 2-3.** CDFs for annual and MRI 300, 700, and 1,700 years, for Omaha, Nebraska. (Note: Lines top to bottom in key are left to right in figure.)

**Table 2-5.** Statistical parameters of wind speed for Omaha, Nebraska.

Omaha, NE	Mean	Cov
Annual	55.0	0.195
300 Years	102	0.105
700 Years	109	0.100
1,700 Years	117	0.095

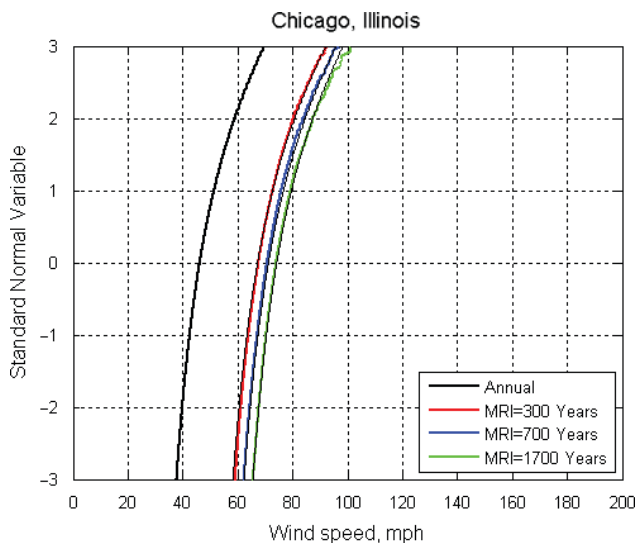


**Figure 2-2.** CDFs for annual and MRI 300, 700, and 1,700 years, for Chicago, Illinois. (Note: Lines top to bottom in key are left to right in figure.)

**Table 2-4.** Statistical parameters of wind speed for Chicago, Illinois.

Chicago, IL	Mean	Cov
Annual	47.0	0.102
300 Years	68	0.075
700 Years	72	0.070
1,700 Years	75	0.066

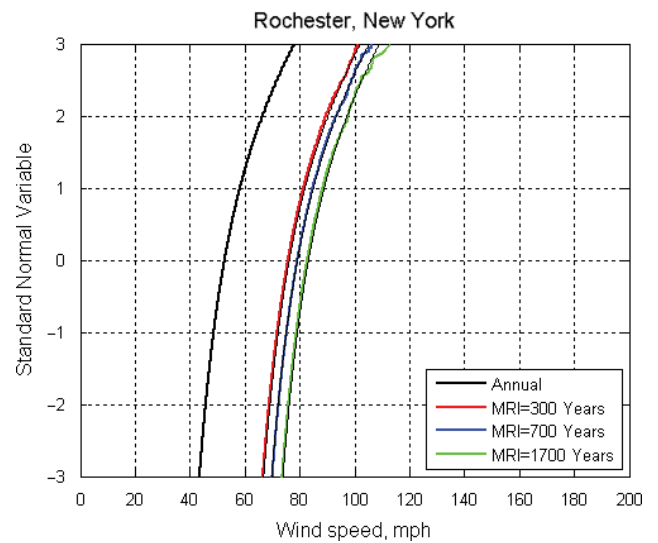


**Figure 2-4.** CDFs for annual and MRI 300, 700, and 1,700 years, for Rochester, New York. (Note: Lines top to bottom in key are left to right in figure.)

**Table 2-6.** Statistical parameters of wind speed for Rochester, New York.

Rochester, NY	Mean	Cov
Annual	53.5	0.097
300 Years	77	0.069
700 Years	80	0.067
1,700 Years	84	0.063

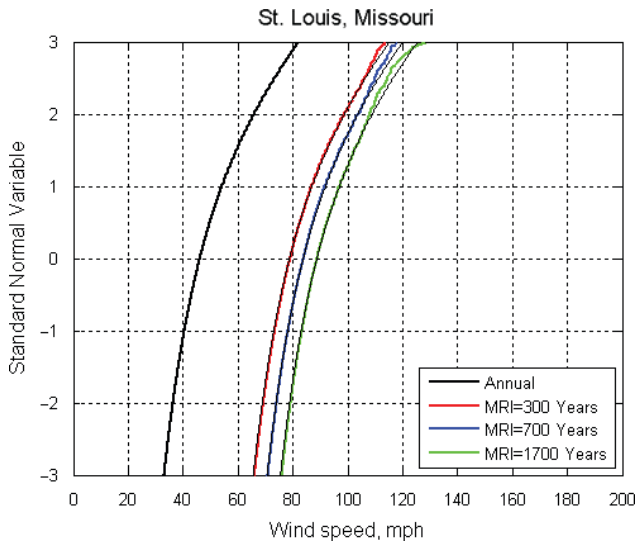


Figure 2-5. CDFs for annual and MRI 300, 700, and 1,700 years, for St. Louis, Missouri. (Note: Lines top to bottom in key are left to right in figure.)

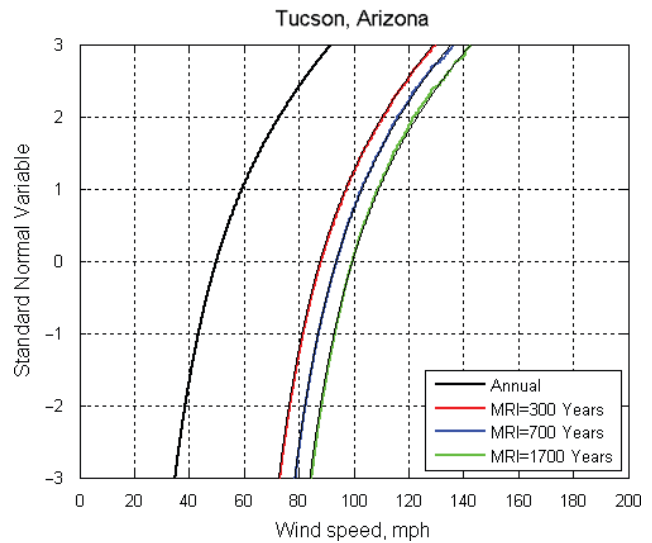


Figure 2-6. CDFs for Annual and MRI 300, 700, and 1,700 years, for Tucson, Arizona. (Note: Lines top to bottom in key are left to right in figure.)

Table 2-7. Statistical parameters of wind speed for St. Louis, Missouri.

St. Louis, MO	Mean	Cov
Annual	47.4	0.156
300 Years	80	0.094
700 Years	85	0.088
1,700 Years	90	0.084

Table 2-8. Statistical parameters of wind speed for Tucson, Arizona.

Tucson, AZ	Mean	Cov
Annual	51.4	0.167
300 years	89	0.096
700 years	95	0.091
1,700 years	101	0.089

Table 2-9. Summaries of statistical parameters of wind speed for Central United States.

	n	Annual			300 Year		700 Year		1,700 Year	
		Mean	Cov	Max	Mean	Cov	Mean	Cov	Mean	Cov
Average	32	52.1	0.144	71.6	85.1	0.088	90.0	0.083	95.2	0.079
Max	48	62.8	0.226	104.0	110.0	0.114	118.0	0.109	127.0	0.104
Min	10	40.9	0.087	53.4	66.0	0.063	69.0	0.060	72.0	0.056

Table 2-10. Summaries of statistical parameters of wind speed for the West Coast.

	n	Annual			300 Year		700 Year		1,700 Year	
		Mean	Cov	Max	Mean	Cov	Mean	Cov	Mean	Cov
Average	30	47.2	0.140	64.8	76.6	0.085	80.9	0.082	85.5	0.077
Max	54	71.5	0.223	104.4	116.0	0.112	123.0	0.108	130.0	0.098
Min	10	34.4	0.080	41.9	50.0	0.060	52.0	0.058	54.0	0.056

The most important parameters are the mean, bias factor, and the coefficient of variation. The bias factor is the ratio of mean to nominal. Mean values were taken as an extreme peak gust wind speed from the literature (Vickery et al., 2010). Bias factors were calculated as follows:

$$\lambda_{50} = \frac{\mu_{50}}{V_{50}} \quad \lambda_{300} = \frac{\mu_{300}}{V_{300}} \quad \lambda_{700} = \frac{\mu_{700}}{V_{700}} \quad \lambda_{1700} = \frac{\mu_{1700}}{V_{1700}}$$

where:

$\mu_{50}, \mu_{300}, \mu_{700}, \mu_{1700}$  = are wind speeds with MRI = 50 years, 300 years, 700 years, and 1,700 years, respectively, taken from maps included in literature (Vickery et al., 2010); and

$V_{50}, V_{300}, V_{700}, V_{1700}$  = are wind speeds with MRI = 50 years, 300 years, 700 years, and 1,700 years, respectively, taken from maps included in ASCE/SEI 7-10.

To find standard deviation of distribution, multiple Monte Carlo simulations were conducted. The results are shown in Figures 2-1 to 2-6. The symbol markers in the graphs represent mean values of wind occurring in a considered period of time. The curves are CDFs of basic wind speed for different MRIs fitted using a Fisher-Tippett Type I extreme value distribution.

## Conclusions

The CDFs of peak gust wind speed were plotted on normal probability paper as the best fit to the statistical parameters available from 129 locations. The distribution for annual wind speed was defined as Fisher-Tippet Type I extreme value distribution (Peterka and Shahid, 1993). Based on the type of distribution and statistical parameters, a Monte Carlo sim-

**Table 2-11. Summary of statistical parameters of 300-year return period peak gust wind speeds.**

Location	$V_{300}$ (mph)	$\lambda_{300} =$ $\mu_{300}/V_{300}$	$Cov_{300}$
Central United States	105	0.80	0.090
West Coast	100	0.75	0.085
Alaska	105 – 150	0.80*	0.095*
Coastal Segments	105 – 170	0.80	0.130

\*Statistical parameters determined by analogy.

**Table 2-12. Summary of statistical parameters of 700-year return period peak gust wind speeds.**

Location	$V_{700}$ (mph)	$\lambda_{700} =$ $\mu_{700}/V_{700}$	$Cov_{700}$
Central United States	115	0.80	0.085
West Coast	110	0.75	0.080
Alaska	110 – 160	0.80*	0.090*
Coastal Segments	115 – 180	0.80	0.125

\*Statistical parameters determined by analogy.

**Table 2-13. Summary of statistical parameters of 1,700-year return period peak gust wind speeds.**

Location	$V_{1700}$ (mph)	$\lambda_{1700} =$ $\mu_{1700}/V_{1700}$	$Cov_{1700}$
Central United States	120	0.80	0.080
West Coast	115	0.75	0.075
Alaska	115 – 165	0.80*	0.085*
Coastal Segments	120 – 200	0.80	0.115

\*Statistical parameters determined by analogy.

ulation was used to determine the statistical parameters of wind speed. For each location, four distributions were plotted: annual, 300 years, 700 years, and 1,700 years. Statistical parameter for 300-year, 700-year, and 1,700-year MRI were used for extreme wind combinations. Recommended values are listed in Tables 2-11 to 2-13.

## SECTION 3

## Ice Load Parameters

**Information from ASCE/SEI 7-10 and Available Literature**

Atmospheric ice loads due to freezing rain, snow, and in-cloud icing have to be considered in the design of ice-sensitive structures. According to ASCE/SEI 7-10, the equivalent uniform radial thickness  $t$  of ice due to freezing rain for a 50-year mean recurrence interval is presented on maps in Figures 10-2 through 10-6 in ASCE/SEI 7-10. The 50-year MRI ice thicknesses shown in ASCE/SEI 7-10 are based on studies using an ice accretion model and local data. The historical weather data were collected from 540 National Weather Service, military, Federal Aviation Administration, and Environment Canada weather stations. The period of record of the meteorological data is typically 20 to 50 years. At each station, the maximum ice thickness and the maximum wind-on-ice load were determined for each storm. Based on maps in ASCE/SEI 7-10, the ice thickness zones in Table 3-1 can be defined.

These ice thicknesses should be used for Risk Category II. For other categories, thickness should be multiplied by the MRI factor. For Risk Category I, it is required to use MRI = 25 years, and for Risk Category III and IV, it is required to use MRI = 100 years. The mean recurrence interval factors are listed in Table 3-2.

Using the mean recurrence interval factor for each zone, the ice thicknesses for different MRIs were calculated and are presented in Table 3-3.

In addition, ice accreted on structural members, components, and appurtenances increases the projected area of the structures exposed to wind. Wind load on this increased projected area should be used in design of ice-sensitive structures. Figures 10-2 through 10-6 in ASCE/SEI 7-10 include 3-s gust wind speeds that are concurrent with the ice loads due to freezing rain. Table 3-4 summarizes the 3-s gust for different localizations across the United States. As opposed to ice thickness, 3-s concurrent gust speed does not have a multiplication factor for different risk categories. The values on the map are the same for each risk category. The statistical

parameters for 3-s concurrent gust speed can be taken as an average of statistical parameters of wind speed.

**Development of Statistical Parameters for Uniform Radial Ice Thickness**

The statistical parameters of load components are necessary to develop load factors and conduct reliability analysis. The shape of the CDF is an indication of the type of distribution.

Extreme ice thicknesses were determined from an extreme value analysis using the peak-over-threshold method and generalized Pareto distribution (GPD) (Hosking and Wallis, 1987, and Wang, 1991). The analysis of the weather data and the calculation of extreme ice thickness are described in more detail in Jones et al. (2002).

Based on the GPD, ice thicknesses for long return periods (Table 3-3), and the probability of being exceeded, a Monte Carlo simulation was used to determine parameters for annual extremes.

The family of GPDs has three parameters:  $k$  – shape,  $\alpha$  – scale, and  $\theta$  – threshold. The typical generalized Pareto probability density function and cumulative distribution function (CDF) are shown in Figures 3-1 and 3-2.

The results of Monte Carlo simulation for annual extremes are shown in Figure 3-2 and Table 3-5. The threshold,  $\theta$ , for each simulation was zero. This means that in some years, the maximum ice thickness is zero, which would have to be considered part of an extreme population in the epochal method. The shape parameter,  $k$ , is constant for each zone because mean recurrence interval factors are the same for each zone.

However, these parameters are for annual events. The design minimum load from ASCE/SEI 7-10 is based on 25-year, 50-year, and 100-year events, depending on risk category. To estimate statistical parameters for these recurrence intervals, additional analyses should be performed. Based on the avail-

**Table 3-1. Ice thickness zones.**

Ice Load Zones	Zone 0	Zone 1	Zone 2	Zone 3	Zone 4	Zone 5	Zone 6
MRI = 50 years	0.00"	0.25"	0.5"	0.75"	1.0"	1.25"	1.5"

**Table 3-2. Mean recurrence interval factors.**

Mean Recurrence Interval	Multiplier on Ice Thickness
25 years	0.80
50 years	1.00
100 years	1.25
200 years	1.50
250 years	1.60
300 years	1.70
400 years	1.80
500 years	2.00
1,000 years	2.30
1,400 years	2.50

able literature, the sample results of annual extremes were found. These data were plotted on normal probability paper to find the most important parameters, such as the mean, bias factor, and coefficient of variation. Bias factor is the ratio of the mean to nominal. The nominal value was taken from Table 3-3, depending on the zone and risk category.

The first group of sample results was found in *CRREL Report 96-2* (Jones, 1996). The results include uniform equivalent radial ice thicknesses hind-cast for the 316 freezing-rain events in 45 years that occurred at Des Moines, Iowa, between 1948 and 1993 (see Figure 3-3).

The second group of sample results was found in research work of Lott and Jones from 1998. The data were recorded from three weather stations in Indiana, south of the Great Lakes in the central region of the United States (in Indianapolis, at Grissom AFB, and in Lafayette). Ice loads from these three stations, presented as uniform radial ice thicknesses calculated by simple model (Jones, 1998), are shown in Figure 3-4. Only episodes with a freezing-rain storm at one

or more of these three stations are shown, with the graphs divided in decades.

The CDFs of the ice thickness were plotted on normal probability paper, as shown in Figures 3-5 through 3-16. The construction and use of normal probability paper can be found in textbooks on probability [e.g., Nowak and Collins (2000)]. Probability paper allows for an easy evaluation of the most important statistical parameters as well as the type of the distribution function. The horizontal axis represents the considered variable; in this case it is the uniform radial ice thickness. The vertical axis is the inverse normal probability, and it is equal to the distance from the mean value in terms of standard deviations. It can also be considered as the corresponding probability of being exceeded. The test data plotted on the normal probability paper can be analyzed by observing the shape of the resulting curve representing the CDF. The annual extremes for each localization as well as the long return periods predicted from ASCE/SEI 7-10 create a curve that characterizes the generalized Pareto distribution. The dashed line in the graphs is related to the corresponding probability of exceedance for 25-year, 50-year, and 100-year returned periods. The points on the graph marked with stars represent extreme events in 25 years, 50 years, and 100 years. These points were calculated by moving the dashed line to the position of the horizontal axis (standard normal variable = 0). The  $x$  coordinate (ice thickness) was treated as a constant, and the  $y$  coordinate (standard normal variable) was recalculated for the new probability of occurrence. Next, the statistical parameters were determined by fitting a straight line to the CDF. The mean value can be read directly from the graph, as the horizontal coordinate of intersection of the CDF. The standard deviation can also be determined by the inverse of the slope of the line.

**Table 3-3. Ice thickness in long return periods.**

Ice Load Zones	Zone 1	Zone 2	Zone 3	Zone 4	Zone 5	Zone 6
Mean Recurrence Interval	Ice Thicknesses, in.					
25 years	0.20	0.40	0.60	0.80	1.00	1.20
<b>50 years</b>	<b>0.25</b>	<b>0.50</b>	<b>0.75</b>	<b>1.00</b>	<b>1.25</b>	<b>1.50</b>
100 years	0.31	0.63	0.94	1.25	1.56	1.88
200 years	0.38	0.75	1.13	1.50	1.88	2.25
250 years	0.40	0.80	1.20	1.60	2.00	2.40
300 years	0.43	0.85	1.28	1.70	2.13	2.55
400 years	0.45	0.90	1.35	1.80	2.25	2.70
500 years	0.50	1.00	1.50	2.00	2.50	3.00
1,000 years	0.58	1.15	1.73	2.30	2.88	3.45
1,400 years	0.63	1.25	1.88	2.50	3.13	3.75

**Table 3-4. 3-s gust speed concurrent with the ice loads.**

Gust Speed Zones	V <sub>50</sub> (mph)	Cov	σ (mph)
Zone 1	30	0.15	4.5
Zone 2	40	0.15	6.0
Zone 3	50	0.15	7.5
Zone 4	60	0.15	9.0
Zone 5	70	0.15	10.5
Zone 6	80	0.15	12

**Conclusions**

The CDFs of ice thicknesses recorded in four weather stations were plotted on normal probability paper for a better interpretation of the results. Then, the statistical parameters were calculated for different localizations and for different recurrence intervals. The average of coefficient of variation and bias factor can be used as statistical parameters for uniform ice thickness (see Table 3-6). However, the analysis is based on the limited database available in the literature. It is recommended to expand the database and verify the statistical parameters in the future.

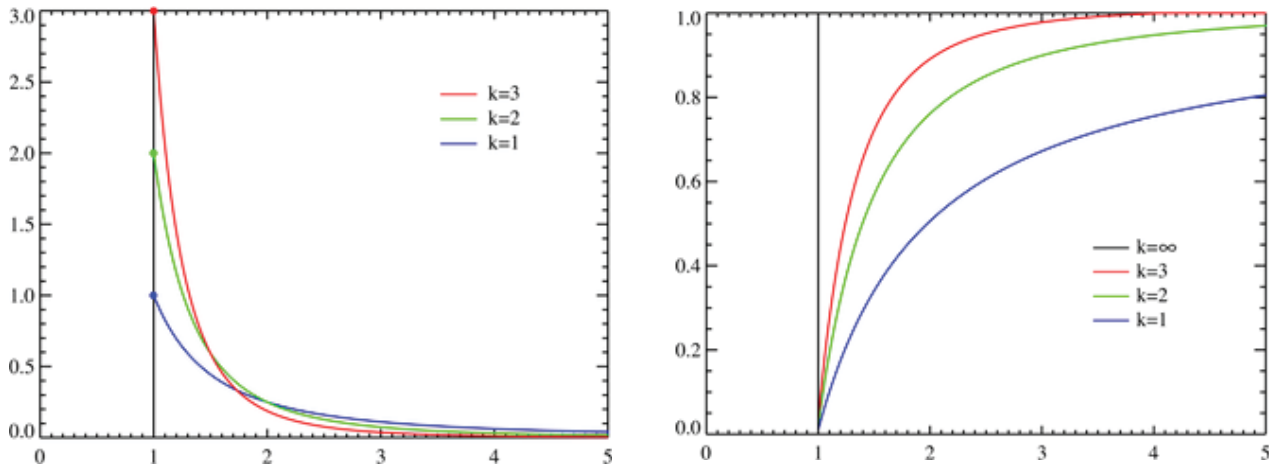


**Figure 3-1. Generalized Pareto probability density function, PDF  $f(x) = \frac{1}{\sigma} (1 + k \cdot z)^{-1/k+1}$  and generalized Pareto cumulative distribution function, CDF  $F(x) = 1 - (1 + k \cdot z)^{-1/k}$ . (Note: Key for left portion of figure corresponds to top to bottom in the graph; key for right portion of figure is left to right.)**

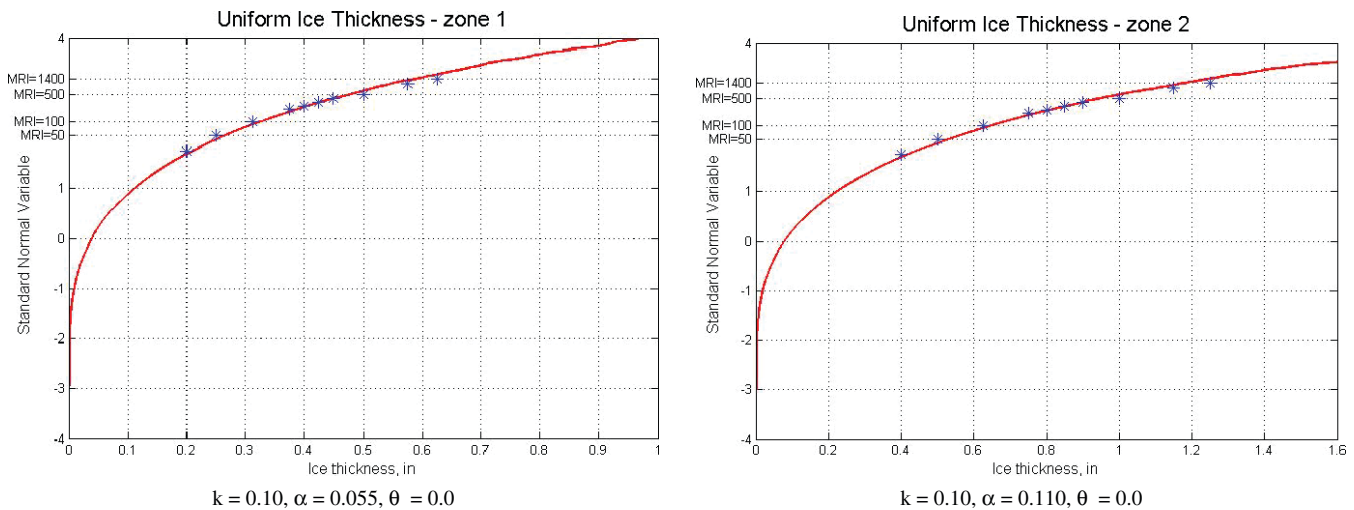


**Figure 3-2. Generalized Pareto distribution of uniform ice thickness for different zones with three most important parameters.**

(continued on next page)

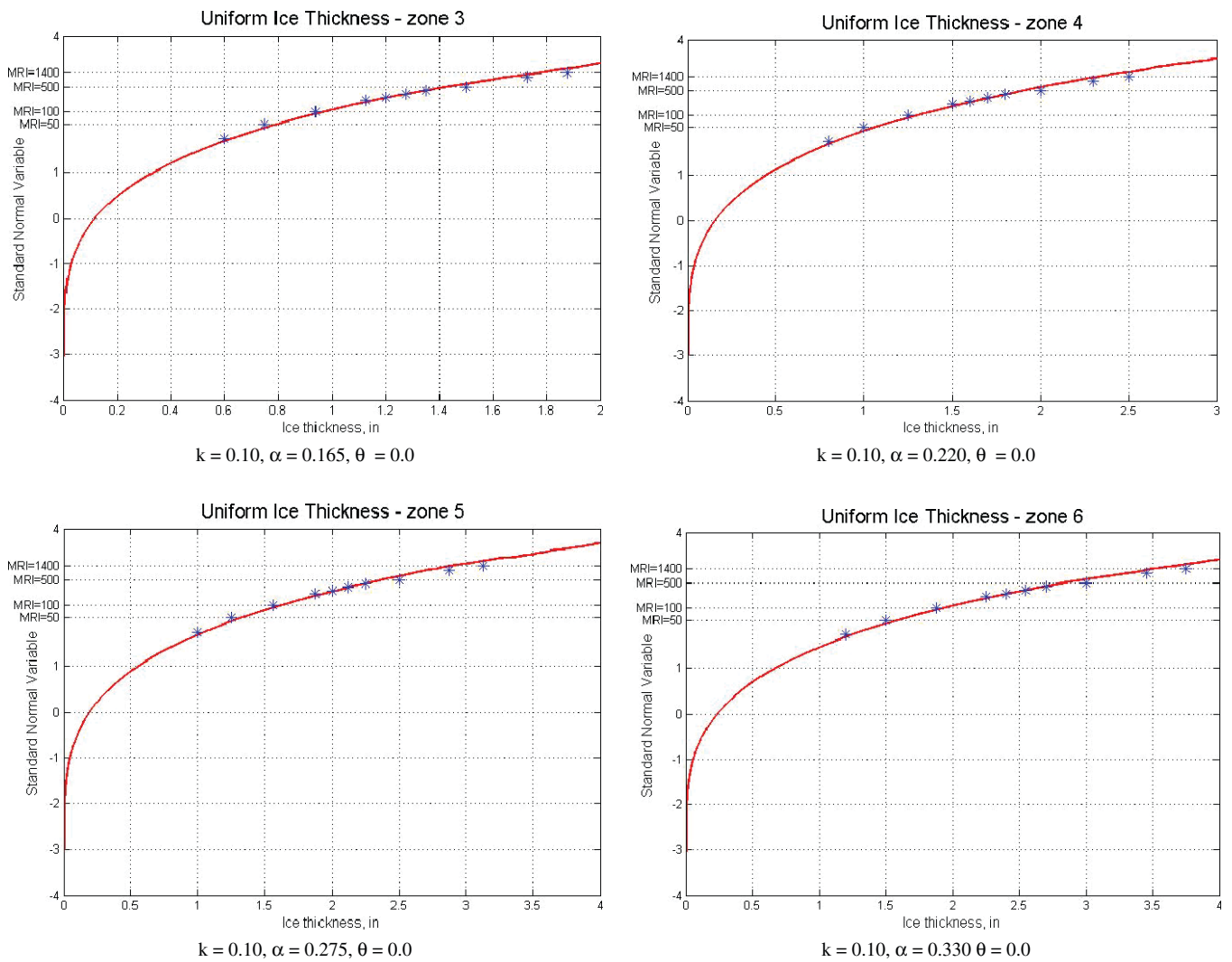


Figure 3-2. (Continued).

Table 3-5. Summaries of statistical parameters of GPD for annual extremes.

Ice Load Zones	Zone 1	Zone 2	Zone 3	Zone 4	Zone 5	Zone 6
Generalized Pareto Distribution						
$k$ - shape	0.10	0.10	0.10	0.10	0.10	0.10
$\alpha$ - scale	0.055	0.110	0.165	0.220	0.275	0.330
$\theta$ - threshold	0	0	0	0	0	0

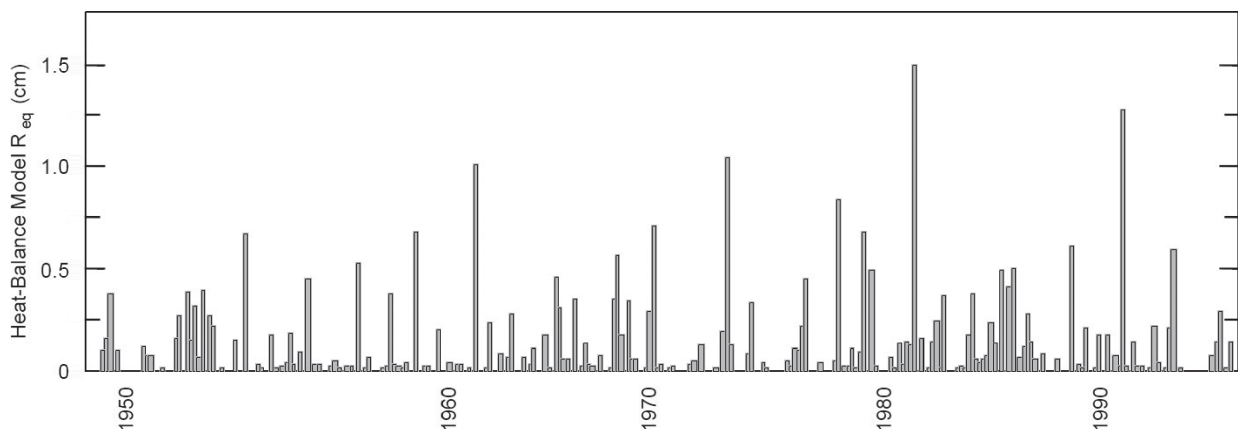


Figure 3-3. Uniform radial ice thickness hind-cast by the heat-balanced model for freezing events at the Des Moines airport from 1948 to 1993.

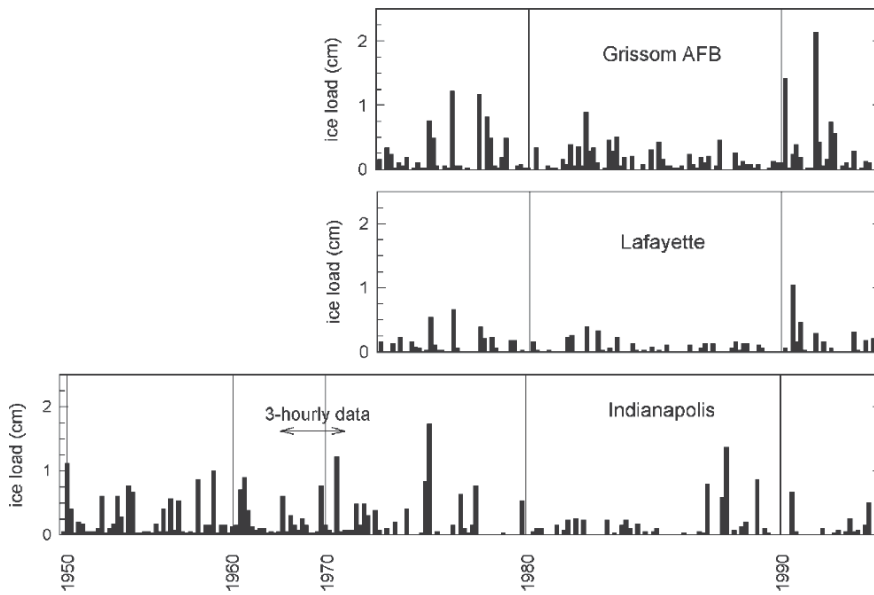


Figure 3-4. Uniform radial ice thickness calculated using historical weather data—three station in Indiana, from the simple model.

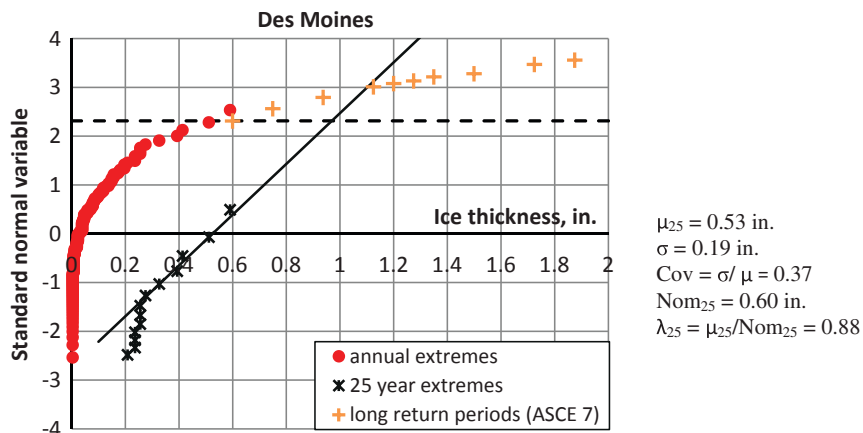


Figure 3-5. CDF of uniform radial ice thickness recorded at the Des Moines airport and simulation results for 25-year extremes.

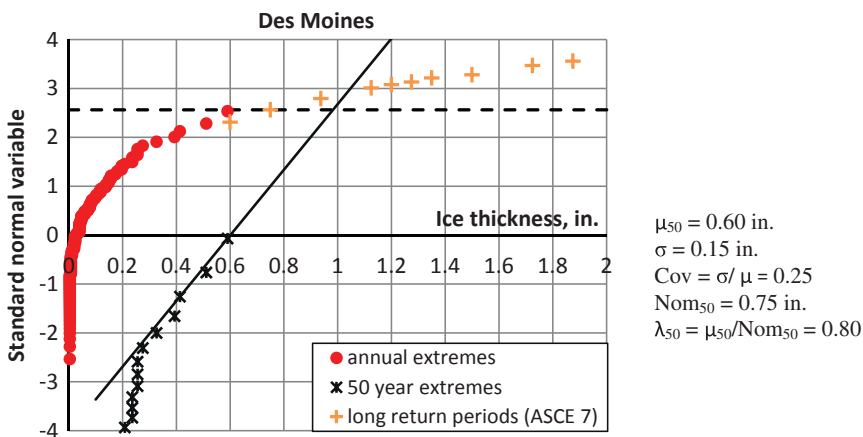
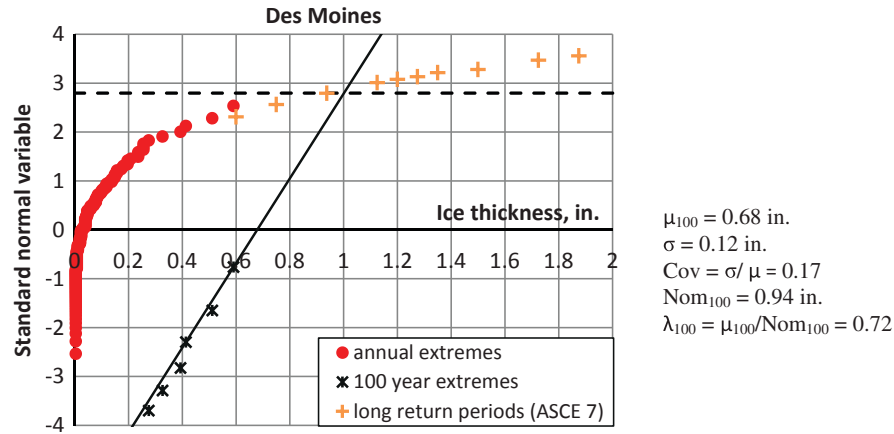
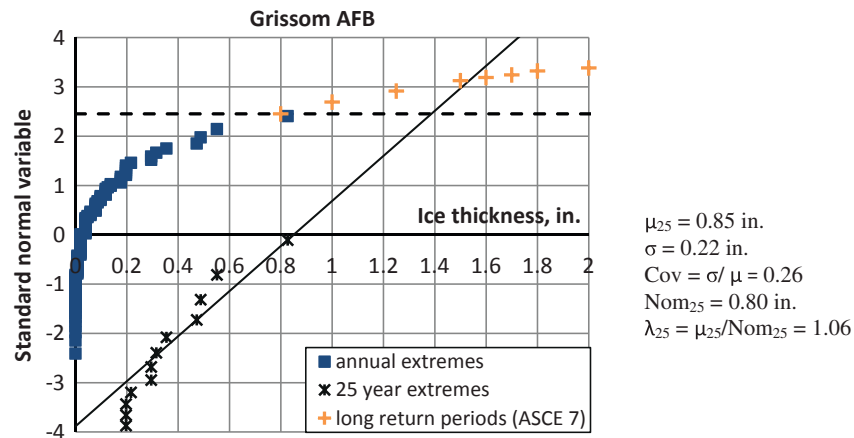


Figure 3-6. CDF of uniform radial ice thickness recorded at the Des Moines airport and simulation results for 50-year extremes.



**Figure 3-7. CDF of uniform radial ice thickness recorded at the Des Moines airport and simulation results for 100-year extremes.**



**Figure 3-8. CDF of uniform radial ice thickness recorded at Grissom AFB and simulation results for 25-year extremes.**

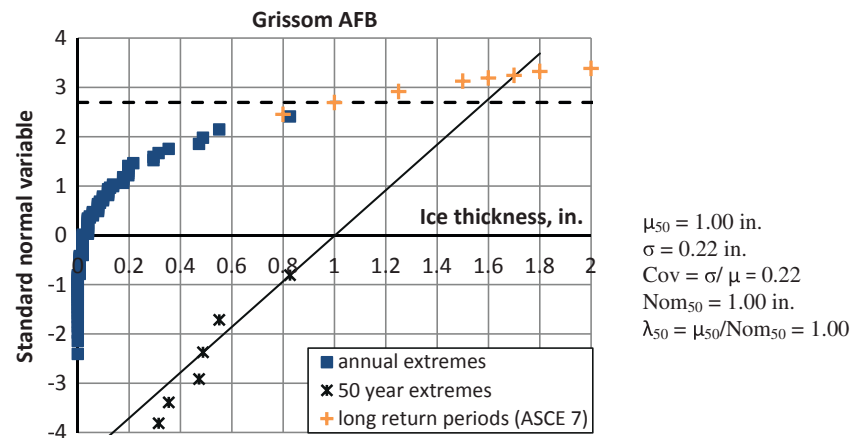


**Figure 3-9. CDF of uniform radial ice thickness recorded at Grissom AFB and simulation results for 50-year extremes.**

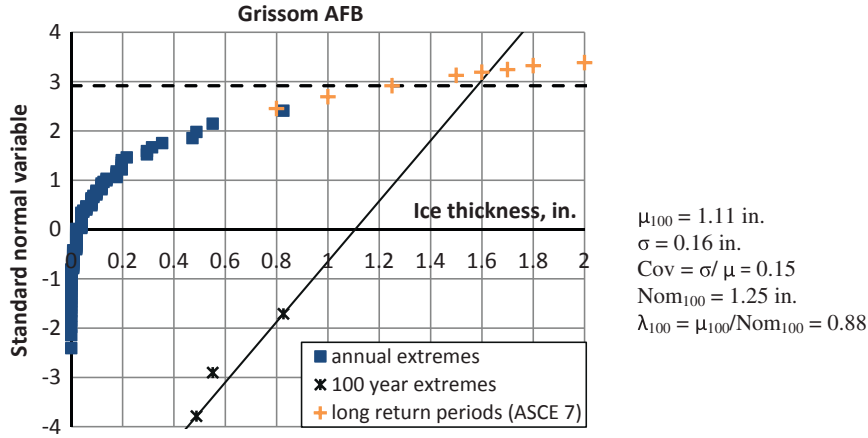


**Figure 3-10. CDF of uniform radial ice thickness recorded at Grissom AFB and simulation results for 100-year extremes.**

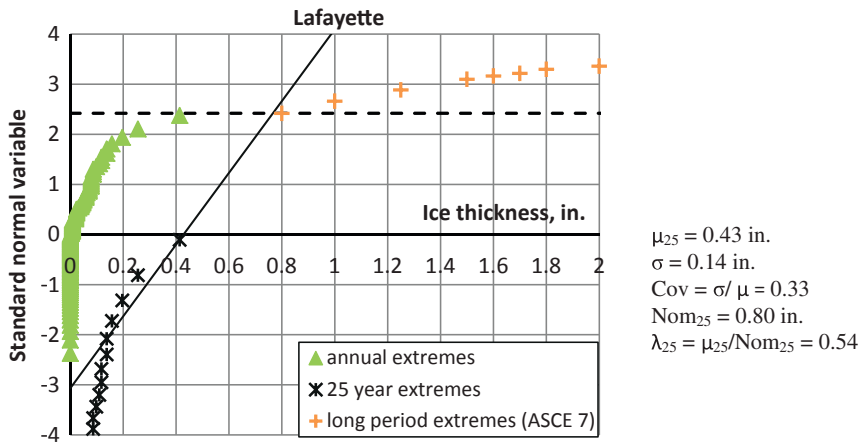


**Figure 3-11. CDF of uniform radial ice thickness recorded in Lafayette and simulation results for 25-year extremes.**

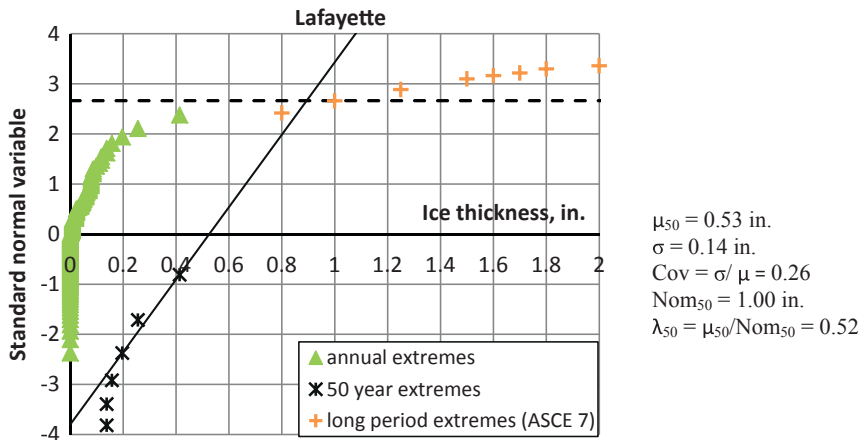


**Figure 3-12. CDF of uniform radial ice thickness recorded in Lafayette and simulation results for 50-year extremes.**

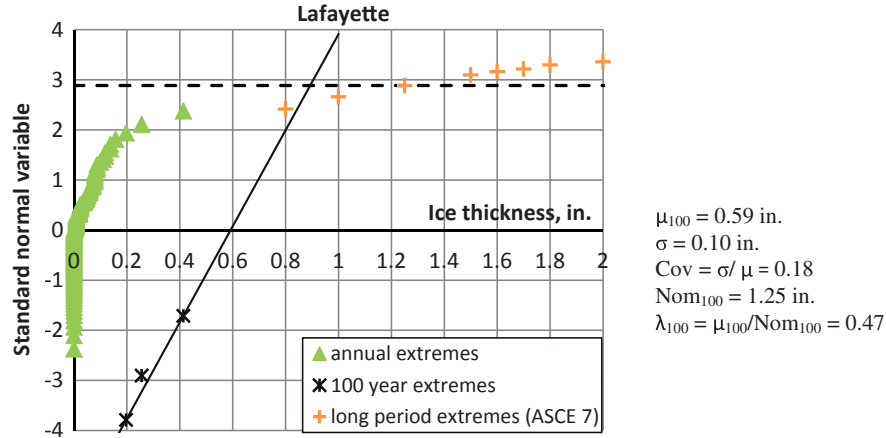


**Figure 3-13. CDF of uniform radial ice thickness recorded in Lafayette and simulation results for 100-year extremes.**

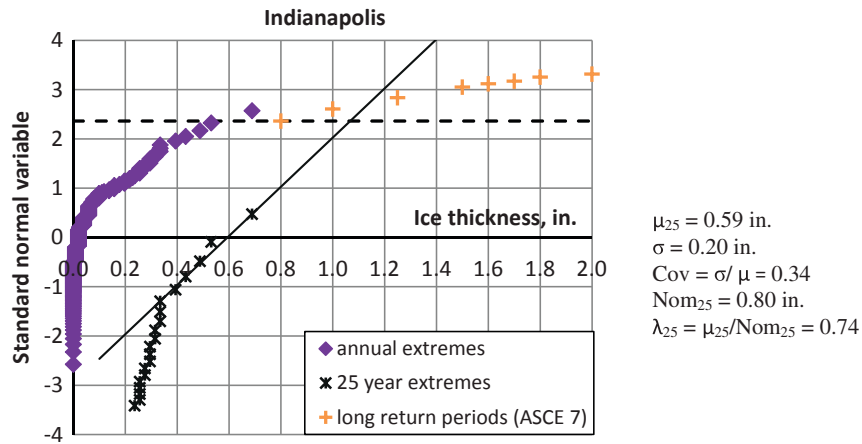


**Figure 3-14. CDF of uniform radial ice thickness recorded in Indianapolis and simulation results for 25-year extremes.**

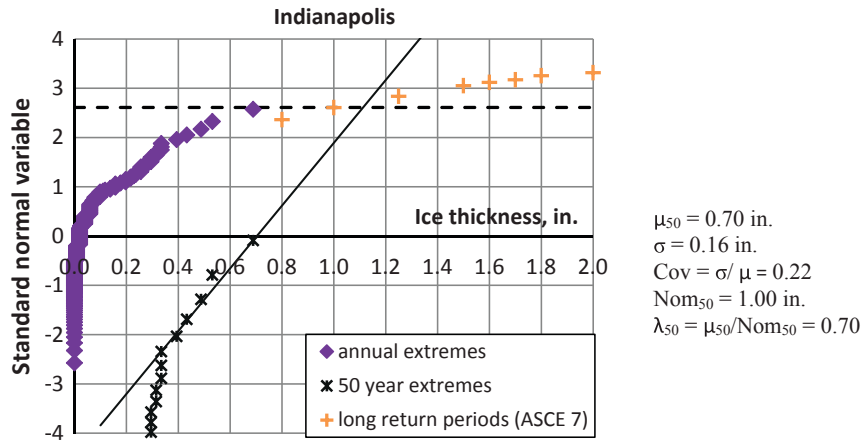


**Figure 3-15. CDF of uniform radial ice thickness recorded in Indianapolis and simulation results for 50-year extremes.**

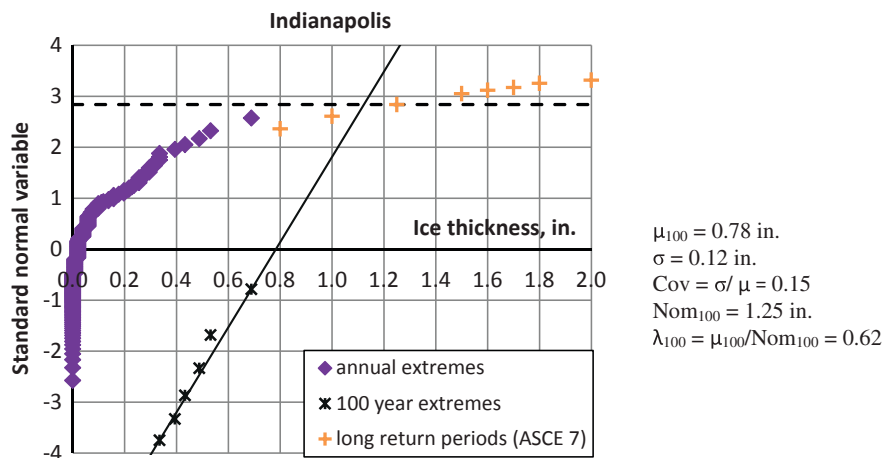


**Figure 3-16. CDF of uniform radial ice thickness recorded in Indianapolis and simulation results for 100-year extremes.**

**Table 3-6. Average statistical parameters for different mean recurrence interval.**

	MRI = 25 Years	MRI = 50 Years	MRI = 100 Years
Cov	0.32	0.24	0.16
$\lambda$	0.80	0.76	0.68

## SECTION 4

# Correlation Between Ice Thickness and Concurrent 3-s Gust Wind

## Information from ASCE/SEI 7-10 and Available Literature

Ice accreted on structural members, components, and appurtenances increases the projected area of the structures exposed to wind. The projected area will be increased by adding  $t$  to all free edges of the projected area. Wind load on this increased projected area is to be applied in the design of ice-sensitive structures. Figures 10-2 through 10-6 in ASCE/SEI 7-10 include the equivalent uniform radial thickness  $t$  of ice due to freezing rain for a 50-year MRI and 3-s gust wind speeds that are concurrent with the ice loads due to freezing rain.

The amount of ice that accretes on a component is affected by the wind speed that accompanies the freezing rain. Wind speeds during freezing rain are typically moderate. However, the accreted ice may last for days or even weeks after the freezing rain ends, as long as the weather remains cold.

Table 4-1 summarizes the 3-s gust for different locations across the United States. As opposed to ice thickness, 3-s concurrent gust speed does not have a multiplication factor for different risk categories. Values on the map are the same for each risk category. The statistical parameters for 3-s concurrent gust speed can be taken as an average of the statistical parameters of wind speed.

It is often important to know the wind load on a structure both during a freezing-rain storm and for as long after the storm as ice remains on the structure. The projected area of the structure is larger because of the ice accretion, so at a given wind speed the wind load is greater than it could be on a bare structure. The wind load results are useful for identifying the combination of wind and ice in each event that causes the largest horizontal load. This combination is independent of drag coefficient as long as it can be assumed to be the same for both the pole-ice accretion and the icicle.

## Possible Combination of Uniform Radial Ice Thickness and Concurrent 3-s Gust Speeds

Based on Figures 10-2 through 10-6 from ASCE/SEI 7-10, 24 different combinations of ice thickness and concurrent wind speed were identified. All possible combinations are marked in Table 4-2 as highlighted cells, as shown here:

	- Possible combination
-	- Not found

The response of traffic sign supports (given example) was calculated using a complex interaction equation for load combination that produces torsion, shear, flexure, and axial force [Equation C-H3-8, AISC *Steel Construction Manual* (AISC, 2010)].

$$\left(\frac{P_r}{P_c} + \frac{M_r}{M_c}\right) + \left(\frac{V_r}{V_c} + \frac{T_r}{T_c}\right)^2 \leq 1.0$$

where:

- $P$  = axial force,
- $M$  = bending moment,
- $V$  = shear,
- $T$  = torsion,

and the terms with the subscript  $r$  represent the required strength (load effect), and those with the subscript  $c$  represent the corresponding available strengths (load carrying capacity). The interaction values for the various combinations are illustrated in Figures 4-1 to 4-8.

## Conclusions

The combination that governs in most cases is the extreme wind combination. The combination with ice and wind on ice governs only in a few cases. All possible values of response

**Table 4-1. 3-s gust speed concurrent with ice load.**

Gust speed zones	$V_{50}$ (mph)	Cov	$\sigma$ (mph)
Zone 1	30	0.15	4.5
Zone 2	40	0.15	6.0
Zone 3	50	0.15	7.5
Zone 4	60	0.15	9.0
Zone 5	70	0.15	10.5
Zone 6	80	0.15	12

calculated using the interaction equation [Equation C-H3-8, AISC *Steel Construction Manual* (AISC, 2010)] are summarized in Tables 4-3 and 4-4. The shaded cells are the cases governed by ice and wind on ice. It appears that ice and wind can be reasonably omitted from the required combinations for traffic signal structures.

### Secondary Analysis for Wind on Ice

A second study was conducted to determine whether the wind-on-ice limit state is likely to control for LTS structures. The loads on a horizontal circular tube were considered. The combined loading for maximum wind and dead load was compared to the combined loading for wind on ice, ice weight, and load. The maximum ice thickness and wind speed were selected from ASCE/SEI 7-10. The minimum wind speed was selected from ASCE/SEI 7-10, Figure 3.8-1. By using these extreme values, it was envisioned that the wind-on-ice limit state will control only in extremely rare circumstances.

A spreadsheet was used to compute the distributed load on the horizontal member (see Figure 4-9). The loads acting about different axes (dead load and ice weight acting vertically versus wind loads acting horizontally) were combined using vector addition (the square root of the sum of the squares). Note that the level arms and so forth are the same for both load effects so that nominal loading can be considered directly (e.g., a cantilever traffic signal pole).

A parametric study was conducted varying the diameter from 12 in. to 16 in., the thickness from 0.25 in. to 0.50 in., while holding the steel density at 0.490 kcf and the ice density at 0.058 kcf.

With the wind and ice loadings selected to make the wind-on-ice limit state as large as possible, the load for that limit state was varied from 91% to 97.5% of the loading from the extreme wind case. This ratio does not prohibit the wind-on-ice case from controlling (see Table 4-5).

Next, the wind-on-ice speed was increased to determine the speed necessary for the wind-on-ice limit state to control with 1.5 in. of ice. The results of this analysis are presented in Table 4-6.

In order to get the load effect from the wind-on-ice limit state equal to the extreme wind limit state, the speed had to be increased to at least 95 mph, which is more than a 50% increase from the maximum value from ASCE/SEI coincident wind speeds.

Next, using the maximum (anywhere in the United States) wind-on-ice speed per ASCE/SEI, the ice thickness was increased to determine the thickness required for the wind-on-ice limit state to control. The results of this analysis are presented in Table 4-7.

Finally, two examples were computed; first, a design wind of 110 mph was compared to the load effect of that with an ice load of 1.5 in. The coincident wind to equal to the wind-only load effect was 95 mph to 97.5 mph, which is much larger than the fastest coincident wind in the United States (60 mph).

The second example compares a design wind of 110 mph with the load effect of the maximum coincident wind in the United States (60 mph). To create the same load effect, the ice thickness would be greater than 3 in. (see Table 4-8).

This simple study appears to validate the much more complex statistically based analysis.

### Conclusion

Two independent analyses indicate that the wind-on-ice load combination may be eliminated from the typical limit-state analysis because it will not control. This is not to suggest that wind on icing will not occur and that the LRFD-LTS specifications should ignore or neglect it. Rather, it considers it and does not require the computation because of the research presented herein.

**Table 4-2. Possible combination of uniform radial ice thickness and concurrent 3-s gust speeds.**

Ice Load Zones Gust Speed Zones	0.00"	0.25"	0.5"	0.75"	1.0"	1.25"	1.5"
30 mph							-
40 mph						-	
50 mph						-	-
60 mph				-			-
70 mph	-		-	-	-	-	-
80 mph	-		-	-	-	-	-

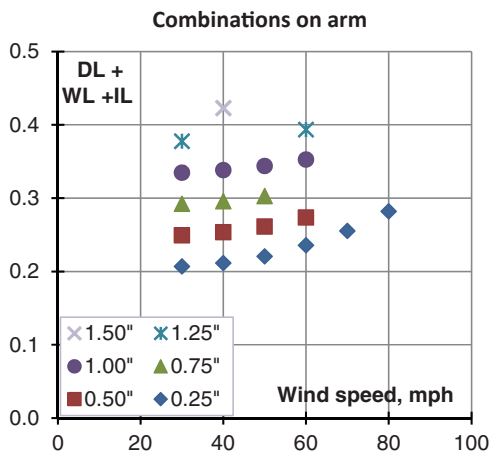


**Figure 4-1.** Values of the interaction equation at the critical section as a function of wind speed on ice—arm.

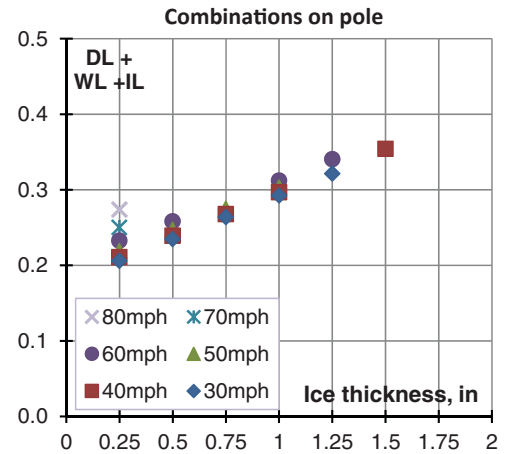


**Figure 4-4.** Values of the interaction equation at the critical section as a function of ice thickness—pole.

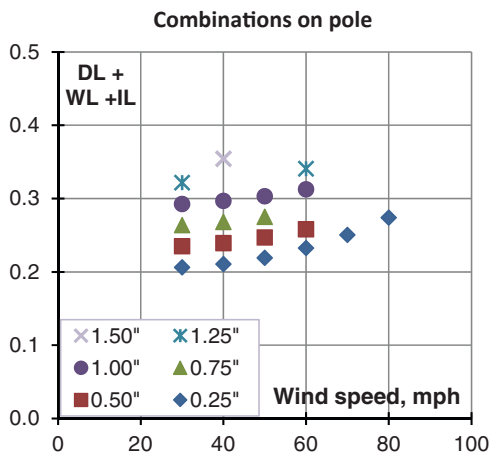


**Figure 4-2.** Values of the interaction equation at the critical section as a function of wind speed on ice—pole.

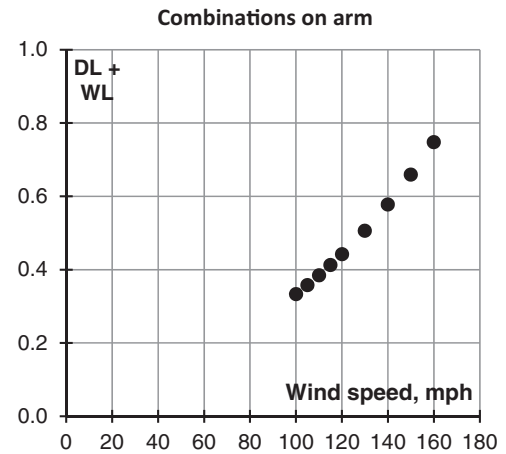


**Figure 4-5.** Values of the interaction equation at the critical section as a function of wind speed in combination of extreme wind and dead load—arm.

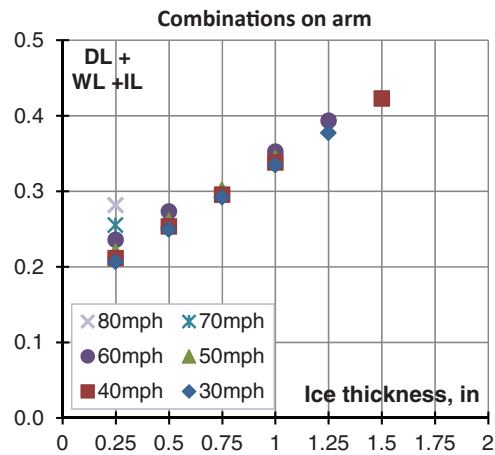


**Figure 4-3.** Values of the interaction equation at the critical section as a function of ice thickness—arm.

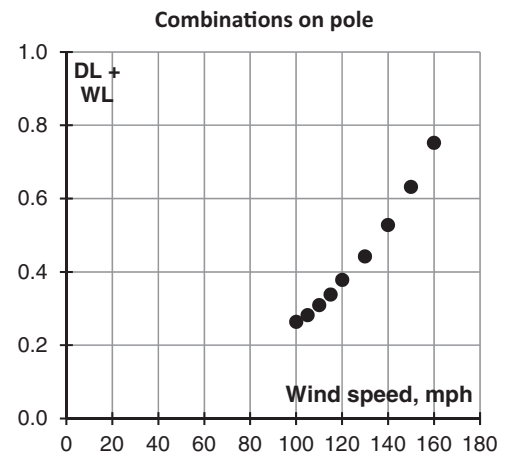


**Figure 4-6.** Values of the interaction equation at the critical section as a function of wind speed in combination of extreme wind and dead load—pole.

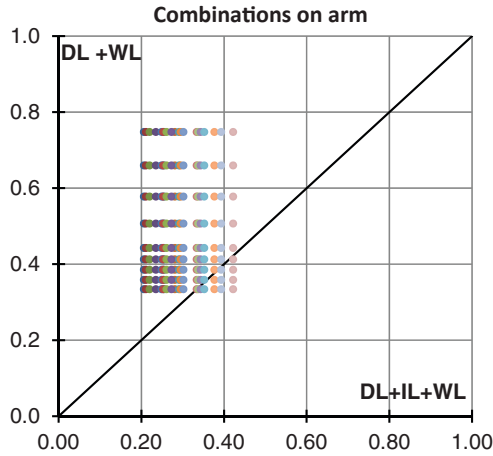


Figure 4-7. Values of the interaction equation at the critical section due to combination of extreme wind and dead load versus combination of ice load, wind on ice, and dead load—arm.

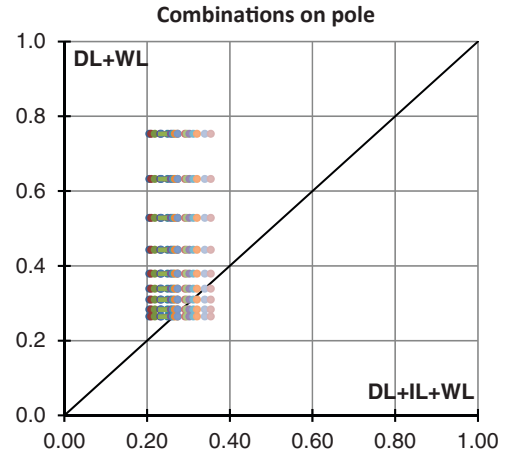


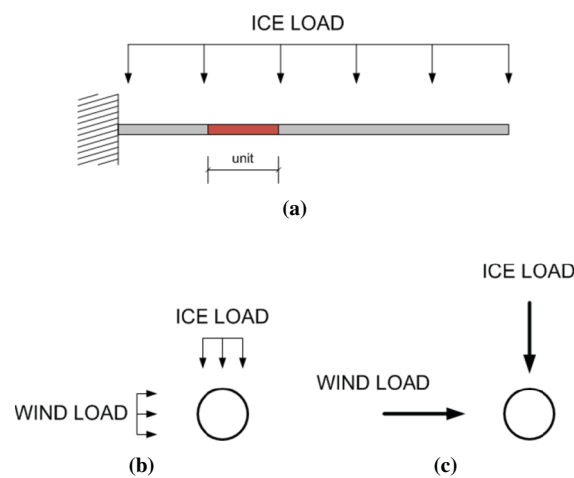
Figure 4-8. Values of the interaction equation at the critical section due to combination of extreme wind and dead load versus combination of ice load, wind on ice, and dead load—pole.

Table 4-3. Values of response at the critical section on an arm calculated using interaction equation.

DL + WL		100 mph	105 mph	110 mph	115 mph	120 mph	130 mph	140 mph	150 mph	160 mph
DL + WL + IL		0.33	0.36	0.38	0.41	0.44	0.51	0.58	0.66	0.75
Ice	Wind									
0.25"	30 mph	0.21	0.21	0.21	0.21	0.21	0.21	0.21	0.21	0.21
	40 mph	0.21	0.21	0.21	0.21	0.21	0.21	0.21	0.21	0.21
	50 mph	0.22	0.22	0.22	0.22	0.22	0.22	0.22	0.22	0.22
	60 mph	0.24	0.24	0.24	0.24	0.24	0.24	0.24	0.24	0.24
	70 mph	0.26	0.26	0.26	0.26	0.26	0.26	0.26	0.26	0.26
	80 mph	0.28	0.28	0.28	0.28	0.28	0.28	0.28	0.28	0.28
0.50"	30 mph	0.25	0.25	0.25	0.25	0.25	0.25	0.25	0.25	0.25
	40 mph	0.25	0.25	0.25	0.25	0.25	0.25	0.25	0.25	0.25
	50 mph	0.26	0.26	0.26	0.26	0.26	0.26	0.26	0.26	0.26
	60 mph	0.27	0.27	0.27	0.27	0.27	0.27	0.27	0.27	0.27
0.75"	30 mph	0.29	0.29	0.29	0.29	0.29	0.29	0.29	0.29	0.29
	40 mph	0.30	0.30	0.30	0.30	0.30	0.30	0.30	0.30	0.30
	50 mph	0.30	0.30	0.30	0.30	0.30	0.30	0.30	0.30	0.30
1.00"	30 mph	0.33	0.33	0.33	0.33	0.33	0.33	0.33	0.33	0.33
	40 mph	0.34	0.34	0.34	0.34	0.34	0.34	0.34	0.34	0.34
	50 mph	0.34	0.34	0.34	0.34	0.34	0.34	0.34	0.34	0.34
	60 mph	0.35	0.35	0.35	0.35	0.35	0.35	0.35	0.35	0.35
1.25"	30 mph	0.38	0.38	0.38	0.38	0.38	0.38	0.38	0.38	0.38
	60 mph	0.39	0.39	0.39	0.39	0.39	0.39	0.39	0.39	0.39
1.50"	40 mph	0.42	0.42	0.42	0.42	0.42	0.42	0.42	0.42	0.42

**Table 4-4. Values of response at the critical section on a pole calculated using interaction equation.**

DL + WL		100 mph	105 mph	110 mph	115 mph	120 mph	130 mph	140 mph	150 mph	160 mph
DL + WL + IL		0.26	0.28	0.31	0.34	0.38	0.44	0.53	0.63	0.75
Ice	Wind									
0.25''	30 mph	0.21	0.21	0.21	0.21	0.21	0.21	0.21	0.21	0.21
	40 mph	0.21	0.21	0.21	0.21	0.21	0.21	0.21	0.21	0.21
	50 mph	0.22	0.22	0.22	0.22	0.22	0.22	0.22	0.22	0.22
	60 mph	0.23	0.23	0.23	0.23	0.23	0.23	0.23	0.23	0.23
	70 mph	0.25	0.25	0.25	0.25	0.25	0.25	0.25	0.25	0.25
	80 mph	0.27	0.27	0.27	0.27	0.27	0.27	0.27	0.27	0.27
0.50''	30 mph	0.23	0.23	0.23	0.23	0.23	0.23	0.23	0.23	0.23
	40 mph	0.24	0.24	0.24	0.24	0.24	0.24	0.24	0.24	0.24
	50 mph	0.25	0.25	0.25	0.25	0.25	0.25	0.25	0.25	0.25
	60 mph	0.26	0.26	0.26	0.26	0.26	0.26	0.26	0.26	0.26
0.75''	30 mph	0.26	0.26	0.26	0.26	0.26	0.26	0.26	0.26	0.26
	40 mph	0.27	0.27	0.27	0.27	0.27	0.27	0.27	0.27	0.27
	50 mph	0.27	0.27	0.27	0.27	0.27	0.27	0.27	0.27	0.27
1.00''	30 mph	0.29	0.29	0.29	0.29	0.29	0.29	0.29	0.29	0.29
	40 mph	0.30	0.30	0.30	0.30	0.30	0.30	0.30	0.30	0.30
	50 mph	0.30	0.30	0.30	0.30	0.30	0.30	0.30	0.30	0.30
	60 mph	0.31	0.31	0.31	0.31	0.31	0.31	0.31	0.31	0.31
1.25''	30 mph	0.32	0.32	0.32	0.32	0.32	0.32	0.32	0.32	0.32
	60 mph	0.34	0.34	0.34	0.34	0.34	0.34	0.34	0.34	0.34
1.50''	40 mph	0.35	0.35	0.35	0.35	0.35	0.35	0.35	0.35	0.35



**Figure 4-9. Mast arm loads with ice and wind.**

**Table 4-5. Wind on ice with extreme icing (1.5 in.).**

$V_{steel}$ (lb/ft <sup>3</sup> )	$V_{ice}$ (lb/ft <sup>3</sup> )	Center Diameter (inches)	Tube Thickness (inches)	Outer Diameter (inches)	Inner Diameter (inches)	Ice Thickness (inches)	V (mph)	$V_{ice}$ (mph)	$C_D$	Inner diameter of ice (inches)	Outer diameter of ice (inches)	$P_z$ (psf)	$P_{z,ice}$ (psf)	Area for Wind (in <sup>2</sup> /ft)	Area for Wind on Ice (in <sup>2</sup> /ft)	Area of Pole (self weight) in <sup>2</sup> /ft	Ice area (in <sup>2</sup> /ft)	$W_{pole}$ (plf)	$W_{ice}$ (plf)	$W_{wind}$ (plf)	$W_{wind, on, ice}$ (plf)	$W_{total} (plf)$ [vectorially added] (1)	$W_{total, ice}$ (plf)[vectorially added] (2)	% of total (1)/(2)
<b>Loads from maximum wind on ice and maximum ice thickness. The wind on structure value is the lowest on the map. (summary results are bolded)</b>																								
<b>Input Parameters</b>										<b>Computations</b>														
490	58	16	0.250	16.3	15.8	1.5	110	60	0.55	16.3	19.3	17.0	5.07	195	231	12.6	20.9	42.8	8.42	23.07	8.13	48.59	44.33	<b>91.2%</b>
490	58	16	0.313	16.3	15.7	1.5	110	60	0.55	16.3	19.3	17.0	5.07	196	232	15.7	21.0	53.5	8.45	23.16	8.16	58.25	54.73	<b>93.9%</b>
490	58	16	0.375	16.4	15.6	1.5	110	60	0.55	16.4	19.4	17.0	5.07	197	233	18.8	21.1	64.1	8.48	23.25	8.18	68.22	65.21	<b>95.6%</b>
490	58	16	0.438	16.4	15.6	1.5	110	60	0.55	16.4	19.4	17.0	5.07	197	233	22.0	21.1	74.8	8.51	23.34	8.21	78.39	75.76	<b>96.7%</b>
490	58	16	0.500	16.5	15.5	1.5	110	60	0.55	16.5	19.5	17.0	5.07	198	234	25.1	21.2	85.5	8.54	23.43	8.24	88.67	86.34	<b>97.4%</b>
490	58	14	0.250	14.3	13.8	1.5	110	60	0.55	14.3	17.3	17.0	5.07	171	207	11.0	18.6	37.4	7.47	20.23	7.29	42.53	38.84	<b>91.3%</b>
490	58	14	0.313	14.3	13.7	1.5	110	60	0.55	14.3	17.3	17.0	5.07	172	208	13.7	18.6	46.8	7.50	20.32	7.31	50.99	47.93	<b>94.0%</b>
490	58	14	0.375	14.4	13.6	1.5	110	60	0.55	14.4	17.4	17.0	5.07	173	209	16.5	18.7	56.1	7.53	20.41	7.34	59.72	57.10	<b>95.6%</b>
490	58	14	0.438	14.4	13.6	1.5	110	60	0.55	14.4	17.4	17.0	5.07	173	209	19.2	18.8	65.5	7.56	20.50	7.37	68.61	66.32	<b>96.7%</b>
490	58	14	0.500	14.5	13.5	1.5	110	60	0.55	14.5	17.5	17.0	5.07	174	210	22.0	18.8	74.8	7.59	20.59	7.39	77.61	75.58	<b>97.4%</b>
490	58	12	0.250	12.3	11.8	1.5	110	60	0.55	12.3	15.3	17.0	5.07	147	183	9.4	16.2	32.1	6.52	17.39	6.44	36.48	33.36	<b>91.4%</b>
490	58	12	0.313	12.3	11.7	1.5	110	60	0.55	12.3	15.3	17.0	5.07	148	184	11.8	16.3	40.1	6.55	17.48	6.47	43.73	41.13	<b>94.1%</b>
490	58	12	0.375	12.4	11.6	1.5	110	60	0.55	12.4	15.4	17.0	5.07	149	185	14.1	16.3	48.1	6.58	17.57	6.49	51.21	48.99	<b>95.7%</b>
490	58	12	0.438	12.4	11.6	1.5	110	60	0.55	12.4	15.4	17.0	5.07	149	185	16.5	16.4	56.1	6.61	17.66	6.52	58.84	56.89	<b>96.7%</b>
490	58	12	0.500	12.5	11.5	1.5	110	60	0.55	12.5	15.5	17.0	5.07	150	186	18.8	16.5	64.1	6.64	17.75	6.55	66.55	64.82	<b>97.4%</b>

**Table 4-6. Wind on ice controlling the limit state.**

$V_{steel}$ (lb/ft <sup>3</sup> )	$V_{ice}$ (lb/ft <sup>3</sup> )	Center Diameter (inches)	Tube Thickness (inches)	Outer Diameter (inches)	Inner Diameter (inches)	Ice Thickness (inches)	V (mph)	$V_{ice}$ (mph)	$C_D$	Inner diameter of ice (inches)	Outer diameter of ice (inches)	$P_z$ (psf)	$P_{z,ice}$ (psf)	Area for Wind (in <sup>2</sup> /ft)	Area for Wind on Ice (in <sup>2</sup> /ft)	Area of Pole (self weight) in <sup>2</sup> /ft	Ice area (in <sup>2</sup> /ft)	$W_{pole}$ (plf)	$W_{ice}$ (plf)	$W_{wind}$ (plf)	$W_{wind, on, ice}$ (plf)	$W_{total} (plf)$ [vectorially added] (1)	$W_{total, ice}$ (plf)[vectorially added] (2)	% of total (1)/(2)
<b>Maximum ice thickness, the wind speed needed for wind on ice to control (summary results are bolded)</b>																								
<b>Input Parameters</b>										<b>Computations</b>														
490	58	16	0.250	16.3	15.8	1.5	110	<b>97.5</b>	0.55	16.3	19.3	17.0	13.38	195	231	12.6	20.9	42.8	8.42	23.07	21.47	48.59	48.58	<b>100.0%</b>
490	58	16	0.313	16.3	15.7	1.5	110	<b>97.5</b>	0.55	16.3	19.3	17.0	13.38	196	232	15.7	21.0	53.5	8.45	23.16	21.54	58.25	58.24	<b>100.0%</b>
490	58	16	0.375	16.4	15.6	1.5	110	<b>97.5</b>	0.55	16.4	19.4	17.0	13.38	197	233	18.8	21.1	64.1	8.48	23.25	21.61	68.22	68.21	<b>100.0%</b>
490	58	16	0.438	16.4	15.6	1.5	110	<b>97.5</b>	0.55	16.4	19.4	17.0	13.38	197	233	22.0	21.1	74.8	8.51	23.34	21.68	78.39	78.37	<b>100.0%</b>
490	58	16	0.500	16.5	15.5	1.5	110	<b>97.5</b>	0.55	16.5	19.5	17.0	13.38	198	234	25.1	21.2	85.5	8.54	23.43	21.75	88.67	88.66	<b>100.0%</b>
490	58	14	0.250	14.3	13.8	1.5	110	<b>96.5</b>	0.55	14.3	17.3	17.0	13.11	171	207	11.0	18.6	37.4	7.47	20.23	18.85	42.53	42.56	<b>100.0%</b>
490	58	14	0.313	14.3	13.7	1.5	110	<b>96.5</b>	0.55	14.3	17.3	17.0	13.11	172	208	13.7	18.6	46.8	7.50	20.32	18.92	50.99	51.00	<b>100.0%</b>
490	58	14	0.375	14.4	13.6	1.5	110	<b>96.5</b>	0.55	14.4	17.4	17.0	13.11	173	209	16.5	18.7	56.1	7.53	20.41	18.98	59.72	59.72	<b>100.0%</b>
490	58	14	0.438	14.4	13.6	1.5	110	<b>96.5</b>	0.55	14.4	17.4	17.0	13.11	173	209	19.2	18.8	65.5	7.56	20.50	19.05	68.61	68.61	<b>100.0%</b>
490	58	14	0.500	14.5	13.5	1.5	110	<b>96.7</b>	0.55	14.5	17.5	17.0	13.17	174	210	22.0	18.8	74.8	7.59	20.59	19.20	77.61	77.63	<b>100.0%</b>
490	58	12	0.250	12.3	11.8	1.5	110	<b>95</b>	0.55	12.3	15.3	17.0	12.71	147	183	9.4	16.2	32.1	6.52	17.39	16.15	36.48	36.49	<b>100.0%</b>
490	58	12	0.313	12.3	11.7	1.5	110	<b>95</b>	0.55	12.3	15.3	17.0	12.71	148	184	11.8	16.3	40.1	6.55	17.48	16.21	43.73	43.74	<b>100.0%</b>
490	58	12	0.375	12.4	11.6	1.5	110	<b>95</b>	0.55	12.4	15.4	17.0	12.71	149	185	14.1	16.3	48.1	6.58	17.57	16.28	51.21	51.21	<b>100.0%</b>
490	58	12	0.438	12.4	11.6	1.5	110	<b>95</b>	0.55	12.4	15.4	17.0	12.71	149	185	16.5	16.4	56.1	6.61	17.66	16.35	58.84	58.83	<b>100.0%</b>
490	58	12	0.500	12.5	11.5	1.5	110	<b>95</b>	0.55	12.5	15.5	17.0	12.71	150	186	18.8	16.5	64.1	6.64	17.75	16.41	66.55	66.54	<b>100.0%</b>

**Table 4-7. Example 1.**

Design wind load	110 mph
$C_D$	0.55
Max ice load on ASCE map	1.5 in
Coincident wind for equivalent load effect	95 mph to 97.5 mph

**Table 4-8. Example 2.**

Design wind load	110 mph
$C_D$	0.55
Max coincident wind	60 mph
Ice thickness for equivalent load effect	3.2 in. to 3.4 in.

---

## SECTION 5

## Resistance Model

**Statistical Parameters of Resistance**

Load carrying capacity is a function of the nominal value of resistance,  $R_n$ , and three factors: material factor,  $m$ , representing material properties, fabrication factor,  $f$ , representing the dimensions and geometry, and professional factor,  $p$ , representing uncertainty in the analytical model:

$$R = R_n \cdot m \cdot f \cdot p$$

The statistical parameters for  $m$ ,  $f$ , and  $p$  were considered by various researchers, and the results were summarized by Ellingwood et al. (1980) based on material test data available in the 1970s.

The actual strength in the structure can differ from structure to structure, but these differences are included in the fabrication and professional bias factors ( $\lambda_f$  and  $\lambda_p$ ). Material parameters for steel were established based on the yield strength data.

The considered parameters are listed in Tables 5-1 through 5-4:

The resistance (load carrying capacity) is formulated for each of the considered limit states and structural components.

$$\text{Bending resistance, elastic state: } M = f_y \cdot S$$

$$\text{Bending resistance, plastic state: } M = f_y \cdot Z$$

$$\text{Shear resistance: } V = A_{\text{shear}} \cdot 0.57 \cdot f_y$$

$$\text{Torsion capacity: } T = \frac{J}{0.5 \cdot d} \cdot 0.57 \cdot f_y$$

$$\text{Axial capacity: } P = A \cdot f_y$$

The limit state that controls design of luminaries is calculated using an interaction equation for load combination that produces torsion, shear, flexure, and axial force [Section C-H3-8, AISC *Steel Construction Manual* (AISC, 2010)].

$$\left( \frac{P_r}{P_c} + \frac{M_r}{M_c} \right) + \left( \frac{V_r}{V_c} + \frac{T_r}{T_c} \right)^2 \leq 1.0$$

where:

$P$  = axial force,

$M$  = bending moment,

$V$  = shear, and

$T$  = torsion.

The terms with the subscript  $r$  represent the required strength (load effect), and those with the subscript  $c$  represent the corresponding available strengths (load carrying capacity).

The limit-state function can be written:

$$g(Q_i, R_i) = 1.0 - \left( \frac{Q_1}{R_1} + \frac{Q_2}{R_2} \right) - \left( \frac{Q_3}{R_3} + \frac{Q_4}{R_4} \right)^2$$

The interaction equation is a nonlinear function; therefore, to calculate combined load carrying capacity, Monte Carlo simulation was used by generating one million values for each of the random variables. This procedure allows for finding function  $g$  and calculating reliability index  $\beta$ . For calibration purposes, using a first-order second-moment approach, the resistance parameters were assumed to have a bias factor of 1.05 and a coefficient of variation of 10%.

**Conclusion**

The resistance model and the parametric statistics for resistance parameters are presented and available for calibration.

**Table 5-1. Statistical parameters for material and dimensions (Ellingwood et al., 1980).**

Parameters	$\lambda$	Cov
Static yield strength, flanges	1.05	0.10
Static yield strength, webs	1.10	0.11
Young's modulus	1.00	0.06
Static yield strength in shear	1.11	0.10
Tensile strength of steel	1.10	0.11
Dimensions, $f$	1.00	0.05

**Table 5-2. Resistance statistics for hot-rolled steel elements (Ellingwood et al., 1980).**

Limit State	Professional		Material		Fabrication		Resistance	
	$\lambda$	Cov	$\lambda$	Cov	$\lambda$	Cov	$\lambda$	Cov
Tension member, yield	1.00	0	1.05	0.10	1.00	0.05	<b>1.05</b>	<b>0.11</b>
Tension member, ultimate	1.00	0	1.10	0.10	1.00	0.05	<b>1.10</b>	<b>0.11</b>
Elastic beam, LTB	1.03	0.09	1.00	0.06	1.00	0.05	<b>1.03</b>	<b>0.12</b>
Inelastic beam, LTB	1.06	0.09	1.05	0.10	1.00	0.05	<b>1.11</b>	<b>0.14</b>
Plate girders in flexure	1.03	0.05	1.05	0.10	1.00	0.05	<b>1.08</b>	<b>0.12</b>
Plate girders in shear	1.03	0.11	1.11	0.10	1.00	0.05	<b>1.14</b>	<b>0.16</b>
Beam columns	1.02	0.10	1.05	0.10	1.00	0.05	<b>1.07</b>	<b>0.15</b>

**Table 5-3. Resistance statistics for cold-formed steel members (Ellingwood et al., 1980).**

Limit State	Resistance	
	$\lambda$	Cov
Tension member	1.10	0.11
Braced beams in flexure, flange stiffened	1.17	0.17
Braced beams in flexure, flange unstiffened	1.60	0.28
Laterally unbraced beams	1.15	0.17
Columns, flexural buckling, elastic	0.97	0.09
Columns, flexural buckling, inelastic, compact	1.20	0.13
Columns, flexural buckling, inelastic, stiffened	1.07	0.20
Columns, flexural buckling, inelastic, unstiffened	1.68	0.26
Columns, flexural buckling, inelastic, cold work	1.21	0.14
Columns, torsional-flexural buckling, elastic	1.11	0.13
Columns, torsional-flexural buckling, inelastic	1.32	0.18

**Table 5-4. Resistance statistics for aluminum structures (Ellingwood et al., 1980).**

Limit State	Resistance	
	$\lambda$	Cov
Tension member, limit-state yield	1.10	0.08
Tension member, limit-state ultimate	1.10	0.08
Beams, limit-state yield	1.10	0.08
Beams, limit-state lateral buckling	1.03	0.13
Beams, limit-state inelastic local buckling	1.00	0.09
Columns, limit-state yield	1.10	0.08
Columns, limit-state local buckling	1.00	0.09

## SECTION 6

## Fatigue Resistance for High-Mast Luminaires

**Background**

The previous AASHTO *Standard Specifications for Structural Supports for Highway Signs, Luminaires, and Traffic Signals* (AASHTO, 2009) requires for certain structures to be designed for fatigue to resist wind-induced stresses.

Accurate load spectra for defining fatigue loadings are generally not available or are very limited. Assessment of stress fluctuations and the corresponding number of cycles for all wind-induced events (lifetime loading histogram) are difficult to assess. However, it is predicted that signs, high-level luminaires, and traffic signal supports are exposed to a large number of cycles. Therefore, an infinite-life fatigue design approach is recommended.

The infinite-life fatigue design approach should ensure that a structure performs satisfactorily for its design life to an acceptable level of reliability without significant fatigue damage. While some fatigue cracks may initiate at local stress concentrations, there should not be any time-dependent propagation of these cracks. This is typically the case for structural supports where the wind-load cycles in 25 years or more are expected to exceed 100 million cycles, whereas typical weld details exhibit a constant-amplitude fatigue threshold (CAFT) at 10 to 20 million cycles.

Figure 6-1 presents the design S-N relations for all types of design categories. The design specifications present eight S-N curves for eight categories of weld details, defined as the detail categories A, B, B', C, C', D, E, and E' (AASHTO, 2009, Standard Specifications).

Table 6-1 presents the values of factor  $A$ , which is a basis for S-N curves for different fatigue categories, and values of constant-amplitude fatigue limit (CAFL) that correspond to the stress range at constant-amplitude loading below which the fatigue life appears to be infinite.

**Stress Range Versus Number of Cycles Relationship from Test Results**

Based on data available in the literature (Stam et al., 2011 and Roy et al., 2011), about 200 samples tested under a constant stress range were used for analysis (see Table 6-2 and Figures 6-2 to 6-14). For each sample, a fatigue category has been assigned based on provided information and design specification provided in Table 11.9.3.1-1—Fatigue Details of Cantilevered and Non-cantilevered Support Structures (AASHTO, 2009, Standard Specifications). Each category group has been plotted separately on a logarithmic scale along with the S-N limit.

**Stress Range Versus Number of Cycles Relationship for Infinite Life**

Because the details should be designed for infinite fatigue life, each of the test results has been recalculated for number of cycles at the CAFL using Miner's rule.

Miner's rule is a linear damage accumulation method developed by Miner in 1945. It assumes that the damage fraction due to a particular stress range level is a linear function of the number of cycles that take places at the stress range. An effective, or equivalent, constant-amplitude stress range  $S_{Re}$  that would cause an equivalent amount of fatigue damage as the variable stress range at a given number of cycles can be defined as follows:

$$S_{Re} = \left( \sum_{i=1}^k \gamma_i S_{Ri}^3 \right)^{1/3}$$

where:

$\gamma_i$  = fraction of cycles at stress range  $i$  to total cycles, and  
 $S_{Ri}$  = magnitude of stress range  $i$ .

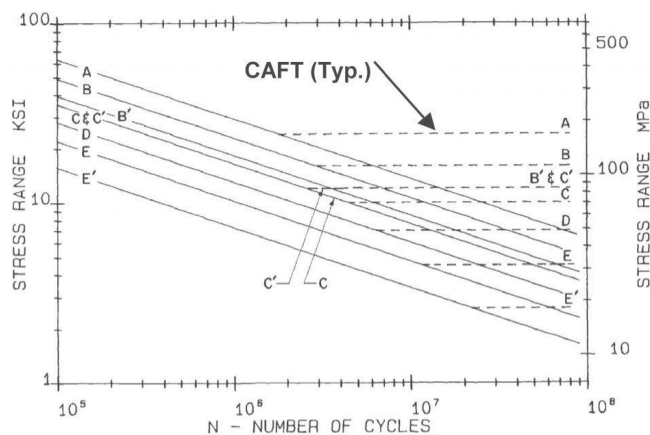


Figure 6-1. Stress range versus number of cycles.

Results for each category were separately plotted on a logarithmic scale along with design S-N curves.

### Statistical Parameters for Resistance

Presented S-N data have a scatter associated with number of cycles under this same stress range. For this case, fatigue resistance should be presented in terms of probability. The fatigue resistance design can be expressed in the form of the cube root of the number of cycles times the stress to the third power,  $(S^3N)^{1/3}$ . Therefore, the CDFs of the fatigue resistance were plotted on normal probability paper for each category of details, as shown in Figures 6-15 through 6-18. The shape of the CDF is an indication of the type of distribution, and if the resulting CDFs are close to straight lines, they can be considered as normal random variables.

Table 6-1. Detail category constant (A) with CAFL summary.

Category	A Times $10^8$ (ksi <sup>3</sup> )	CAFL (ksi)
A	250.0	24
B	120.0	16
B'	61.0	12
C	44.0	10
C'	44.0	10
D	22.0	7
E	11.0	4.5
E'	3.9	2.6
Et	–	≤1.2

Table 6-2. Summary of assigned samples.

Category	No. of Samples
A	2
B	15
B'	–
C	24
C'	–
D	61
E	43
E'	40
Et	3

In addition, the statistical parameters are determined by fitting a straight line to the lower tail of the CDF. The most important parameters are the mean value, standard deviation, and coefficient of variation. Figures 6-15 through 6-18 present the CDF of fatigue resistance for Category C, D, E, and E'. For the remaining details, the number of tested specimens was not sufficient to consider their distribution. The statistical parameters determined by fitting the lower tail with straight lines are summarized in Table 6-3.

For comparison, statistical parameters developed for SHRP 2 Project 19B are presented in Table 6-4.

### Reliability Analysis for Fatigue Limit State

The limit-state function for fatigue can be expressed in terms of the damage ratio as:

$$D = \frac{\sqrt[3]{\sum_i S_{Q_i}^3 \cdot N_{Q_i}}}{\sqrt[3]{\sum_i S_{R_i}^3 \cdot N_{R_i}}} = 1$$

By replacing the nominator by Q and denominator by R, we can obtain the simple limit-state function:

$$g(Q, R) = \frac{\sqrt[3]{\sum_i S_{Q_i}^3 \cdot N_{Q_i}}}{\sqrt[3]{\sum_i S_{R_i}^3 \cdot N_{R_i}}} = \frac{Q}{R} = 1$$

$$\Rightarrow \frac{Q}{R} = 1 \Rightarrow Q = R \Rightarrow R - Q = 0$$

$$g(Q, R) = R - Q = \sqrt[3]{\sum_i S_{R_i}^3 \cdot N_{R_i}} - \sqrt[3]{\sum_i S_{Q_i}^3 \cdot N_{Q_i}}$$

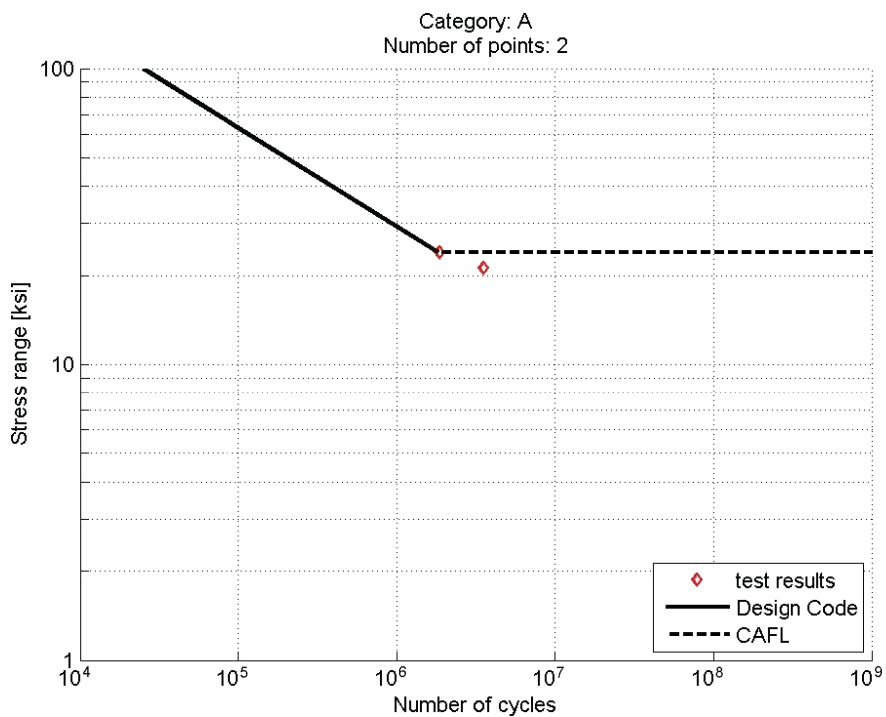


Figure 6-2. Stress range versus number of cycles for Category A.

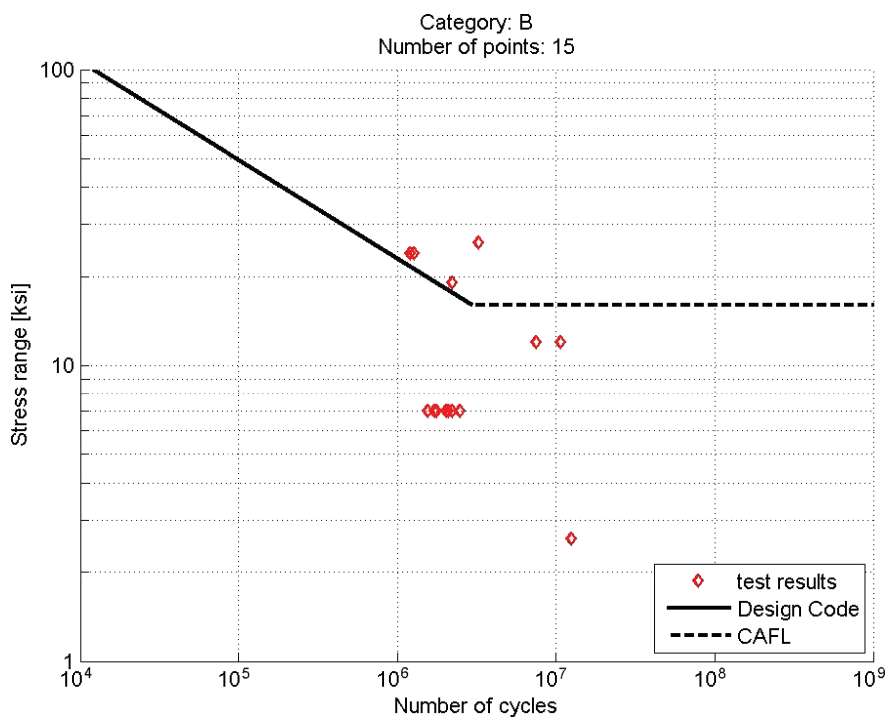


Figure 6-3. Stress range versus number of cycles for Category B.

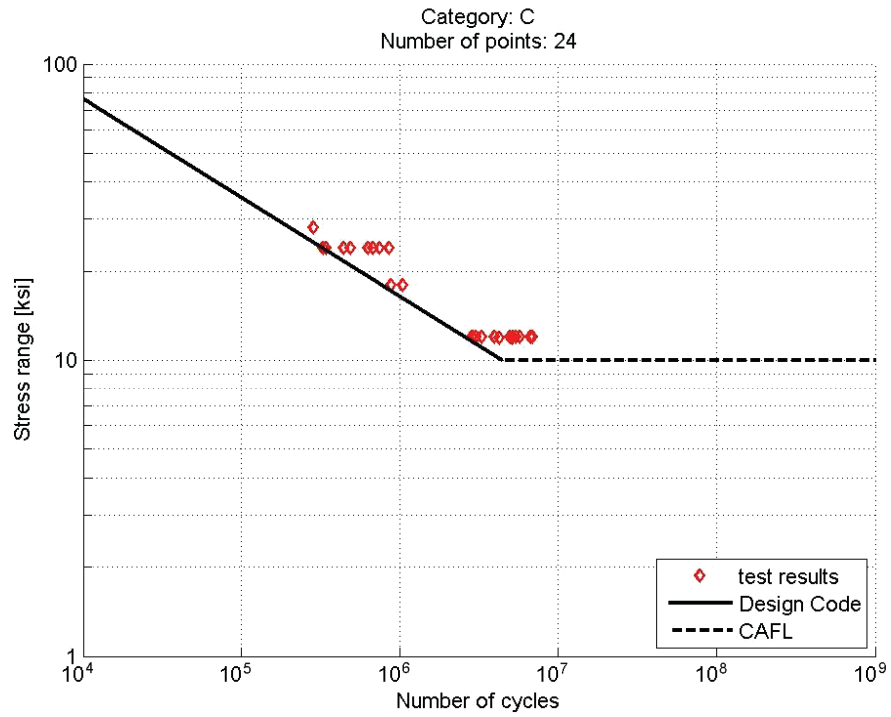


Figure 6-4. Stress range versus number of cycles for Category C.

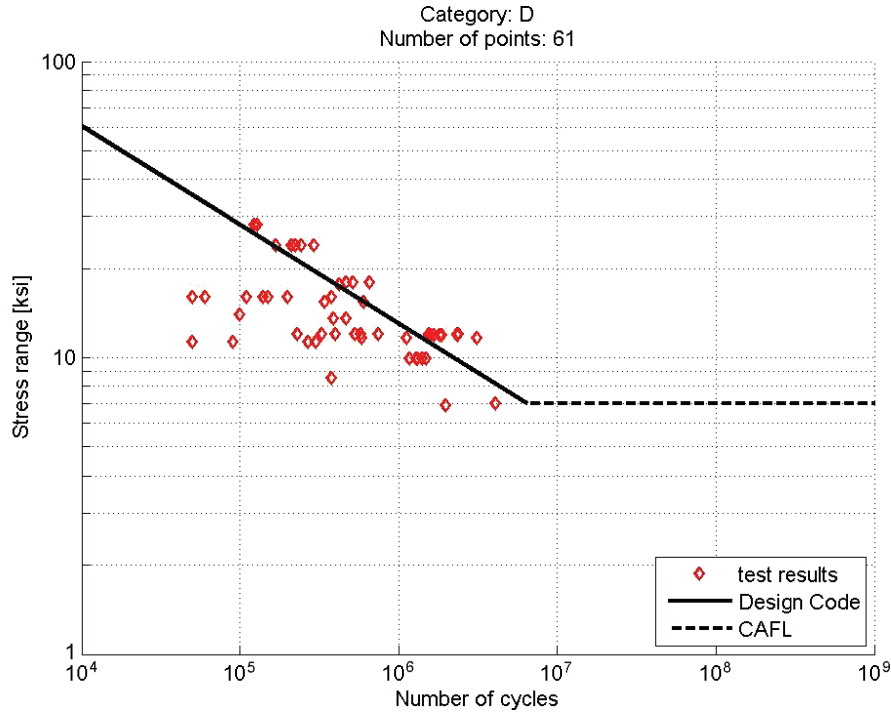


Figure 6-5. Stress range versus number of cycles for Category D.

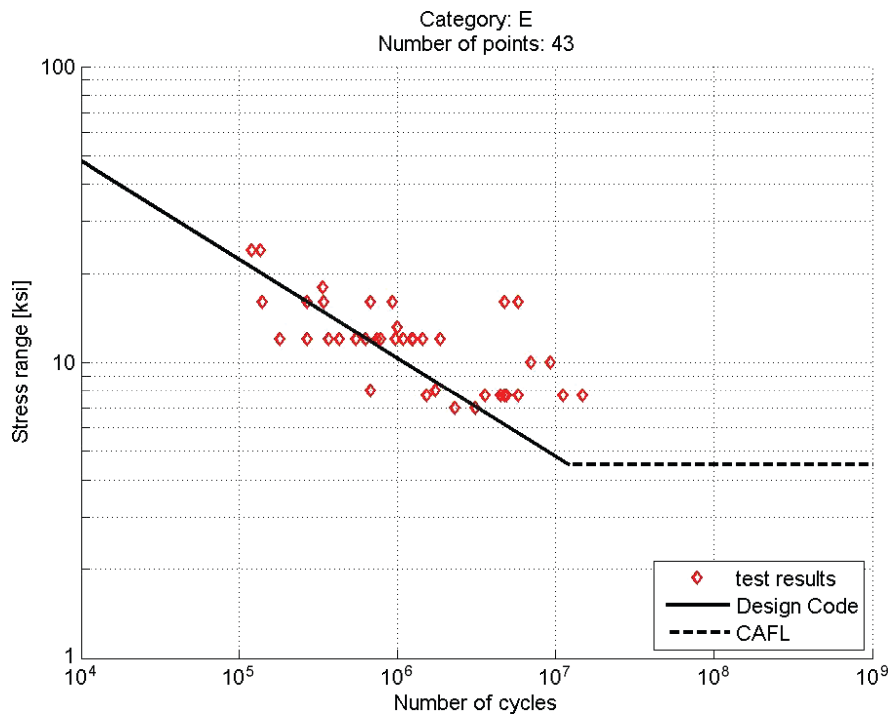


Figure 6-6. Stress range versus number of cycles for Category E.

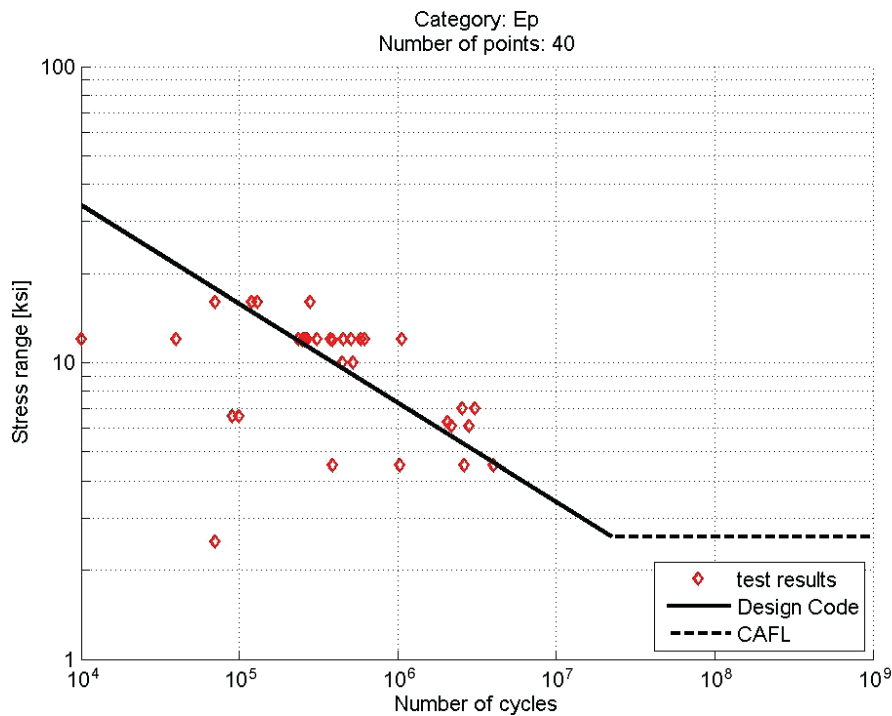


Figure 6-7. Stress range versus number of cycles for Category E'.

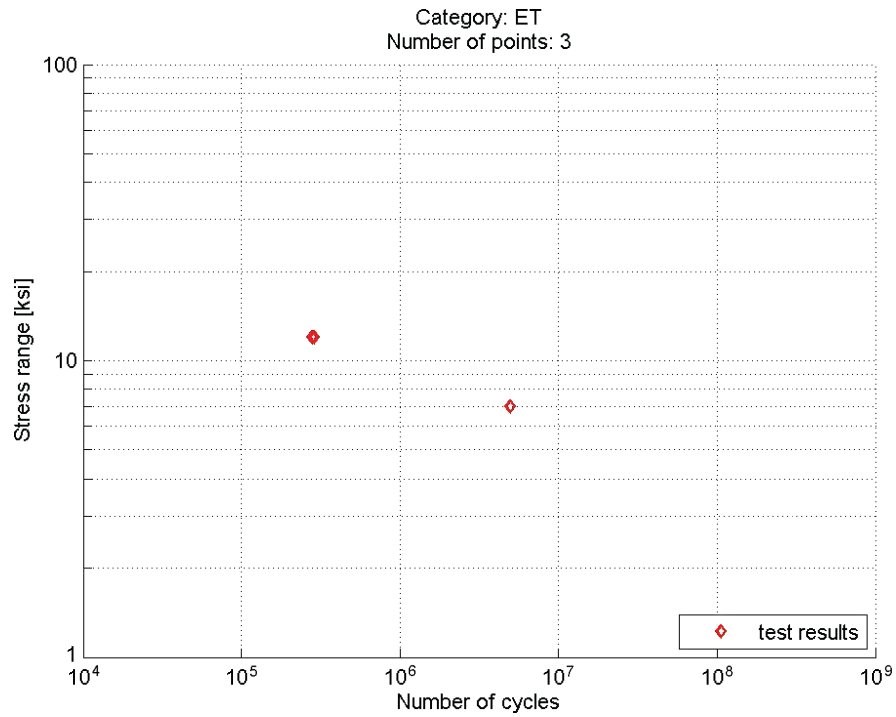


Figure 6-8. Stress range versus number of cycles for Category Et.

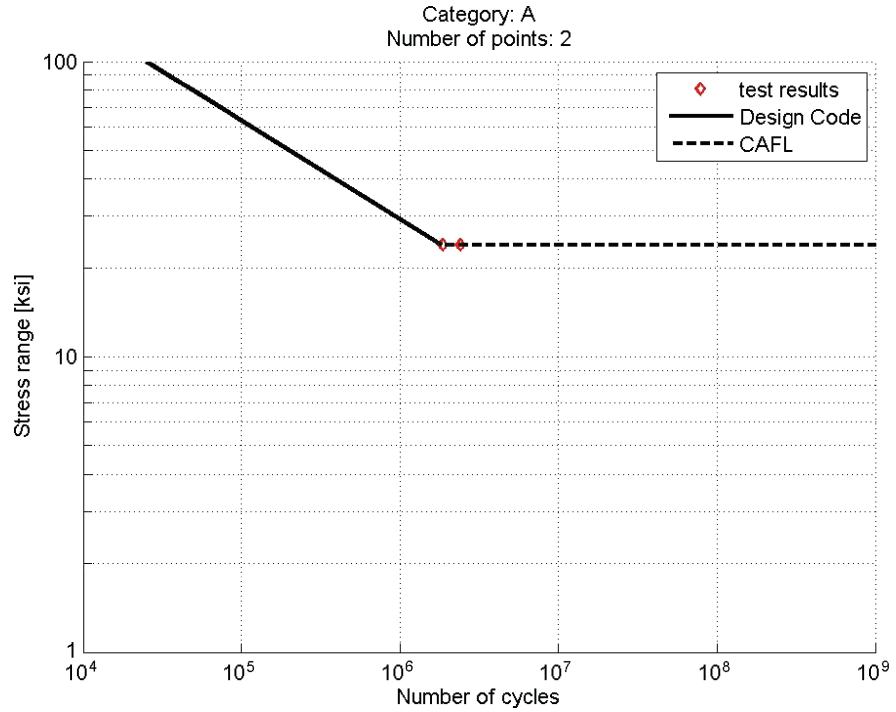


Figure 6-9. Number of cycles at CAFL for Category A.

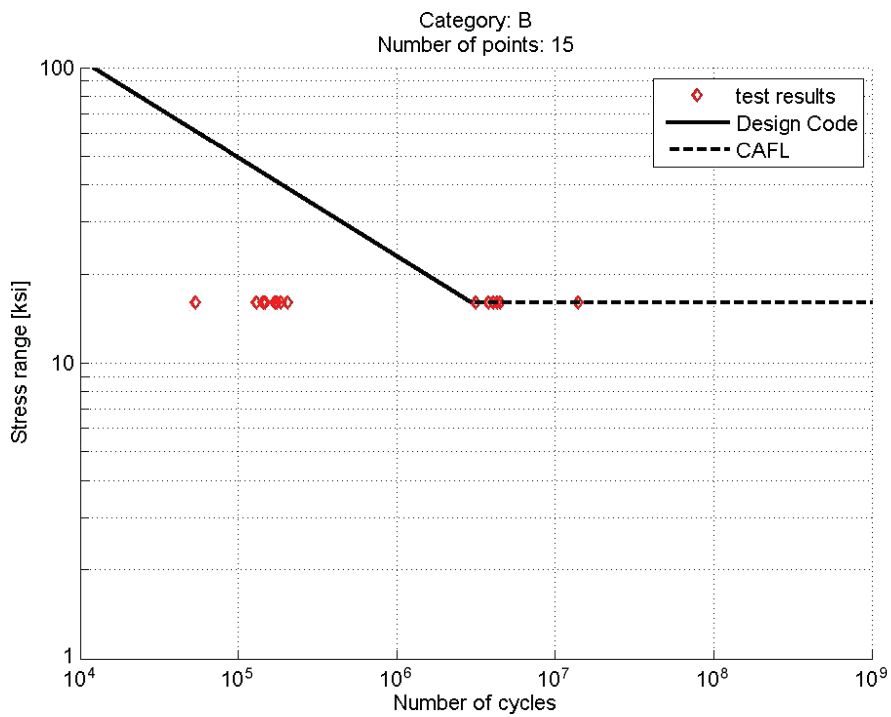


Figure 6-10. Number of cycles at CAFL for Category B.

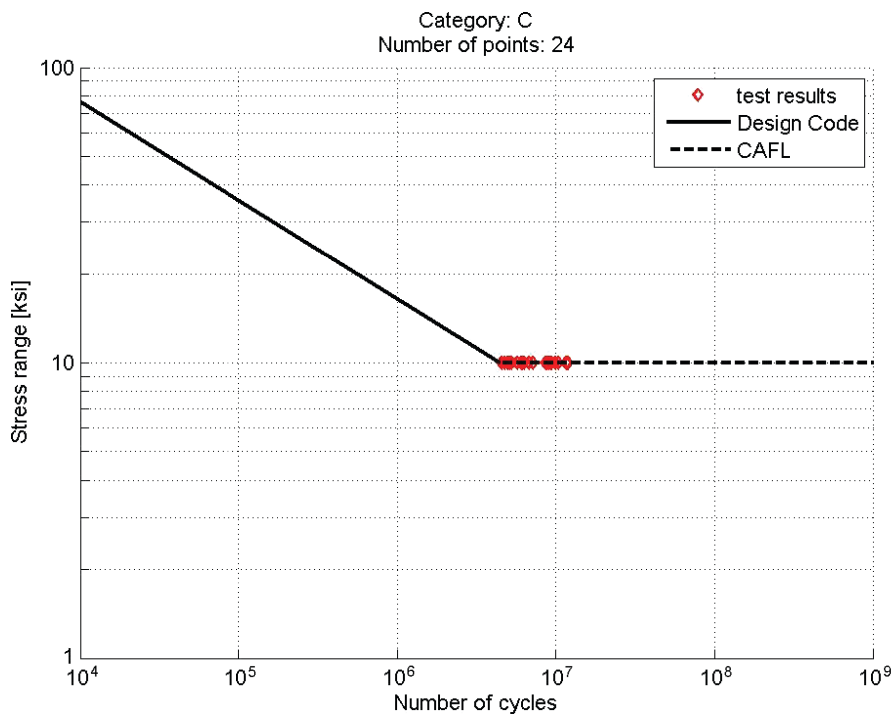


Figure 6-11. Number of cycles at CAFL for Category C.

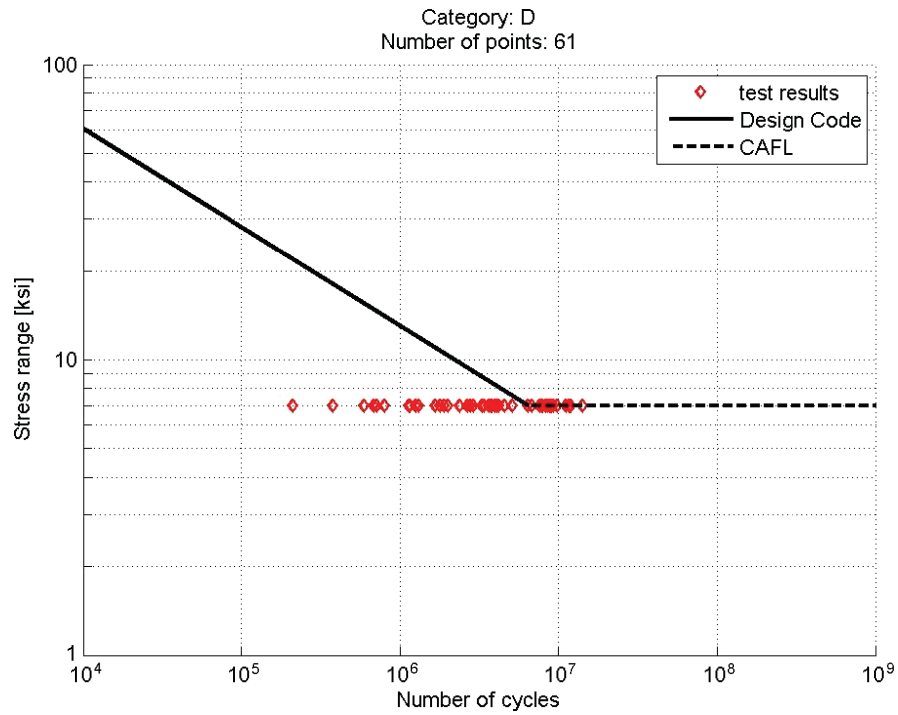


Figure 6-12. Number of cycles at CAFL for Category D.

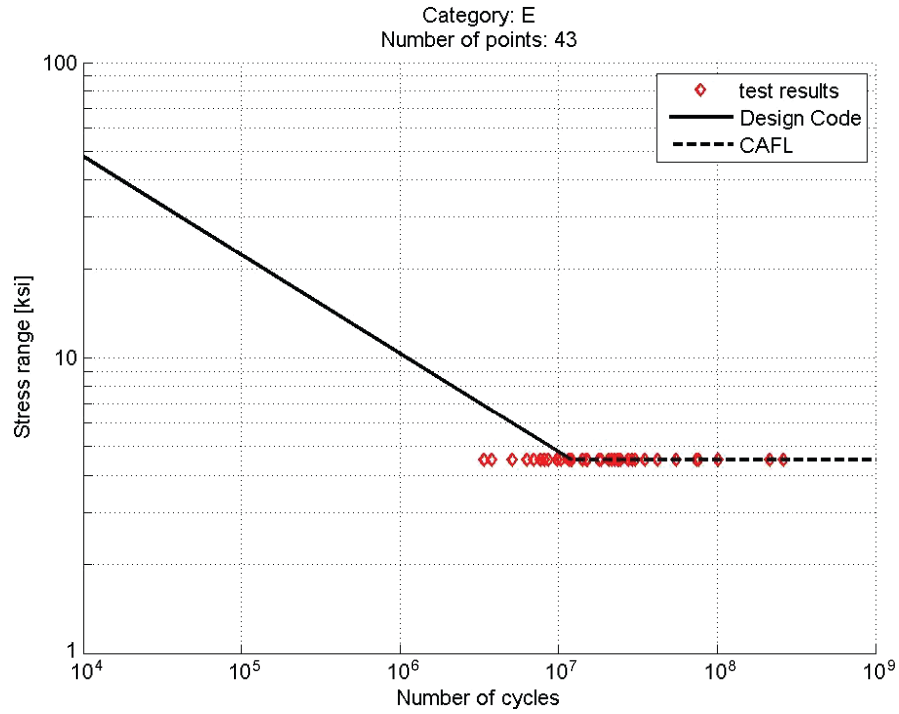


Figure 6-13. Number of cycles at CAFL for Category E.

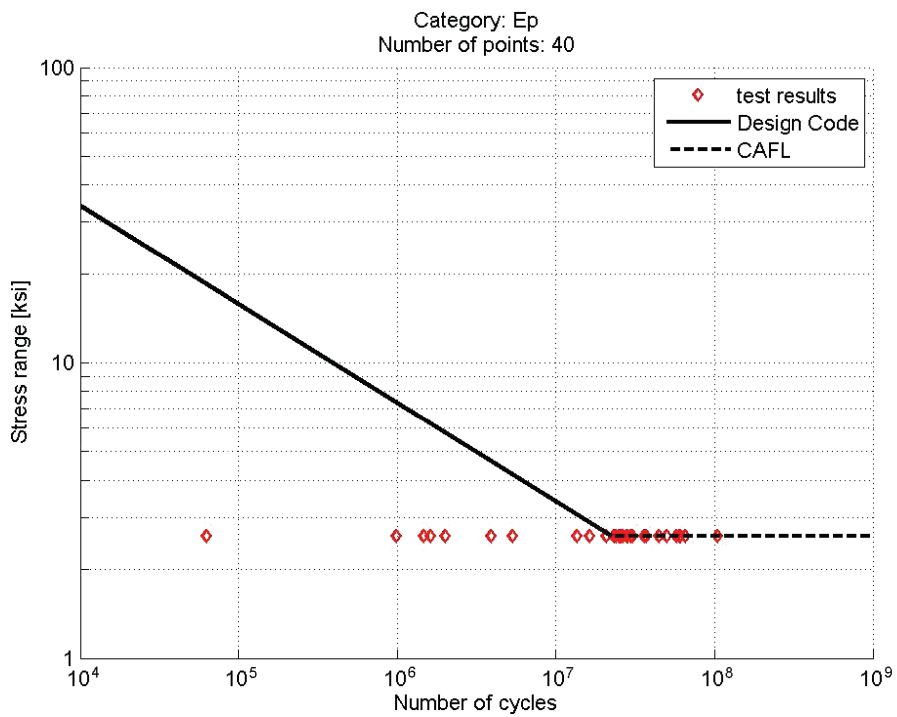


Figure 6-14. Number of cycles at CAFL for Category E'.

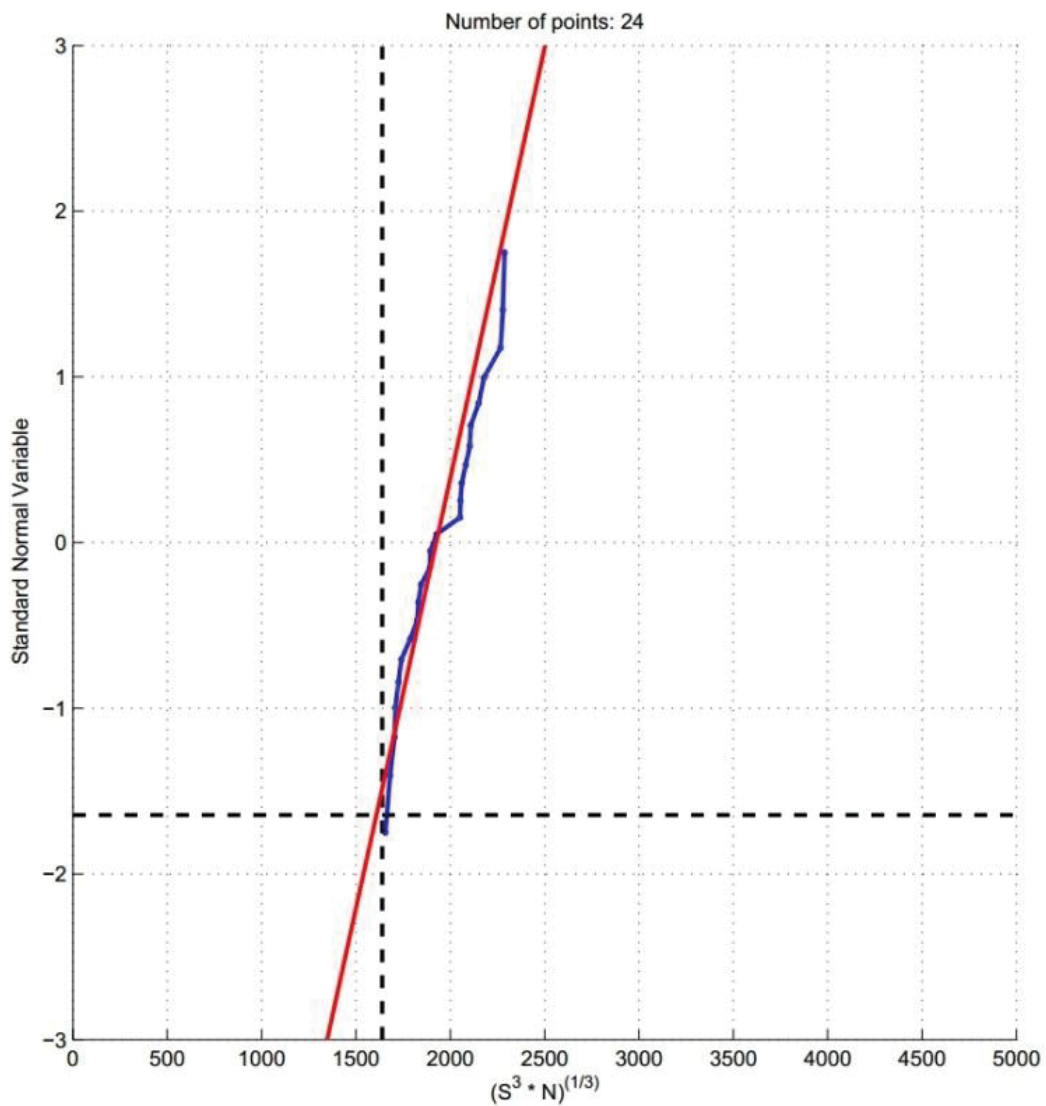


Figure 6-15. CDF for Category C.

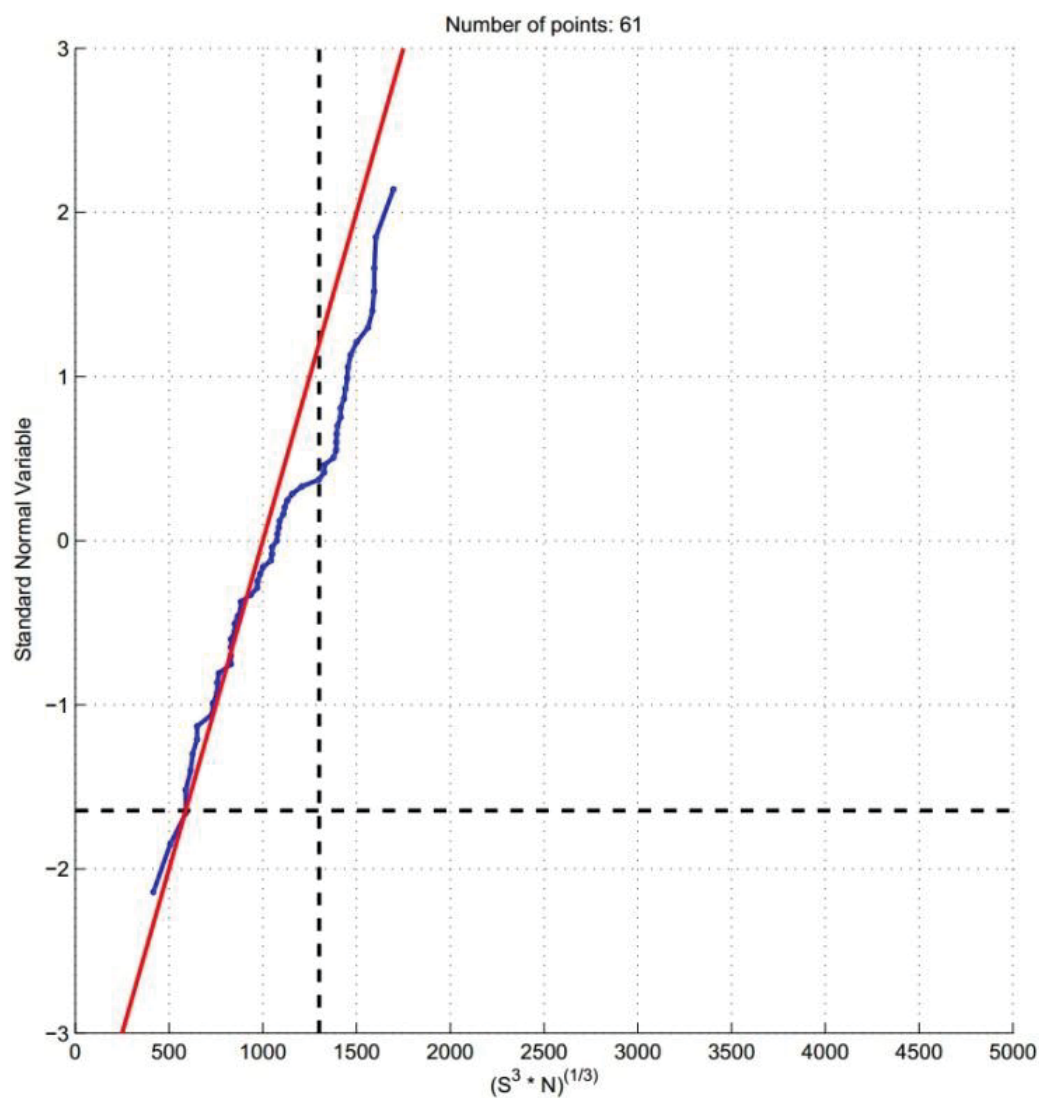


Figure 6-16. CDF for Category D.

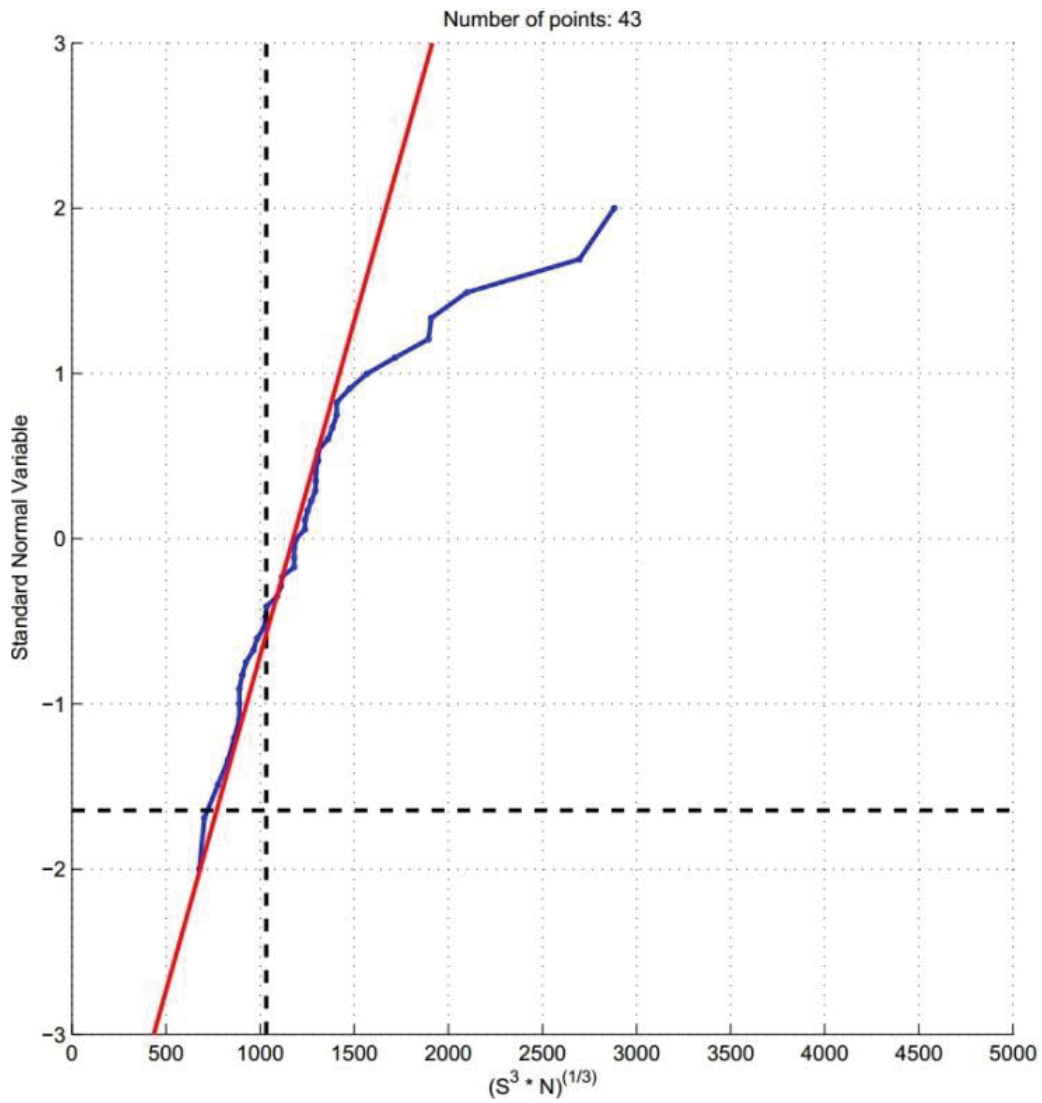


Figure 6-17. CDF for Category E.

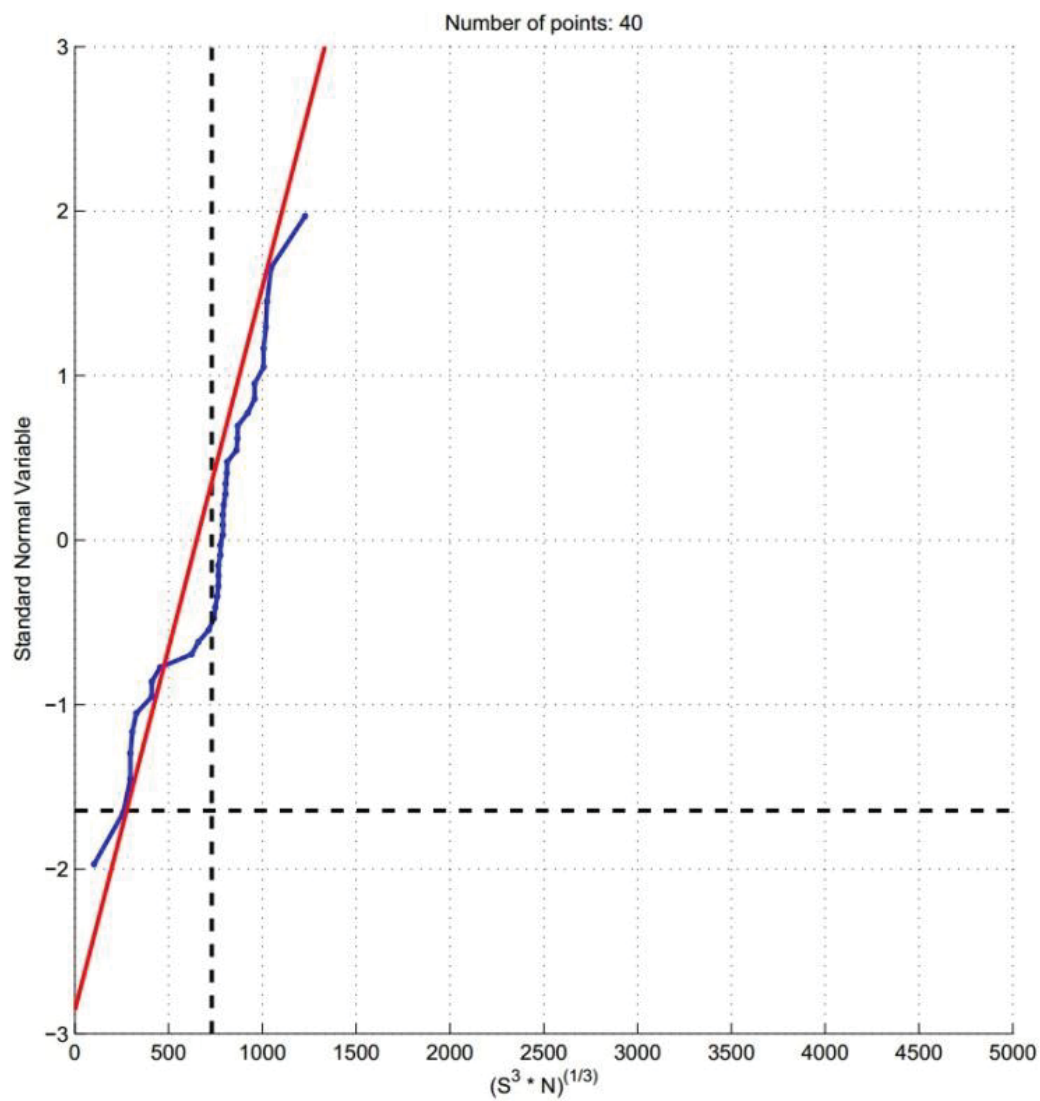


Figure 6-18. CDF for Category E'.

**Table 6-3. Statistical parameters of fatigue resistance based on the data presented for luminaries and sign supports.**

Category	A	B	B'	C and C'	D	E	E'
Nominal, psi	–	–	–	1,639	1,301	1,032	731
Mean, psi	–	–	–	1,925	1,000	1,175	675
Bias, psi	–	–	–	1.17	0.77	1.14	0.92
Cov	–	–	–	10%	25%	21%	35%
St dev, psi	–	–	–	193	250	247	236
No. of data points	–	–	–	24	61	43	40

**Table 6-4. Statistical parameters of fatigue resistance based on data presented for SHRP 2 Project 19B (Report still in progress).**

Category	A	B	B'	C and C'	D	E	E'
Nominal, psi	2,924	2,289	1,827	1,639	1,301	1,032	731
Mean, psi	4,250	2,900	2,225	2,175	1,875	1,200	1,125
Bias	1.45	1.27	1.22	1.33	1.44	1.16	1.54
Cov	22%	13%	9%	17.50%	15%	12.50%	19.50%
St dev, psi	935	377	200	381	281	150	219
No. of data points	72	623	86	358	114	647	319

The statistical parameters of resistance were developed in the previous section and load model is presented in *NCHRP Report 718: Fatigue Loading and Design Methodology for High-Mast Lighting Towers*. Resistance,  $R$ , demonstrates characteristics of normal distribution, and the basic statistical parameters, which are required for reliability analysis, were developed based on the straight line fitted to the lower tail. The load data provided in *NCHRP Report 718* show very little variation. Moreover, even a coefficient of variation equal to 10% does not change the reliability index significantly. Distribution of fatigue resistance definitely has a dominant effect on the entire limit-state function.

For special cases, such as a case of two normal-distributed, uncorrelated random variables,  $R$  and  $Q$ , the reliability index is given by:

$$\beta = \frac{\mu_R - \mu_Q}{\sqrt{\sigma_R^2 + \sigma_Q^2}}$$

To calculate the reliability index, the specific fatigue category and total load on the structure are used. The data presented in *NCHRP Report 718* are summarized in Table 6-5. (Test site and stream gage abbreviations are as presented in *NCHRP Report 718*.)

The reliability indices were calculated for all tested high masts presented in *NCHRP Report 718*. The reliability indices

were calculated for the period of 10 to 50 years. The results are presented in Figures 6-19 to 6-22 for truncation level  $> 0.5$  ksi and in Figures 6-23 to 6-26 for truncation level  $> 1.0$  ksi. (In the figures, site and gage abbreviations are as presented in *NCHRP Report 718*.) The results show that all tested high masts are able to carry a load in 50 years with  $\beta$ s above 0. This means that the components and connections have a small probability of damage due to fatigue in these periods of time. Reliability index  $\beta = 4$  corresponds to 0.001% of probability of failure,  $P_f$ ,  $\beta = 3$  corresponds to  $P_f = 0.1\%$ ,  $\beta = 2$  corresponds to  $P_f = 2.0\%$ ,  $\beta = 1$  corresponds to  $P_f = 15.0\%$ , and  $\beta = 0$  corresponds to  $P_f = 50.0\%$ . For Category D, the reliability indices are close to 0, and this is the effect of low bias and high coefficient of variation of resistance. Verifying the fatigue resistance model is highly recommended.

## Conclusions

The results presented in Figures 6-9 to 6-14 show that many specimens do not fit into a CAFL design line. This indicates that for some details, the finite fatigue life methodology should be considered instead of using infinite fatigue life, or a more conservative category should be assigned. Hence, further research is needed in this area that will provide more data points.

Table 6-5. Summary of load based on NCHRP Report 718.

Test Site	Strain Gage	Detail Category	≥0.5 ksi		≥1.0 ksi	
			$S_{\text{Reff}}$ (ksi)	N/Day	$S_{\text{Reff}}$ (ksi)	N/Day
CA-A	CH_3	D	1.28	5,820	1.8	1,793
CA-X	CH_5	D	1.12	5,016	1.63	1,234
IAN-A (MT)	CH_9	D	1.36	5,927	1.94	1,788
IAN-X (MT)	CH_12	D	1.19	7,173	1.7	2,016
IAS-A	CH_2	E	0.92	2,805	1.47	356
IAS-X	CH_1	E	0.87	3,468	1.41	350
KS-A	CH_2	C	1.55	12,730	2.12	4,622
KS-X	CH_6	C	1.64	14,359	2.2	5,593
ND-A	CH_1	E	0.92	4,547	1.46	579
ND-X	CH_5	E	0.97	6,170	1.46	1,100
OKNE-A	CH_3	D	1.11	8,294	1.64	1,942
OKNE-X	CH_5	E	1.04	8,872	1.55	1,845
OKSW-A	CH_8	E	1.08	13,997	1.61	3,165
OKSW-X	CH_6	D	1.05	16,832	1.55	3,856
PA-A	CH_6	E'	0.81	294	1.35	16
PA-X	CH_1	E'	0.83	441	1.36	33
SD-A	CH_6	E	0.93	11,515	1.51	1,453
SD-X	CH_8	E	0.98	12,750	1.6	1,827
CJE-A (FR)	CH_8	E	1.02	18,693	1.57	3,472
CJE-X (FR)	CH_6	D	1.08	35,437	1.58	8,254
CJE-A (MT)	CH_4	D	1.08	6,037	1.62	1,345
CJE-X (MT)	CH_6	D	1.1	7,598	1.62	1,800
CJW-A (FR)	CH_8	D	1.06	28,228	1.61	5,721
CJW-X (FR)	CH_6	D	1.13	36,382	1.65	9,083
CJW-A (MT)	CH_1	E	1.03	6,688	1.59	1,252
CJW-X (MT)	CH_2	E	1.02	6,934	1.59	1,258

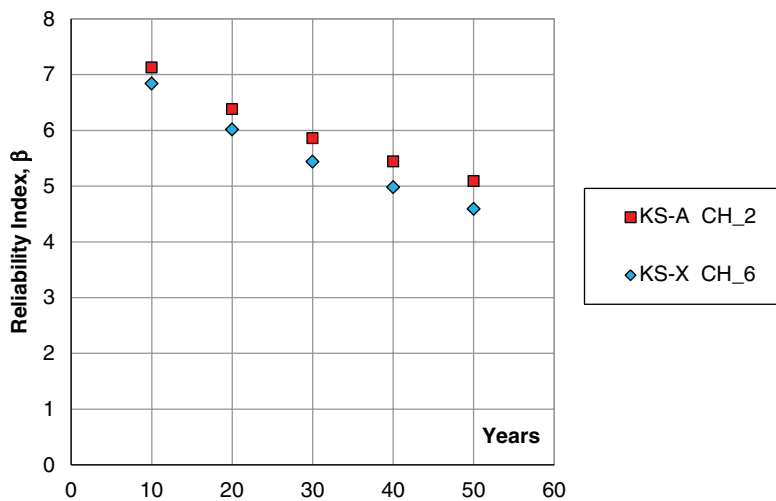


Figure 6-19. Reliability index versus time for Category C, with truncation level &gt; 0.5 ksi.

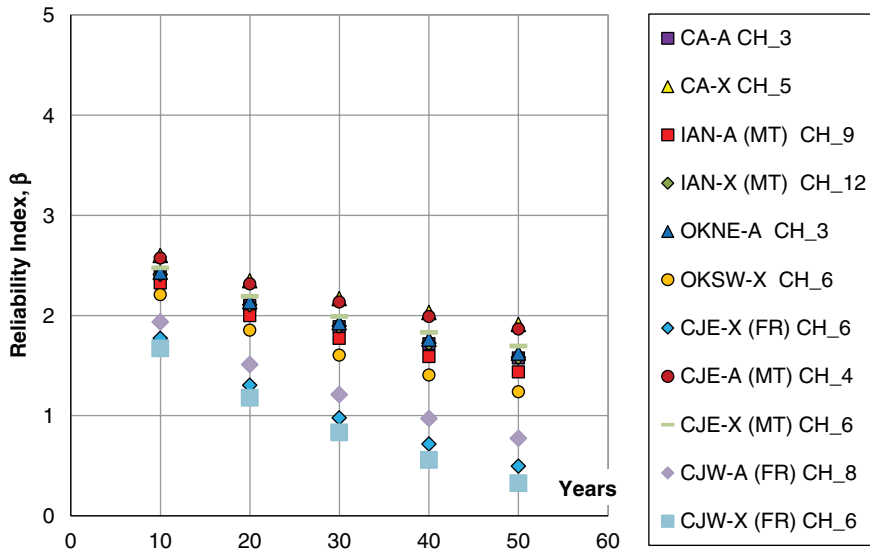


Figure 6-20. Reliability index versus time for Category D, with truncation level > 0.5 ksi.

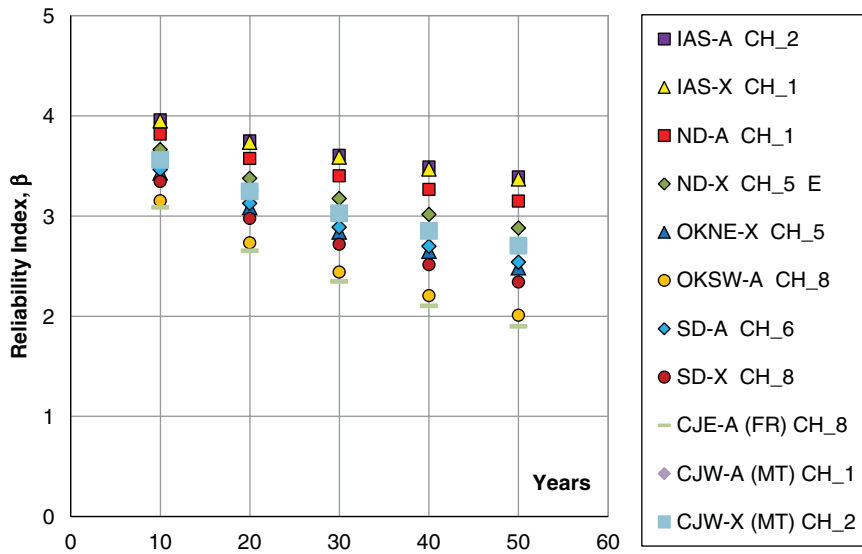


Figure 6-21. Reliability index versus time for Category E, with truncation level > 0.5 ksi.

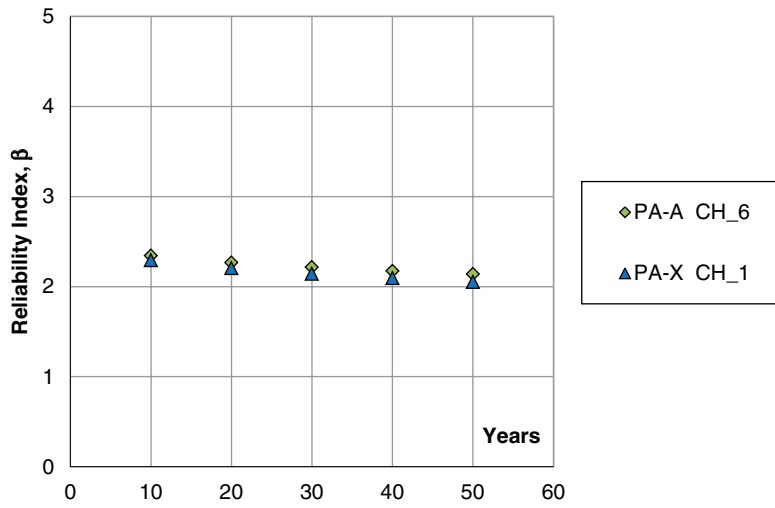


Figure 6-22. Reliability index versus time for Category E', with truncation level > 0.5 ksi.

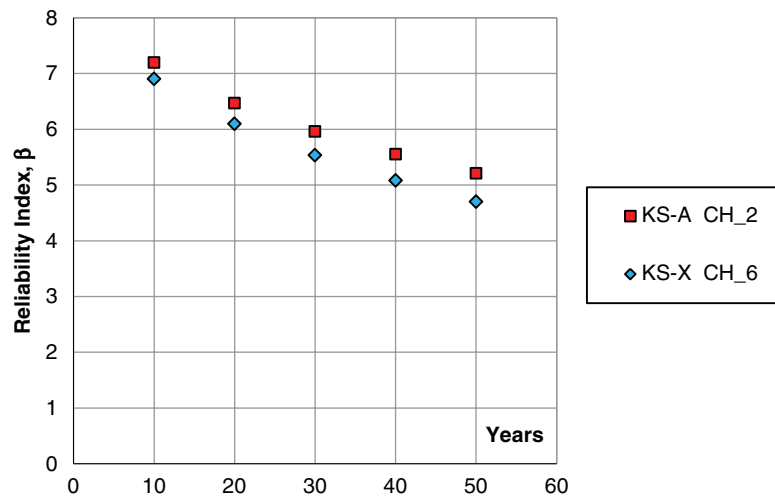


Figure 6-23. Reliability index versus time for Category C, with truncation level > 1.0 ksi.

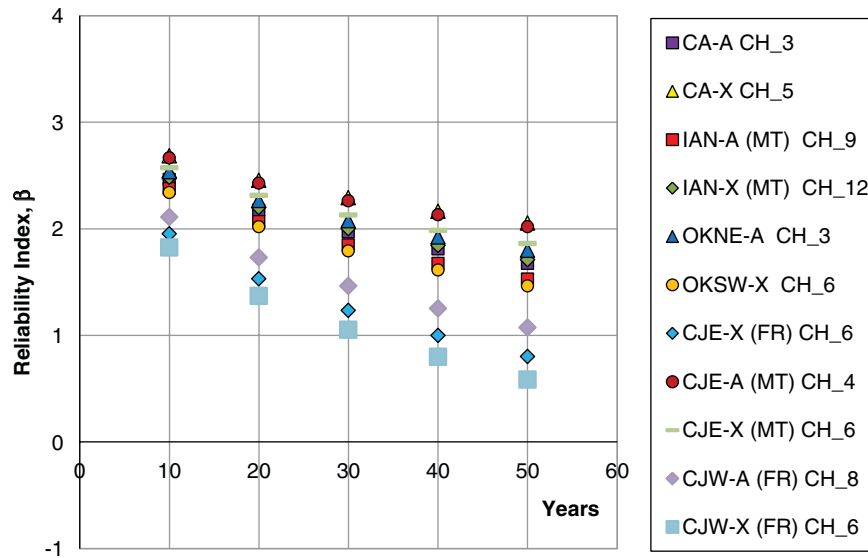


Figure 6-24. Reliability index versus time for Category D, with truncation level > 1.0 ksi.

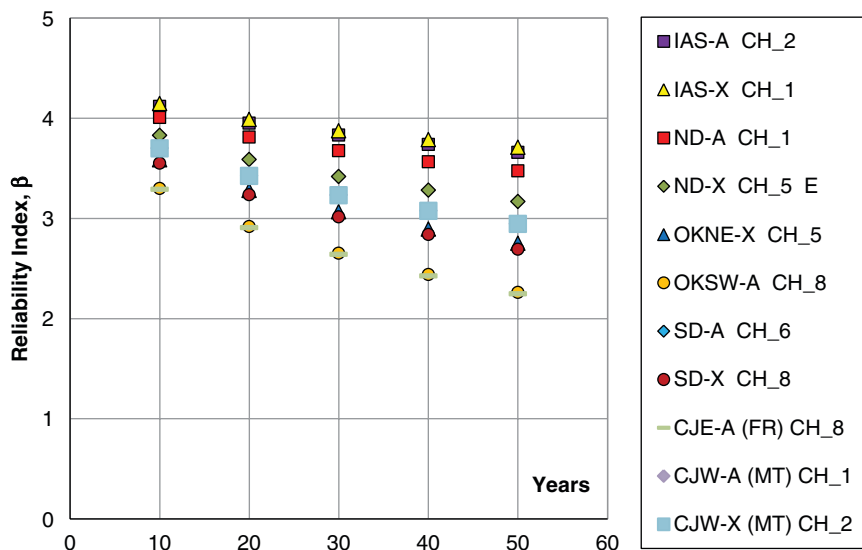


Figure 6-25. Reliability index versus time for Category E, with truncation level > 1.0 ksi.

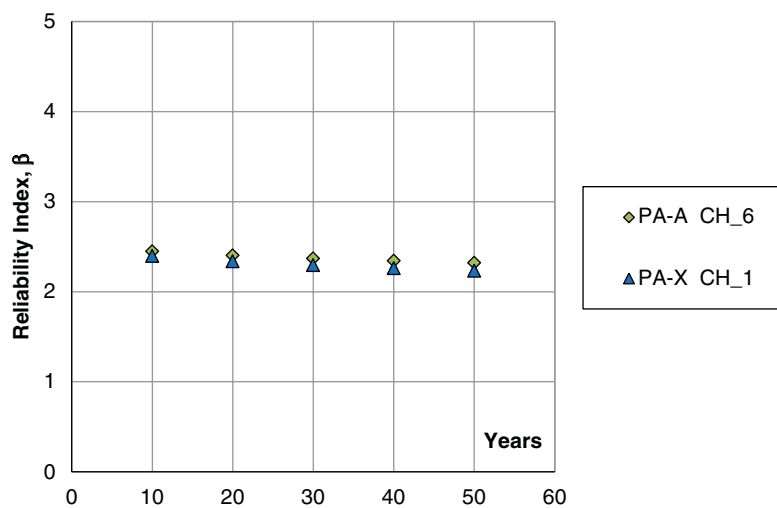


Figure 6-26. Reliability index versus time for Category E', with truncation level > 1.0 ksi.

## SECTION 7

## Reliability Analysis

## LRFD Reliability Analysis—Flexure

The calibration between ASD and LRFD is based on the calibration of ASCE/SEI 7-05 50-year  $V_{50}$  wind speed and ASCE/SEI 7-10 700-year  $V_{700}$  wind speed. The ASCE/SEI 7-10 wind speed maps for a 700-year wind are calibrated to the ASCE/SEI 7-05 50-year wind speed where the difference between LRFD design wind load factors (ASCE/SEI 7-05  $\gamma_W = 1.6$  vs. ASCE/SEI 7-10  $\gamma_W = 1.0$ ) is equal to  $(V_{700}/V_{50})^2 = 1.6$ . Thus, the LRFD ASCE/SEI 7-05  $V_{50}$  wind speed is equivalent (for pressures that are proportional to  $V^2$ ) to the ASCE/SEI 7-10  $V_{700}$ -year wind speed. Likewise, the ASCE/SEI 7-10  $V_{300}$  and  $V_{1700}$  winds speeds are equivalent to ASCE/SEI 7-05  $V_{50}$  wind speeds adjusted for importance [low  $I_{low} = 0.87 = (V_{300}/V_{700})^2$  and high  $I_{high} = 1.15 = (V_{1700}/V_{700})^2$ ]. The ASCE/SEI 7-05  $V_{50}$  wind speed is used as the mean wind speed (adjusted for design map values compared to statistical means) for the reliability analyses.

## Flexural Resistance

The LRFD design requirement for a structure at the optimal design limit is:

$$\phi R_n = \max \left\{ \begin{array}{l} \gamma_{D2} M_D \\ \gamma_{D1} M_D + \gamma_W M_W \end{array} \right.$$

where:

- $R_n$  = nominal resistance,
- $M_D$  = nominal dead load moment,
- $M_W$  = nominal wind load,
- $\gamma_{D1}$  = dead load design load factor (used in conjunction with dead + wind case),
- $\gamma_{D2}$  = dead load design load factor (dead load only case),
- $\gamma_W$  = wind load design load factor, and
- $\phi$  = phi factor.

To meet the design limit, the nominal resistance is:

$$R_n = \max \left\{ \begin{array}{l} \frac{1}{\phi} \gamma_{D2} M_D \\ \frac{1}{\phi} [ \gamma_{D1} M_D + \gamma_W M_W ] \end{array} \right.$$

The mean resistance is:

$$\bar{R} = \lambda_R R_n$$

where:

- $\lambda_R$  = bias factor for strength variable  $R$ , and
- $\bar{R}$  = statistical mean of variable  $R$ .

At the optimal design limit, the mean of  $R$  becomes:

$$\bar{R} = \max \left\{ \begin{array}{l} \frac{\lambda_R}{\phi} \gamma_{D2} M_D \\ \frac{\lambda_R}{\phi} [ \gamma_{D1} M_D + \gamma_W M_W ] \end{array} \right.$$

The coefficient of variation for the strength is  $Cov_R$ .

## Load

The total applied nominal moment at the ASCE/SEI 7-10 700-year wind speed is:

$$M_{T1} = M_D + M_{700}$$

where:

- $M_{T1}$  = total nominal moment at ASCE/SEI 7-10 700-year wind speed,
- $M_D$  = dead load moment, and
- $M_{700}$  = nominal moment from wind at ASCE/SEI 7-10 700-year wind speed.

## A-46

To standardize the comparisons between ASD and LRFD, and for any specified year of wind, all analyses and comparisons are based on the total nominal moment for the LRFD 700-year total applied moment equal to 1.0:

$$M_T = M_D + M_{700} = 1.0$$

and, the dead load moment can be represented by:

$$M_D = 1 - M_{700}$$

The calibration and comparison varies  $M_{700}$  from 1.0 to 0.0, while  $M_D$  varies from 0.0 to 1.0 so that the total applied nominal moment at the ASCE/SEI 7-10 700-year load remains 1.0. The total applied nominal moments for ASD and other LRFD year wind speeds are adjusted to be equivalent to the ASCE/SEI 7-10 700-year wind speed load case.

Given that the nominal moment from wind for any year wind can be determined by:

$$M_{WT} = \left( \frac{V_T}{V_{700}} \right)^2 M_{700}$$

where:

$V_T$  = wind speed for any year  $T$  wind speed, and

$M_{WT}$  = nominal wind moment at any year  $T$ ,

and the total applied nominal moment becomes:

$$M_T = M_D + M_{WT} = (1 - M_{700}) + \left( \frac{V_T}{V_{700}} \right)^2 M_{700}$$

where

$M_T$  = total applied nominal moment at any year  $T$  wind speed.

To determine the mean wind moment for the reliability analyses, the mean moment at the 50-year wind speed is determined from the ASCE/SEI 7-10 wind speed relation:

$$V_T = [0.36 + 0.10 \ln(12T)] V_{50}$$

or:

$$V_{50} = \frac{V_T}{0.36 + 0.10 \ln(12T)} = \lambda_V V_T$$

where:

$\lambda_V$  = bias factor for wind speed at year  $T$ ,

and the nominal wind moment at the 50-year wind speed becomes:

$$M_{50} = \lambda_V^2 M_{700}$$

The nominal moment at the 50-year wind speed is proportional to  $V^2$  by:

$$M_{50} \propto K_d K_z G C_d V_{50}^2$$

where:

$K_d$  = directionality coefficient,

$K_z$  = elevation coefficient,

$G$  = gust factor, and

$C_d$  = drag coefficient.

The mean wind moment for the reliability analyses is:

$$\bar{M}_{50} \propto \bar{K}_d \bar{K}_z \bar{G} \bar{C}_d \bar{V}_{50}^2$$

where the variables are the means. Assuming that  $K_d$  does not vary, the other non-wind speed variables' nominal values are related to the means by the bias factors. Combining them into a single bias factor  $\lambda_p$  gives:

$$\bar{K}_z \bar{G} \bar{C}_d = \lambda_{K_z} \lambda_G \lambda_{C_d} K_z G C_d = \lambda_p K_z G C_d$$

where:

$$\lambda_p = \lambda_{K_z} \lambda_G \lambda_{C_d}$$

and:

$K_d$  does not vary.

Considering that the map design values may differ from the statistical mean of the 50-year wind speed, the mean 50-year wind speed can be represented by:

$$\bar{V}_{50} = \lambda_X V_{50} = \lambda_X \lambda_V V_{700}$$

where:

$\lambda_X = \frac{\mu_{50}}{V_{50}}$  = bias for the 50-year wind speed,

$\mu_{50}$  = mean 50-year wind speed, and

$V_{50}$  = map design 50-year wind speed.

The mean wind moment for the reliability analyses becomes:

$$\bar{M}_{50} = \lambda_p \lambda_V^2 \lambda_X^2 M_{700}$$

where:

$$M_{700} \propto K_d K_z G C_d V_{700}^2$$

Referring back to the basis that all comparisons are equated with a total ASCE/SEI 7-10 applied nominal moment of:

$$M_D + M_{700} = 1$$

and using that the nominal dead load moment and mean dead load moment are:

$$M_D = 1 - M_{700}$$

$$\bar{M}_D = \lambda_D (1 - M_{700})$$

where:

$\lambda_D$  = bias factor for dead load moment.

The mean load effect on the structure becomes:

$$Q = \bar{M}_D + \bar{M}_{50} = \lambda_D (1 - M_{700}) + \lambda_P \lambda_V^2 \lambda_X^2 M_{700}$$

where  $Q$  = the mean moment.

To find the coefficient of variation for  $Q$ , first the coefficient of variation for the mean wind moment is determined from:

$$Cov_{M_{50}} = \sqrt{(2Cov_V)^2 + Cov_{K_z}^2 + Cov_G^2 + Cov_{C_d}^2}$$

Noting that  $V$  in the  $V^2$  term is 100% correlated, and the coefficient of  $V^2$  ( $Cov_V^2$ ) is two times the coefficient of variation of  $V$  ( $Cov_V$ ).

The combination of the statistical properties for the dead and wind moments to determine the coefficient of variation for the total mean moment  $Q$  results in:

$$Cov_Q = \frac{\sigma_Q}{\bar{Q}} = \frac{\sqrt{[Cov_D \lambda_D (1 - M_{700})]^2 + [Cov_{M_{50}} \lambda_P \lambda_V^2 \lambda_X^2 M_{700}]^2}}{\bar{Q}}$$

## Reliability Indices

Assuming  $Q$  and  $R$  are lognormal and independent:

$$\mu_{\ln R} = \ln \bar{R} - \frac{1}{2} \sigma_{\ln R}^2$$

$$\sigma_{\ln R}^2 = \ln(1 + Cov_R^2)$$

$$\mu_{\ln Q} = \ln \bar{Q} - \frac{1}{2} \sigma_{\ln Q}^2$$

$$\sigma_{\ln Q}^2 = \ln(1 + Cov_Q^2)$$

where  $\sigma$  is the standard deviation of the variable indicated.

The reliability index  $\beta$  is:

$$\beta = \frac{\mu_{\ln R} - \mu_{\ln Q}}{\sqrt{\sigma_{\ln R}^2 + \sigma_{\ln Q}^2}} = \frac{\ln\left(\frac{\bar{R}}{\bar{Q}}\right) - \frac{1}{2}(\sigma_{\ln R}^2 + \sigma_{\ln Q}^2)}{\sqrt{\sigma_{\ln R}^2 + \sigma_{\ln Q}^2}}$$

## Implementation

The LRFD reliability analysis was coded into a spreadsheet to study four different regions in the United States:

- Florida Coastal Region,
- Midwest and Western Region,
- Western Coastal Region, and
- Southern Alaska Region.

Inputs for LRFD reliability analyses spreadsheet:

$V_{300}$ ,  $V_{700}$ ,  $V_{1700}$  per ASCE/SEI 7-10 design wind speeds  
 $\mu_{50}$ ,  $V_{\mu 50}$ ,  $V_{50}$  per ASCE/SEI 7-05 design wind speeds

LRFD reliability analyses inputs are in Table 7-1.

Global inputs (for all regions):

$\lambda_D$ ,  $\lambda_R$ ,  $Cov_D$ ,  $Cov_R$   
 $\lambda_{K_z}$ ,  $\lambda_G$ ,  $\lambda_{C_d}$ ,  $Cov_{K_z}$ ,  $Cov_G$ ,  $Cov_{C_d}$   
 $\phi$ ,  $\gamma_{D1}$ ,  $\gamma_{D2}$ ,  $\gamma_W$

Table 7-2 shows the global inputs (inputs are highlighted). The results for the Midwest and Western Region ASCE/SEI 7-10 700-year wind speed are shown in the Table 7-3 (other regions are similar). For the 300-year wind speed, the results are in Table 7-4. Notice that the total nominal moment,  $M_{T_2}$ , is less than 1.0 since the wind moment,  $M_{300}$ , is less than  $M_{700}$ . Likewise, for the 1,700-year wind speed,  $M_{T_2}$  is larger than 1.0 since  $M_{1700}$  is greater than  $M_{700}$ , as shown in Table 7-5 for the Midwest and Western Region.

Using the 300-year wind speed requires less nominal resistance; conversely, using the 1,700-year wind speed increases the required nominal resistance. Because the mean load  $Q$  and its variation do not change, this difference in required nominal resistance changes the reliability indices  $\beta$  accordingly.

**Table 7-1. LRFD reliability analyses inputs.**

	$V_{50}$	$\mu_{50}$	$COV_{\mu 50}$	$V_{300}$	$V_{700}$	$V_{1700}$
Florida Coastal	150	130	0.14	170	180	200
Midwest & West	90	75	0.1	105	115	120
West Coast	85	67	0.095	100	110	115
Southern Alaska	130	110	0.105	150	160	165

Table 7-2. Global inputs.

			COV	BIAS	
BIAS <sub>D</sub>	1.03		COV <sub>kz</sub>	0.16	1.00
COV <sub>D</sub>	0.08		COV <sub>G</sub>	0.11	1.00
BIAS <sub>R</sub>	1.05		COV <sub>Cd</sub>	0.12	1.00
COV <sub>R</sub>	0.10		Total Bias <sub>p</sub>		1.00
	D+W	D Only			
φ	0.90				
γ <sub>D</sub>	1.10	1.25			
γ <sub>w</sub>	1.00				

### ASD Reliability Analysis—Flexure

Because the LRFD reliability analyses are based on the total nominal moment  $M_D + M_{700} = 1.0$ , the ASD analyses must adjust the moments for a consistent comparison.

Using the ASCE/SEI 7-05 criteria for the ASD design, the wind moment for a 50-year wind speed is:

$$DesignM_{50} = M_{700} \left( \frac{DesignV_{50}}{V_{700}} \right)^2$$

Table 7-3. Results for the Midwest and Western Region, 700-year wind speed.

				700 Year Wind		V <sub>700</sub>	115				
				T	700	V <sub>50</sub>	91.00991	Theory			
				BIAS <sub>x</sub>	0.8241	V <sub>700</sub> /V <sub>700</sub>	1.00	(V <sub>700</sub> /V <sub>700</sub> ) <sup>2</sup>			
				COV <sub>v</sub>	0.100	(V <sub>300</sub> /V <sub>700</sub> ) <sup>2</sup>	1.00	1.00			
Equiv				BIAS <sub>v</sub>	0.79						
M <sub>700</sub>	M <sub>T2</sub>	M <sub>700</sub> /M <sub>T2</sub>	R <sub>n</sub>	R	σ <sub>lnR</sub>	Q	COV <sub>M50</sub>	COV <sub>Q</sub>	σ <sub>lnQ</sub>	LRFD β	
1.00	1.00	1.00	1.11	1.17	0.10	0.43	0.30	0.30	0.30	3.35	
0.90	1.00	0.90	1.12	1.18	0.10	0.49	0.30	0.24	0.24	3.54	
0.80	1.00	0.80	1.13	1.19	0.10	0.55	0.30	0.19	0.19	3.69	
0.70	1.00	0.70	1.14	1.20	0.10	0.61	0.30	0.15	0.15	3.77	
0.60	1.00	0.60	1.16	1.21	0.10	0.67	0.30	0.13	0.13	3.75	
0.50	1.00	0.50	1.17	1.23	0.10	0.73	0.30	0.11	0.10	3.60	
0.40	1.00	0.40	1.18	1.24	0.10	0.79	0.30	0.09	0.09	3.34	
0.30	1.00	0.30	1.19	1.25	0.10	0.85	0.30	0.08	0.08	2.98	
0.20	1.00	0.20	1.20	1.26	0.10	0.91	0.30	0.08	0.08	2.57	
0.10	1.00	0.10	1.25	1.31	0.10	0.97	0.30	0.08	0.08	2.38	
0.00	1.00	0.00	1.39	1.46	0.10	1.03	0.30	0.08	0.08	2.71	

Table 7-4. Results for the Midwest and Western Region, 300-year wind speed.

				300 Year Wind		V <sub>300</sub>	105				
				T	300			Theory			
						V <sub>300</sub> /V <sub>700</sub>	0.91	(V <sub>300</sub> /V <sub>700</sub> ) <sup>2</sup>			
						(V <sub>300</sub> /V <sub>700</sub> ) <sup>2</sup>	0.83	0.87			
Equiv											
M <sub>300</sub>	M <sub>T2</sub>	M <sub>300</sub> /M <sub>T2</sub>	R <sub>n</sub>	R	σ <sub>lnR</sub>	Q	COV <sub>M50</sub>	COV <sub>Q</sub>	σ <sub>lnQ</sub>	LRFD β	
0.83	0.83	1.00	0.93	0.97	0.10	0.43	0.30	0.30	0.30	2.77	
0.75	0.85	0.88	0.96	1.00	0.10	0.49	0.30	0.24	0.24	2.92	
0.67	0.87	0.77	0.99	1.03	0.10	0.55	0.30	0.19	0.19	3.04	
0.58	0.88	0.66	1.02	1.07	0.10	0.61	0.30	0.15	0.15	3.11	
0.50	0.90	0.56	1.04	1.10	0.10	0.67	0.30	0.13	0.13	3.12	
0.42	0.92	0.45	1.07	1.13	0.10	0.73	0.30	0.11	0.10	3.03	
0.33	0.93	0.36	1.10	1.16	0.10	0.79	0.30	0.09	0.09	2.86	
0.25	0.95	0.26	1.13	1.19	0.10	0.85	0.30	0.08	0.08	2.61	
0.17	0.97	0.17	1.16	1.22	0.10	0.91	0.30	0.08	0.08	2.32	
0.08	0.98	0.08	1.25	1.31	0.10	0.97	0.30	0.08	0.08	2.38	
0.00	1.00	0.00	1.39	1.46	0.10	1.03	0.30	0.08	0.08	2.71	

**Table 7-5. Results for the Midwest and Western Region, 1,700-year wind speed.**

				1700 Year Wind		$V_{1700}$	120				
				T	1700			Theory			
						$V_{1700}/V_{700}$	1.04	$(V_{1700}/V_{700})^2$			
						$(V_{1700}/V_{700})^2$	1.09	1.15			
Equiv											
$M_{1700}$	$M_{T2}$	$M_{1700}/M_{T2}$	$R_n$	R	$\sigma_{lnR}$	Q	$COV_{M50}$	$COV_Q$	$\sigma_{lnQ}$	LRFD $\beta$	
1.09	1.09	1.00	1.21	1.27	0.10	0.43	0.30	0.30	0.30	3.62	
0.98	1.08	0.91	1.21	1.27	0.10	0.49	0.30	0.24	0.24	3.84	
0.87	1.07	0.81	1.21	1.27	0.10	0.55	0.30	0.19	0.19	4.01	
0.76	1.06	0.72	1.21	1.27	0.10	0.61	0.30	0.15	0.15	4.09	
0.65	1.05	0.62	1.21	1.28	0.10	0.67	0.30	0.13	0.13	4.06	
0.54	1.04	0.52	1.22	1.28	0.10	0.73	0.30	0.11	0.10	3.89	
0.44	1.04	0.42	1.22	1.28	0.10	0.79	0.30	0.09	0.09	3.58	
0.33	1.03	0.32	1.22	1.28	0.10	0.85	0.30	0.08	0.08	3.17	
0.22	1.02	0.21	1.22	1.28	0.10	0.91	0.30	0.08	0.08	2.69	
0.11	1.01	0.11	1.25	1.31	0.10	0.97	0.30	0.08	0.08	2.38	
0.00	1.00	0.00	1.39	1.46	0.10	1.03	0.30	0.08	0.08	2.71	

Considering that the design  $V_{50}$  may differ from  $V_{50} = (\lambda_V)^2 V_{700}$ , a bias factor,  $\lambda_{Design}$ , is introduced, and:

$$DesignM_{50} = \lambda_{Design}^2 \left( \frac{V_{50}}{V_{700}} \right)^2 M_{700} = \lambda_{Design}^2 \lambda_V^2 M_{700}$$

$$\lambda_{Design} = \frac{DesignV_{50}}{V_{50}}$$

The total ASD design moment,  $M_{T3}$ , consistent with  $M_D + M_{700} = 1.0$ , becomes:

$$M_{T3} = M_D + DesignM_{50} = (1 - M_{700}) + \lambda_{Design}^2 \lambda_V^2 M_{700}$$

## Resistance

The LRFD nominal resistance is assumed to be the plastic moment capacity. To directly compare resistances between LRFD and ASD sections, the nominal resistance for the ASD design is increased by the section shape factor for a compact section:

$$R_n = SF M_y$$

where  $SF$  is the shape factor.

The allowable stress for a compact section using the allowed overstress factor (OSF) of 4/3 for wind loads is:

$$F_{allow} = \frac{4}{3} (0.66) F_y = (OSF)(0.66) F_y$$

Using moments instead of stresses, the allowable moment is  $OSF(0.66) M_y$ , and the design requirement for an optimal design is:

$$(OSF)(0.66) M_y = M_D + DesignM_{50} I$$

where:

$I = I_{low} = 0.87$  (low importance) comparable to ASCE/SEI 7-10 300-year wind speed,

$I = I_{med} = 1.00$  (medium importance) comparable to ASCE/SEI 7-10 700-year wind speed, and

$I = I_{high} = 1.15$  (high importance) comparable to ASCE/SEI 7-10 1,700-year wind speed.

The nominal resistance (to directly compare to the LRFD design) is determined by increasing the design strength by the shape factor:

$$R_n = SF M_y = \frac{SF}{OSF} \frac{1}{0.66} [(1 - M_{700}) + \lambda_{Design}^2 \lambda_V^2 M_{700} I]$$

For the ASD reliability analyses, the statistical properties are:

$$\bar{R} = \lambda_R R_n$$

and:

$Q$ ,  $COV_Q$ , and  $\sigma_{lnQ}$  are unchanged

The coefficient of variation for the strength (resistance) is  $COV_R$ .

**Table 7-6. Results for the Midwest and Western Region for medium importance.**

LRFD				ASD		Strength	
				Total Design		Ratio	
Equiv				Moment		$R_{nLRFD}$	
$R_{nLRFD}$	$M_{50}$	$M_{T3}$	$M_{50}/M_{T3}$	$M_D + M_{50}I$	$R_{nASD}$	$R_{nASD}$	ASD $\beta$
1.11	0.61	0.61	1.00	0.61	0.90	1.23	2.69
1.12	0.55	0.65	0.85	0.65	0.96	1.17	2.94
1.13	0.49	0.69	0.71	0.69	1.02	1.11	3.20
1.14	0.43	0.73	0.59	0.73	1.08	1.06	3.44
1.16	0.37	0.77	0.48	0.77	1.13	1.02	3.63
1.17	0.31	0.81	0.38	0.81	1.19	0.98	3.74
1.18	0.24	0.84	0.29	0.84	1.25	0.94	3.77
1.19	0.18	0.88	0.21	0.88	1.31	0.91	3.71
1.20	0.12	0.92	0.13	0.92	1.36	0.88	3.57
1.25	0.06	0.96	0.06	0.96	1.42	0.88	3.39
1.39	0.00	1.00	0.00	1.00	1.48	0.94	3.19

The equations for determining the reliability indices are identical to those used for the LRFD cases.

### Implementation

For the four regions, the ASD reliability analyses require additional inputs.

Inputs for ASD are:

- Importance factors  $I_{low} = 0.87$ ,  $I_{med} = 1.00$ , and  $I_{high} = 1.15$ ;
- Shape factor  $SF = Z_x/S_x = 1.30$  for a circular section; and
- Wind overstress factor  $OSF = 4/3 = 1.333$ .

The results for the Midwest and Western Region ASCE/SEI 7-05 medium importance  $I_{med} = 1.00$  are shown in Table 7-6.

The LRFD-required nominal strength is shown for direct comparison. For the Midwest and Western Region for low importance  $I_{low} = 0.87$ , the results are as shown in Table 7-7.

Notice that the total nominal moment,  $M_{T3}$ , does not change, but the total design moment  $M_D + M_{50}I$  changes with the importance factor, resulting in different required nominal strength  $R_n$ . Similarly for high importance, the required nominal strength  $R_n$  increases as shown in Table 7-8 for the Midwest and Western Region.

**Table 7-7. Results for the Midwest and Western Region for low importance.**

				Bias <sub>Des</sub> =		0.988903	
LRFD				ASD		Strength	
				Total Design		Ratio	
Equiv				Moment		$R_{nLRFD}$	
$R_{nLRFD}$	$M_{50}$	$M_{T3}$	$M_{50}/M_{T3}$	$M_D + M_{50}I$	$R_{nASD}$	$R_{nASD}$	ASD $\beta$
0.93	0.61	0.61	1.00	0.53	0.79	1.18	2.25
0.96	0.55	0.65	0.85	0.58	0.86	1.12	2.49
0.99	0.49	0.69	0.71	0.63	0.93	1.07	2.75
1.02	0.43	0.73	0.59	0.67	0.99	1.02	3.00
1.04	0.37	0.77	0.48	0.72	1.06	0.98	3.23
1.07	0.31	0.81	0.38	0.77	1.13	0.95	3.39
1.10	0.24	0.84	0.29	0.81	1.20	0.92	3.48
1.13	0.18	0.88	0.21	0.86	1.27	0.89	3.49
1.16	0.12	0.92	0.13	0.91	1.34	0.87	3.43
1.25	0.06	0.96	0.06	0.95	1.41	0.89	3.33
1.39	0.00	1.00	0.00	1.00	1.48	0.94	3.19

**Table 7-8. Results for the Midwest and Western Region for high importance.**

LRFD				ASD			
Equiv				Total Design			
Moment				Ratio			
$R_{nLRFD}$	$M_{50}$	$M_{T3}$	$M_{50}/M_{T3}$	$M_D+M_{50I}$	$R_{nASD}$	$R_{nLRFD}$	ASD $\beta$
1.21	0.61	0.61	1.00	0.70	1.04	1.16	3.14
1.21	0.55	0.65	0.85	0.73	1.08	1.12	3.41
1.21	0.49	0.69	0.71	0.76	1.13	1.07	3.67
1.21	0.43	0.73	0.59	0.79	1.17	1.04	3.90
1.21	0.37	0.77	0.48	0.82	1.22	1.00	4.06
1.22	0.31	0.81	0.38	0.85	1.26	0.97	4.13
1.22	0.24	0.84	0.29	0.88	1.30	0.93	4.09
1.22	0.18	0.88	0.21	0.91	1.35	0.91	3.94
1.22	0.12	0.92	0.13	0.94	1.39	0.88	3.73
1.25	0.06	0.96	0.06	0.97	1.43	0.87	3.47
1.39	0.00	1.00	0.00	1.00	1.48	0.94	3.19

The importance factors directly change the required nominal resistances. Because the mean load  $Q$  and its variation does not change (not shown in these tables and the same as in the LRFD tables), this difference in required nominal resistances changes the reliability indices  $\beta$  accordingly.

## Calibration and Comparison

Using the proposed flexure load and resistance factors, and with the statistical properties incorporated into the reliability analyses, the plots in Figure 7-1 compare the reliability indices for the four regions between current ASD design procedures and the proposed LRFD procedures. The *Minimum Beta* plots represent the minimum indices over the four regions. Similarly, the *Average Beta* plots show the averages over the four regions. For the LRFD 300-year, 700-year, and 1,700-year wind speed cases, the equivalent ASD designs use  $I_{low} = 0.87$ ,  $I_{med} = 1.00$ , and  $I_{high} = 1.15$  importance factors, respectively.

The proposed LRFD procedures result in comparable but more consistent reliability over the range of designs. For low-importance structures (using 300-year wind speeds), the reliability indices are lower, as intended. Likewise, for higher-importance structures (1,700-year wind speeds), the reliability indices are higher. This is shown in Figure 7-2 for the LRFD procedures. The ratios are the averages over the four regions.

At low wind moments ( $\gamma_{D2}M_D$  controls the design), there is no difference. However, for higher wind moments, the required strength increases for high-importance structures and decreases for lower-importance structures.

As expected, the LRFD-required strength at a higher percentage of wind load ( $M_{Wind}/M_{Total}$  high) is greater than that

required for ASD. This behavior is demonstrated in Figure 7-3, where the ratios are the average for the four regions.

At a total moment where the wind is responsible for approximately 60% or more of the total, the proposed LRFD procedures will require more section capacity than the current ASD procedures. Below 60%, the LRFD procedures will require less section capacity than ASD.

## LRFD Reliability Analysis—Torsion

The torsion analysis is similar to the flexure analysis, with a few caveats. The loading  $Q$  (in a torsional sense) and its associated variability do not change. However, two differences from flexure are recommended in the proposed LRFD procedures. First, the bias factor and the phi factor are changed to 0.95 (from 0.90) and 1.10 (from 1.05). This is due to the use of the elastic capacity,  $T_n = C(0.60F_y)$ , instead of the plastic capacity, for the nominal torsion resistance  $T_n$  with this adjustment; a shape factor of 1.0 is used with the plastic limit for both LRFD and ASD.

### Strength

The required nominal resistance and the mean resistance become:

$$\phi T_n = \max \begin{cases} \frac{1}{\phi} \gamma_{D2} M_D \\ \frac{1}{\phi} [\gamma_{D1} M_D + \gamma_w M_w] \end{cases}$$

$$\bar{T} = \lambda_R T_n$$

The coefficient of variation for the resistance remains at  $Cov_R$ .

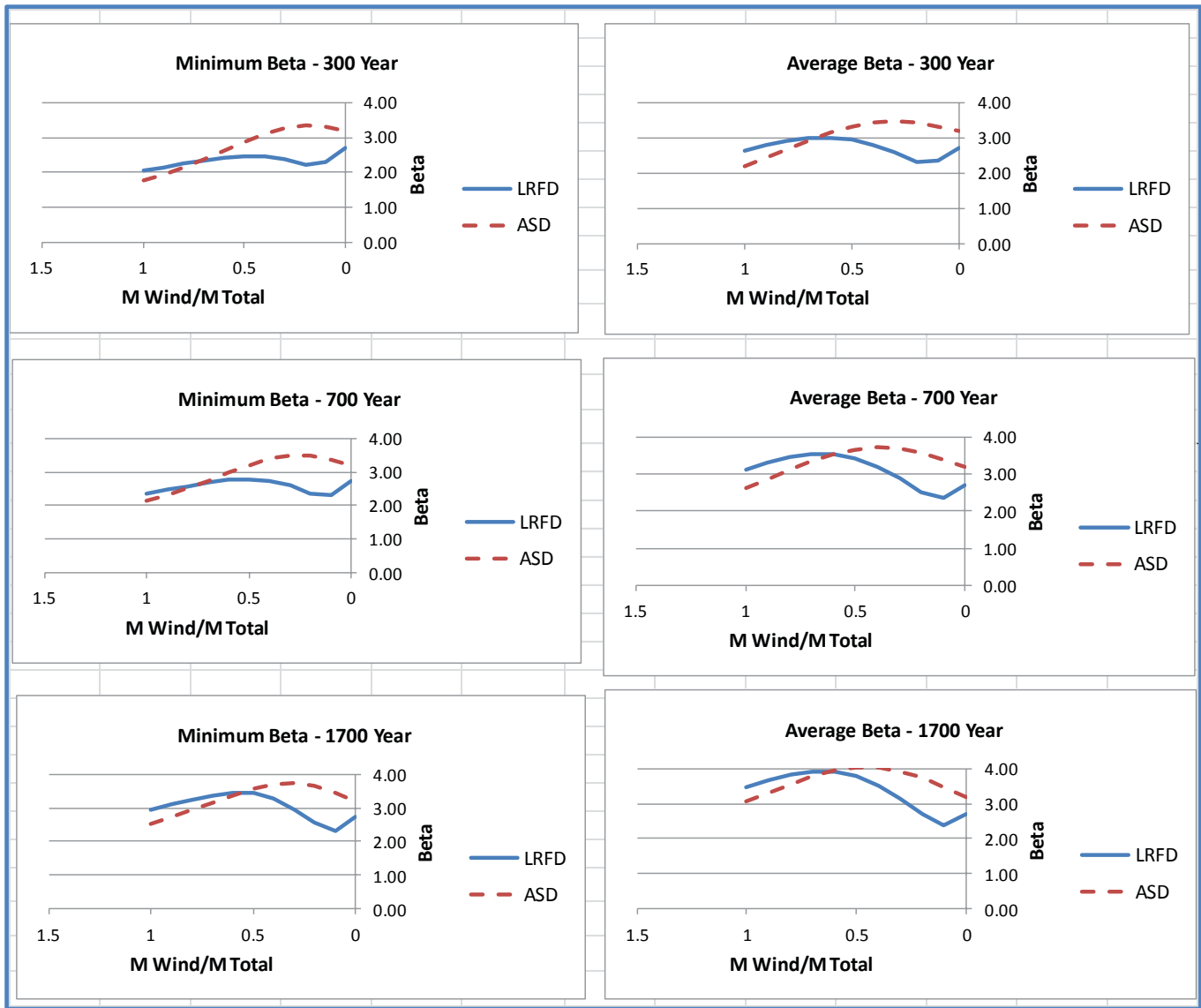


Figure 7-1. Minimum and average reliability indices.

### LRFD Required Resistance Ratios ( $R_nT/R_n700$ )

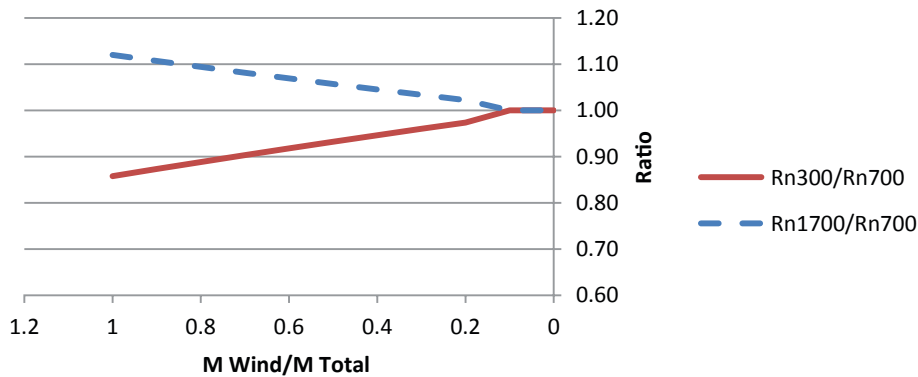


Figure 7-2. Resistance ratios for different return periods.

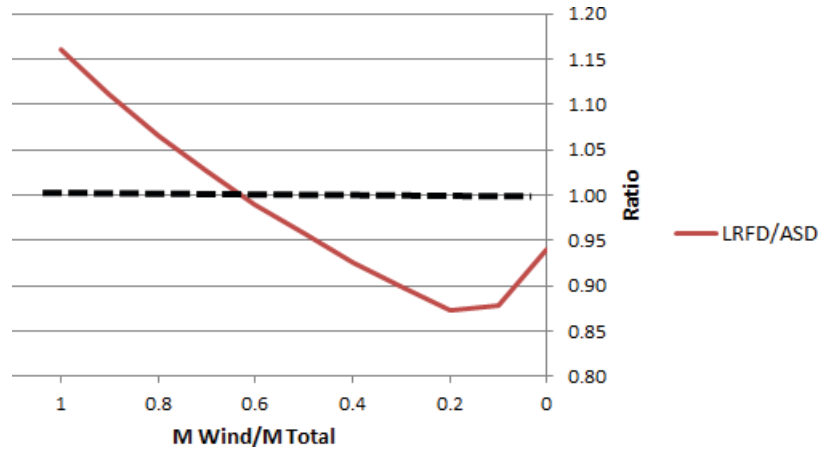


Figure 7-3. Required resistance ratios.

**Load**

Torsion acts similar to flexural moment. Thus:

$$\bar{Q} = \bar{M}_D + \bar{M}_{50} = \lambda_D (1 - M_{700}) + \lambda_P \lambda_V^2 \lambda_X^2 M_{700}$$

$$Cov_Q = \frac{\sigma_Q}{\bar{Q}} = \frac{\sqrt{[Cov_D \lambda_D (1 - M_{700})]^2 + [Cov_{M_{50}} \lambda_P \lambda_V^2 \lambda_X^2 M_{700}]^2}}{\bar{Q}}$$

where *M* is now a torsional moment. The reliability indices equations remain the same as presented for flexure.

**Implementation**

The reliability analyses were coded into a spreadsheet for the four regions where the inputs are the same except for the aforementioned changes, as shown in Table 7-9 (inputs are highlighted).

In Table 7-10, only the results for the Midwest and Western Region ASCE/SEI 7-10 700-year wind speed are shown

Table 7-9. Statistical parameters.

			COV	BIAS
BIAS <sub>D</sub>	1.03	COV <sub>kz</sub>	0.16	1.00
COV <sub>D</sub>	0.08	COV <sub>G</sub>	0.11	1.00
BIAS <sub>R</sub>	1.10	COV <sub>Cd</sub>	0.12	1.00
COV <sub>R</sub>	0.10		Total Bias <sub>p</sub>	1.00
	D+W	D Only		
φ	0.95			
γ <sub>D</sub>	1.10	1.25		
γ <sub>w</sub>	1.00			

because the reliability indices are nearly identical to the flexural cases shown previously.

All of the other regions and wind speed cases show similar results in comparison to the flexural analyses.

**ASD Reliability Analysis—Torsion**

For the calibration and comparison to ASD, again, the load does not change. However, the strength equations are different enough between flexure and torsion that the comparison is necessary.

**Strength**

The ASD allowable torsion stress for a compact section, and using the OSF of 4/3 for wind loads is:

$$F_{allow} = \frac{4}{3} (0.33) F_y = (OSF) (0.33) F_y$$

Given the LRFD elastic strength stress limit of 0.60*F<sub>y</sub>* and the ASD allowable torsion stress of 0.33*F<sub>y</sub>*, the equivalent ASD factor of safety for torsion becomes 1.818 (0.60/0.33) instead of the flexural case of 1.515 (1/0.66). Thus, the nominal resistance for the ASD torsion case becomes:

$$T_n = SF M_y = \frac{SF}{OSF} \frac{1}{0.55} [(1 - M_{700}) + \lambda_{Design}^2 \lambda_V^2 M_{700} I]$$

For the ASD reliability analyses, the statistical properties are:

$$\bar{T} = \lambda_R T_n$$

and: *Q*, *Cov<sub>Q</sub>*, and *σ<sub>lnQ</sub>* are unchanged.

**Table 7-10. Computed values ( $V_{700}$ ).**

				700 Year Wind		$V_{700}$	115			
				T	700	$V_{50}$	91.00991	Theory		
				BIAS <sub>x</sub>	0.8241	$V_{700}/V_{700}$	1.00	$(V_{700}/V_{700})^2$		
				COV <sub>v</sub>	0.100	$(V_{300}/V_{700})^2$	1.00	1.00		
Equiv				BIAS <sub>v</sub>	0.79					
$M_{700}$	$M_{T_2}$	$M_{700}/M_{T_2}$	$R_n$	R	$\sigma_{lnR}$	Q	COV <sub>M50</sub>	COV <sub>Q</sub>	$\sigma_{lnQ}$	LRFD $\beta$
1.00	1.00	1.00	1.05	1.16	0.10	0.43	0.30	0.30	0.30	3.32
0.90	1.00	0.90	1.06	1.17	0.10	0.49	0.30	0.24	0.24	3.51
0.80	1.00	0.80	1.07	1.18	0.10	0.55	0.30	0.19	0.19	3.66
0.70	1.00	0.70	1.08	1.19	0.10	0.61	0.30	0.15	0.15	3.73
0.60	1.00	0.60	1.09	1.20	0.10	0.67	0.30	0.13	0.13	3.70
0.50	1.00	0.50	1.11	1.22	0.10	0.73	0.30	0.11	0.10	3.55
0.40	1.00	0.40	1.12	1.23	0.10	0.79	0.30	0.09	0.09	3.28
0.30	1.00	0.30	1.13	1.24	0.10	0.85	0.30	0.08	0.08	2.92
0.20	1.00	0.20	1.14	1.25	0.10	0.91	0.30	0.08	0.08	2.51
0.10	1.00	0.10	1.18	1.30	0.10	0.97	0.30	0.08	0.08	2.32
0.00	1.00	0.00	1.32	1.45	0.10	1.03	0.30	0.08	0.08	2.65

The coefficient of variation for the strength (resistance) is  $Cov_R$ .

The equations for determining the reliability indices are identical to those used for the LRFD cases.

### Implementation

For the four regions, the ASD reliability analyses require the same additional inputs as for the flexure analyses, except the shape factor is equal to 1.0.

The results for the Midwest and Western Region ASCE/SEI 7-05 medium importance  $I_{med} = 1.00$  is shown in Table 7-11.

The torsional indices are nearly identical to the flexural reliability indices for the different load cases for the four regions.

### Calibration and Comparison

Using the proposed torsion load and resistance factors, and with the statistical properties incorporated into the reliability analyses, the plots in Figure 7-4 compare the reliability indices for the four regions between current ASD design procedures and the proposed LRFD procedures. The *Minimum Beta* plots represent the minimum indices over the four regions. The

**Table 7-11. Results for the Midwest and Western Region for medium importance.**

LRFD				ASD		Strength	
				Total Design		Ratio	
Equiv				Moment		$\frac{R_{nLRFD}}{R_{nASD}}$	
$R_{nLRFD}$	$M_{50}$	$M_{T_3}$	$M_{50}/M_{T_3}$	$M_D+M_{50}$	$R_{nASD}$	$R_{nASD}$	ASD $\beta$
1.05	0.61	0.61	1.00	0.61	0.84	1.26	2.58
1.06	0.55	0.65	0.85	0.65	0.89	1.20	2.81
1.07	0.49	0.69	0.71	0.69	0.94	1.14	3.04
1.08	0.43	0.73	0.59	0.73	0.99	1.09	3.25
1.09	0.37	0.77	0.48	0.77	1.05	1.05	3.42
1.11	0.31	0.81	0.38	0.81	1.10	1.01	3.51
1.12	0.24	0.84	0.29	0.84	1.15	0.97	3.52
1.13	0.18	0.88	0.21	0.88	1.21	0.93	3.45
1.14	0.12	0.92	0.13	0.92	1.26	0.90	3.31
1.18	0.06	0.96	0.06	0.96	1.31	0.90	3.13
1.32	0.00	1.00	0.00	1.00	1.36	0.96	2.93

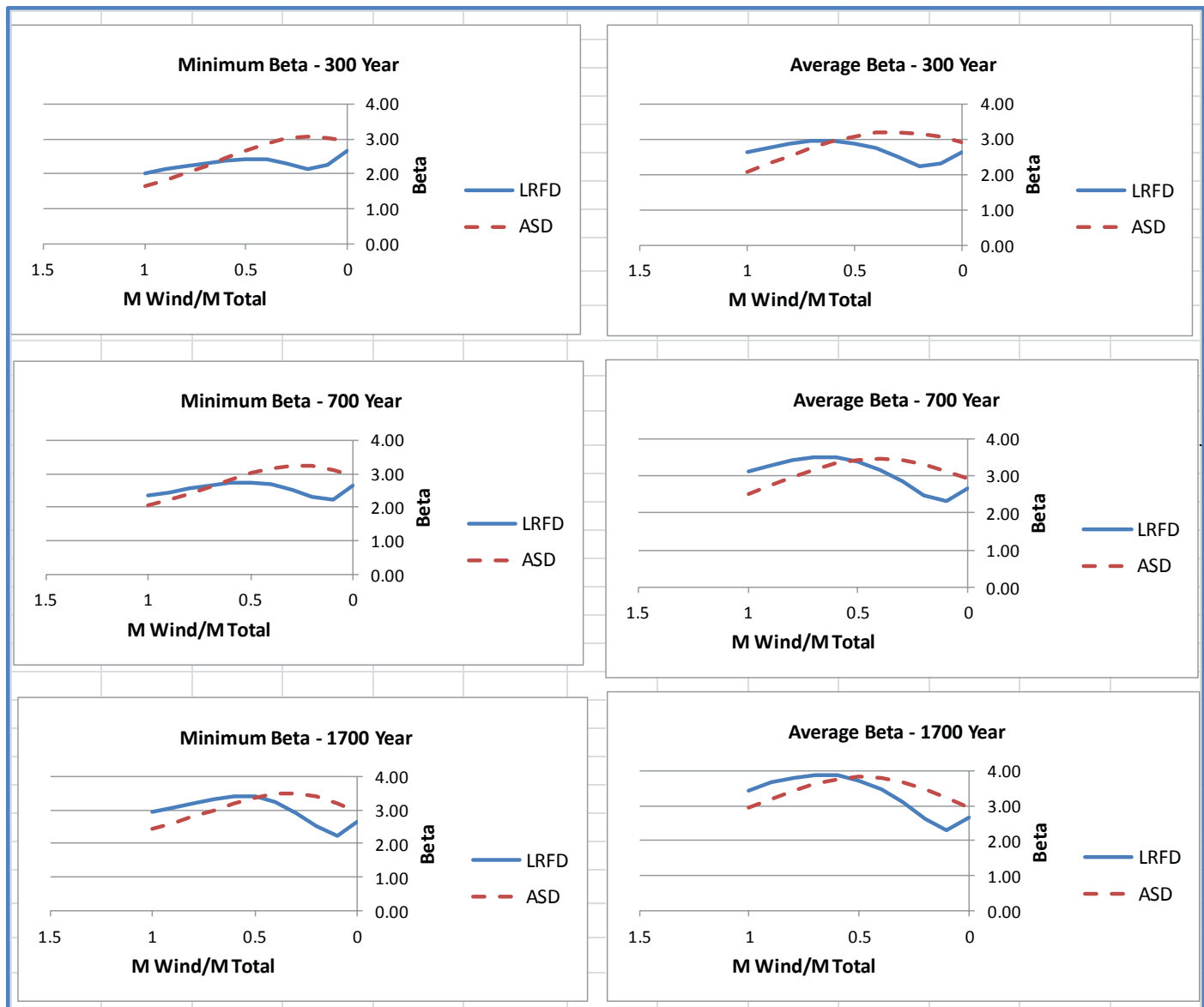


Figure 7-4. Reliability indices for torsion.

Average Beta plots show the averages over the four regions. For the LRFD 300-year, 700-year, and 1,700-year wind speed cases, the equivalent ASD designs use  $I_{low} = 0.87$ ,  $I_{med} = 1.00$ , and  $I_{high} = 1.15$  importance factors, respectively.

The proposed LRFD procedures result in comparable but more consistent reliability over the range of designs for torsion compared to the flexural analyses.

The discussion on flexure in terms of comparisons with ASD and required strengths also applies to torsion.

### LRFD Flexure-Shear Interaction

Monte Carlo simulation (using a spreadsheet) was used to verify target reliability when there is a presence of moment and torsion. It was assumed that the flexural moment com-

prised dead and wind load moment, and that the torsion was from wind load only. This would be consistent with a traffic signal mast arm and pole structure. The interaction design equation limit is in the form:

$$\left( \frac{\gamma_{D1}M_D + \gamma_W M_W}{\phi R_n} \right) + \left( \frac{\gamma_W T_W}{\phi_T T_n} \right)^2 \leq 1.0$$

At the optimum design, the interaction is equal to 1.0. Thus, there is a combination of a certain amount of flexure and a certain amount of torsion that results in an optimum design. Using the flexure and torsion analyses shown previously, where the design capacity  $\phi M_n = [\gamma_{D1}M_D + \gamma_W M_W]$  and  $\phi_T T_n = [\gamma_{D1}M_D + \gamma_W M_W]$  are based on the factored loads (resulting in a performance ratio of 1.0 for the individual

designs), this can be represented by the percentages  $a$  and  $b$  shown as:

$$\left( \frac{a(\gamma_{D1}M_D + \gamma_W M_W)}{\phi R_n} \right) + \left( \frac{b(\gamma_W T_W)}{\phi_T T_n} \right)^2 = a + b^2 = 1.0$$

The terms  $a$  and  $b$  represent the percentage of flexure and torsion, respectively. For instance, if the factored applied flexural moment is 70% of the design capacity ( $a = 0.70$ ), then the factored applied torsion moment would be at 54.8% ( $a + b^2 = 1.0$ ) of the torsion design capacity for an optimal design.

For the reliability analyses, the limit-state equation for the design limit is:

$$\frac{a(M_D + M_W)}{M} + \left( \frac{b(T_W)}{T} \right)^2 \leq 1$$

Each term is a random variable with its associated log-normal statistical properties. The properties are determined from the previous flexure and torsion analyses.

Failure is represented by the limit-state equation exceeding 1.0. The contribution from flexure is the total applied moment compared to the strength and is represented by the term  $a$  from the design limit. The contribution from torsion is the total applied torsion compared to the strength and is represented by the term  $b$  from the design limit. The terms for the flexure moment and strength and the torsion moment and strength can be determined from the previous analyses. The torsion values are for the 100% wind load case. For the flexure values, a choice must be made on percentage of wind and dead load moment.

### Monte Carlo Moment/Shear Interaction Simulation

The reliability analysis for the moment-shear interaction is demonstrated (see Table 7-12). The LRFD ASCE/SEI 7-10

**Table 7-12. Inputs for wind-to-total-load effect ratio.**

		Midwest & Western Region	
		$M_{700}/M_{T1}$	$M_D/M_{T1}$
% Wind of		0.60	0.40
Total Flexure Moment			
% Flexure in Interaction Eqn			
a	b		
0.7	0.548		

700-year wind speed is used for the Midwest and Western Region with the wind load representing 60% of the total  $M_D + M_{700} = 1.0$  ( $M_{700} = 0.60$  and  $M_D = 0.40$ ). The flexure contribution to the interaction is 70% ( $a = 0.70$ ,  $b = 0.548$ ).

The statistical properties for the flexural dead and wind load effects, the torsional wind, and the strengths are as shown in Table 7-13.

Monte Carlo simulation was used for each of the random variables and combines the terms, along with the  $a$  and  $b$  percentage terms, into the interaction equation. To verify the inputs and the analysis, for 10,000 samples, the statistical results shown in Table 7-14 are determined for each of the variables.

Because the analysis computes values for flexure, torsion, and the interaction, the flexure-only case and the torsion-only case can also be verified, along with determining the reliability index for the interaction equation. For instance, the probability distribution for the flexure-only case is shown in Figure 7-5.

Collecting the data and checking for samples that exceed the limit of 1.0 results in typical percentage of failures of 0.0001, which represents a reliability index of  $\beta = 3.72$ . The reliability index determined from the associated flexure analy-

**Table 7-13. Intermediate computations.**

Parameter	$M_D$	$M_W$	$M_{T1}$	$M_n$	T	$T_n$
Assigned						
Mean	0.41	0.26	0.67	1.21	0.43	1.16
COV	0.08	0.30		0.10	0.30	0.10
Std Dev	0.03	0.08		0.12	0.13	0.12
$\mu_{lnX}$	-0.89	-1.41		0.19		0.14
$\sigma_{lnX}$	0.08	0.29		0.10		0.10

**Table 7-14. Intermediate computations.**

Computed	$M_D$	$M_W$	$M_{T1}$	$M_n$	T	$T_n$
Mean	0.41	0.25	0.67	1.21	0.42	1.16
COV	0.08	0.30	0.13	0.10	0.30	0.10
Std Dev	0.03	0.08	0.08	0.12	0.13	0.12

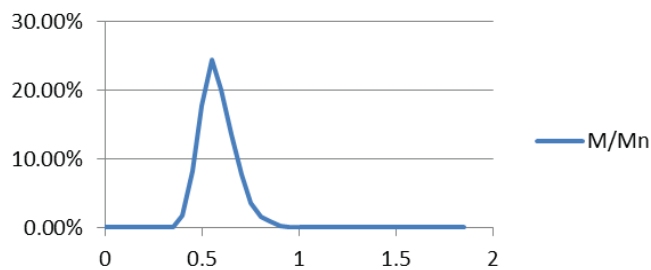


**Figure 7-5. Monte Carlo-generated probability density for flexure only.**

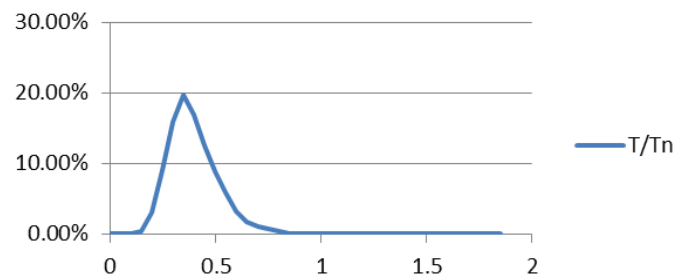


**Figure 7-6. Monte Carlo-generated probability density for torsion only.**

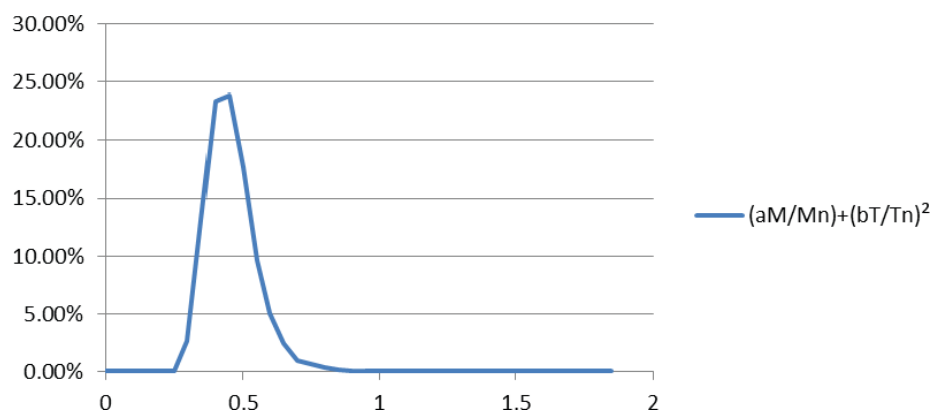


**Figure 7-7. Monte Carlo-generated probability density for moment-torsion interaction only**

sis is  $\beta = 3.75$ . For the torsion case of wind load only, typical percentage of failures is 0.0004, which represents a reliability index of  $\beta = 3.35$ . The reliability index determined from the associated torsion analysis is  $\beta = 3.32$ , with the probability distribution shown in Figure 7-6. This confirms the equation-based analysis in an independent manner.

The interaction probability density results are similar. Application of the interaction equation with the individual

variable sample values results in the probability distribution shown in Figure 7-7.

Collecting the data and checking for samples that exceed the limit of 1.0 results in typical percentage of failures of 0.0003, which represents a reliability index of  $\beta = 3.43$ . The results demonstrate that the reliability indices for moment-torsion interaction are consistent with the moment-only and torsion-only cases.

## SECTION 8

## Implementation

**Setting Target Reliability Indices**

The statistical characterization of the limit-state equation and the associated inputs are presented in the preceding sections. The reliability indices are computed based on the current ASD practice and the LRFD-LTS specifications. The comparisons made and presented previously are based on the recommended load and resistance factors. These factors are illustrated for the 700-year wind speeds (MRI = 700 years). This MRI is for the typical structure; however, some consideration is warranted for structures that are located on travelways with low ADT and/or that are located away from the travelway, whereby failure is unlikely to be a traveler safety issue. Similarly, consideration is also warranted for structures that are located on heavily traveled roads where a failure has a significant chance of harming travelers and/or suddenly stopping traffic, creating an event that causes a traffic collision with the structure and likely chain-reaction impacts of vehicles.

Ultimately, judgment is used to set the target reliability indices for the different applications. This is often based on typical average performance under the previous design specifications (i.e., ASD). However, even in the ASD methods, an importance factor was considered: 0.87 and 1.15 for less important and more important applications, respectively. Some variations are also considered for hurricane versus non-hurricane regions.

There were similar concerns for the LRFD-LTS specifications' assignment of the MRI considered for design. Less important structures are assigned an MRI of 300, while an important structure uses an MRI of 1,700-years. Typical structures are assigned an MRI of 700 years.

The description of this implementation is provided next with the resulting reliability indices for each region.

**Implementation into Specifications**

The possible structure locations were divided into two primary categories:

1. Failures where a structure is likely to cross the travelway and, within those structures, those that are located on a typical travelway versus a lifeline travelway, which are those that are critical for emergency use/egress; and
2. Failures where a structure cannot cross the travelway and that, consequently, are of lesser importance.

Within these categories, the ADT is used to further distinguish the consequence of failure. The traffic speed was initially considered in the research but was not used in the final work based on simplicity and judgment. Table 8-1 summarizes this approach.

From this design approach, Table 8-1 establishes the MRI and the associated wind maps. The maps provide the design wind speed based on the structure's location.

**Computed Reliability Indices**

Based on the load and resistance statistical characteristics, the reliability indices  $\beta$  are computed for the four regions for a wind-to-total-load ratio of 0.5 and 1.0. The 0.5 ratio is typical of traffic signal poles, and the 1.0 ratio is typical of high-mast poles. Other ratios were computed; however, these two are provided for brevity.

Figure 8-1 illustrates the relationship between Table 8-1 and the computed values. For example, assume that a structure is located on a travelway with ADT of between 1,000 and 10,000, and a failure could cross the roadway. The MRI is 700. The statistical properties for the 700-year wind in the region

**Table 8-1. MRI related to structure location and consequence of failure.**

Mean Recurrence Interval			
Traffic Volume	Importance		
	Typical	High	Low
ADT<100	300	1700	300
100<ADT≤1000	700	1700	300
1000<ADT≤ 10000	700	1700	300
ADT>10000	1700	1700	300
Typical: Failure could cross travelway			
High: Support failure could stop a life-line travelway			
Low: Support failure could not cross travelway			
Roadway sign supports: use 10 years			

of interest are then used to compute  $\beta$ . The computed value of  $\beta = 3.89$  is shown Figure 8-1.

Other indices were computed for load ratios in each region. The results are illustrated in Tables 8-2 to 8-5.

Note that for the same region and location, the load ratio of 0.5 has a higher  $\beta$  than that for the ratio of 1.0. This is because a wind-dominated structure will experience a higher load variability (all wind) than one that is 50% dead load. Compare the same application (cell) across regions, and the region with the lower wind variability will have a higher  $\beta$ .

The resulting indices are reasonable for the various applications, and the load and resistance factor were accordingly set. The load factors are summarized in Table 8-6.

The resistance factors  $\phi$  for the primary limit states are illustrated in Table 8-7. For brevity, not all are illustrated. The resistance factors are provided in the individual material resistance sections. The resistance factor for service and fatigue limit states is 1.0.

**Sensitivities**

The previous discussion outlines the results of assignment of load and resistance factors and the resulting reliability indices. It is useful to illustrate the sensitivities of these assignments to the resulting reliability indices. The minimum and average values for all regions are used to demonstrate by varying the dead load, wind load, and resistance factors for steel flexure strength and extreme limit states.

Note that an increase in resistance factor  $\phi$  decreases the reliability index  $\beta$ . An increase in load factor  $\gamma$  increases  $\beta$ .

The typical traffic signal structures have load ratios in the region of one-half, while high-mast poles have very little dead load effect and ratios that are nearer to unity. In Table 8-8, the area contained within the dotted lines indicates the region that is of typical interest.

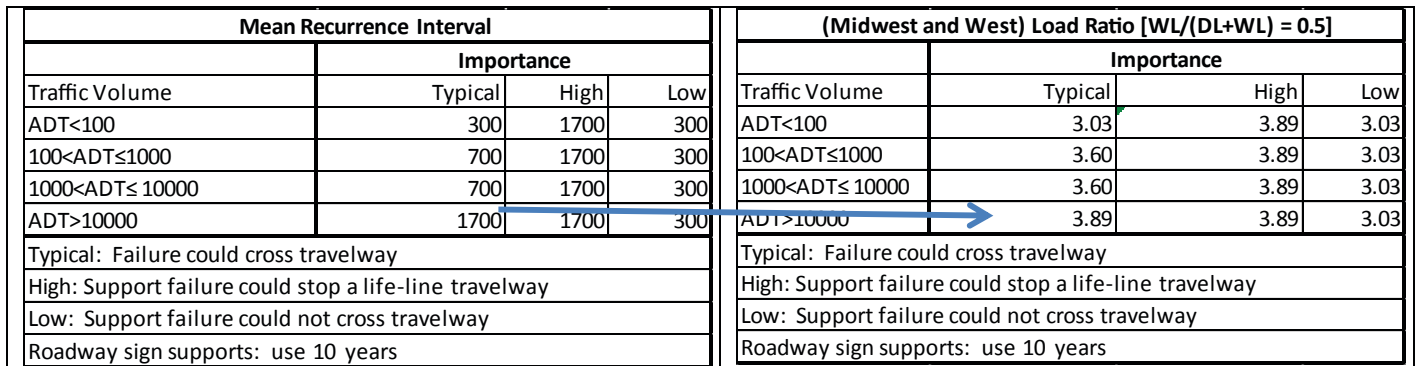


**Figure 8-1. Relationship between MRI and computed reliability indices.**

**Table 8-2. Reliability indices for the Midwest and Western United States.**

(Midwest and West) Load Ratio [WL/(DL+WL) = 0.5]			
Traffic Volume	Importance		
	Typical	High	Low
ADT<100	3.03	3.89	3.03
100<ADT≤1000	3.60	3.89	3.03
1000<ADT≤ 10000	3.60	3.89	3.03
ADT>10000	3.89	3.89	3.03
Typical: Failure could cross travelway			
High: Support failure could stop a life-line travelway			
Low: Support failure could not cross travelway			
Roadway sign supports: use 10 years			

(Midwest and West) Load Ratio [WL/(DL+WL) = 1.0]			
Traffic Volume	Importance		
	Typical	High	Low
ADT<100	2.77	3.62	2.77
100<ADT≤1000	3.35	3.62	2.77
1000<ADT≤ 10000	3.35	3.62	2.77
ADT>10000	3.62	3.62	2.77
Typical: Failure could cross travelway			
High: Support failure could stop a life-line travelway			
Low: Support failure could not cross travelway			
Roadway sign supports: use 10 years			

Table 8-3. Reliability indices for the West Coast.

(West Coast)Load Ratio [WL/(DL+WL) = 0.5]			
Traffic Volume	Importance		
	Typical	High	Low
ADT<100	3.38	4.31	3.38
100<ADT≤1000	4.00	4.31	3.38
1000<ADT≤ 10000	4.00	4.31	3.38
ADT>10000	4.31	4.31	3.38
Typical: Failure could cross travelway			
High: Support failure could stop a life-line travelway			
Low: Support failure could not cross travelway			
Roadway sign supports: use 10 years			

(West Coast)Load Ratio [WL/(DL+WL) = 1.0]			
Traffic Volume	Importance		
	Typical	High	Low
ADT<100	3.23	4.14	3.23
100<ADT≤1000	3.85	4.14	3.23
1000<ADT≤ 10000	3.85	4.14	3.23
ADT>10000	4.14	4.14	3.23
Typical: Failure could cross travelway			
High: Support failure could stop a life-line travelway			
Low: Support failure could not cross travelway			
Roadway sign supports: use 10 years			

Table 8-4. Reliability indices for the Florida coast.

(Coastal)Load Ratio [WL/(DL+WL) = 0.5]			
Traffic Volume	Importance		
	Typical	High	Low
ADT<100	2.46	3.42	2.46
100<ADT≤1000	2.78	3.42	2.46
1000<ADT≤ 10000	2.78	3.42	2.46
ADT>10000	3.42	3.42	2.46
Typical: Failure could cross travelway			
High: Support failure could stop a life-line travelway			
Low: Support failure could not cross travelway			
Roadway sign supports: use 10 years			

(Coastal)Load Ratio [WL/(DL+WL) = 1.0]			
Traffic Volume	Importance		
	Typical	High	Low
ADT<100	2.05	2.94	2.05
100<ADT≤1000	2.37	2.94	2.05
1000<ADT≤ 10000	2.37	2.94	2.05
ADT>10000	2.94	2.94	2.05
Typical: Failure could cross travelway			
High: Support failure could stop a life-line travelway			
Low: Support failure could not cross travelway			
Roadway sign supports: use 10 years			

Table 8-5. Reliability indices for Southern Alaska coast.

(Southern Ak)Load Ratio [WL/(DL+WL) = 0.5]			
Traffic Volume	Importance		
	Typical	High	Low
ADT<100	2.88	3.47	2.88
100<ADT≤1000	3.27	3.47	2.88
1000<ADT≤ 10000	3.27	3.47	2.88
ADT>10000	3.47	3.47	2.88
Typical: Failure could cross travelway			
High: Support failure could stop a life-line travelway			
Low: Support failure could not cross travelway			
Roadway sign supports: use 10 years			

(Southern Ak)Load Ratio [WL/(DL+WL) = 1.0]			
Traffic Volume	Importance		
	Typical	High	Low
ADT<100	2.56	3.15	2.56
100<ADT≤1000	2.96	3.15	2.56
1000<ADT≤ 10000	2.96	3.15	2.56
ADT>10000	3.15	3.15	2.56
Typical: Failure could cross travelway			
High: Support failure could stop a life-line travelway			
Low: Support failure could not cross travelway			
Roadway sign supports: use 10 years			

**Table 8-6. Load factors (same as Table 3.4.1 in the proposed LRFD-LTS specifications).**

Load Combination Limit State	Description	Reference Articles	Permanent		Transient			Fatigue			
			Dead Components (DC)	Live Load (LL)	Wind (W)	Truck Gust (TrG)	Natural Wind Gust Vibration (NWG)	Vortex-Induced Vibration (VVW)	Combined Wind on High-level Towers	Galloping Induced Vibration (GVW)	
			Max/Min	Mean							Apply separately
Strength I	Gravity	3.5, 3.6, and 3.7	1.25		1.6						
Extreme I	Wind	3.5, 3.8, 3.9	1.1/0.9			1.0 <sup>a</sup>					
Service I	Translation	10.4		1.0		1.0 <sup>b</sup>					
Service III	Crack control for Prestressed Concrete			1.0		1.00					
Fatigue I	Infinite-life	11.7		1.0			1.0	1.0	1.0	1.0	1.0
Fatigue II	Evaluation	17.5		1.0			1.0	1.0	1.0	1.0	1.0
a. Use Figures 3.8-1, 3.8-2, or 3.8-3 (for appropriate return period)											
b. Use wind map 3.8-4 (service)											

Note: Table numbers within table are for tables in the LRFD-LTS specifications.

**Table 8-7. Resistance factors for strength and extreme limit states.**

Material	Action	Resistance Factor
<b>Steel</b>	Flexure	0.90
	Torsion and Shear	0.95
	Axial Compression	0.90
	Axial Tension (yield)	0.90
	Axial Tension (rupture)	0.75
	<b>Aluminum</b>	
	Flexure (yield)	0.90
	Flexure (rupture)	0.75
	Torsion and Shear	0.90
	Axial Compression	0.9
	Axial Tension (yield)	0.90
	Axial Tension (rupture)	0.75
<b>Wood</b>		
	Flexure	0.85
	Torsion and Shear	0.75
	Axial compression	0.90
	Tension	0.80
<b>Concrete</b>		
	Flexure	1.00
	Torsion and Shear	0.90
	Axial compression	0.90
<b>FRP</b>		
	Flexure	0.67

Table 8-8. Sensitivity of the reliability index to load and resistance factors.

Parameters	Minimum $\beta$	Average $\beta$	Resistance Ratio
<b>Baseline</b> $\phi = 0.9$ $\gamma_{\text{dead-only}} = 1.25$ $\gamma_{\text{dead}} = 1.1$ $\gamma_{\text{wind}} = 1.0$	<b>Minimum Beta - 700 Year</b> 	<b>Average Beta - 700 Year</b> 	<b>Required Resistance Ratios (LRFD/ASD)</b> 
$\phi = 0.9$ $\gamma_{\text{dead-only}} = 1.35$ $\gamma_{\text{dead}} = 1.1$ $\gamma_{\text{wind}} = 1.0$	<b>Minimum Beta - 700 Year</b> 	<b>Average Beta - 700 Year</b> 	<b>Required Resistance Ratios (LRFD/ASD)</b> 
$\phi = 0.9$ $\gamma_{\text{dead-only}} = 1.25$ $\gamma_{\text{dead}} = 1.2$ $\gamma_{\text{wind}} = 1.0$	<b>Minimum Beta - 700 Year</b> 	<b>Average Beta - 700 Year</b> 	<b>Required Resistance Ratios (LRFD/ASD)</b> 

Table 8-8. (Continued).

<p><math>\phi = 0.95</math>  <math>\gamma_{\text{dead-only}} = 1.25</math>  <math>\gamma_{\text{dead}} = 1.1</math>  <math>\gamma_{\text{wind}} = 1.0</math></p>	<p><b>Minimum Beta - 700 Year</b></p>	<p><b>Average Beta - 700 Year</b></p>	<p><b>Required Resistance Ratios (LRFD/ASD)</b></p>
<p><math>\phi = 1.0</math>  <math>\gamma_{\text{dead-only}} = 1.25</math>  <math>\gamma_{\text{dead}} = 1.1</math>  <math>\gamma_{\text{wind}} = 1.0</math></p>	<p><b>Minimum Beta - 700 Year</b></p>	<p><b>Average Beta - 700 Year</b></p>	<p><b>Required Resistance Ratios (LRFD/ASD)</b></p>
<p><math>\phi = 0.85</math>  <math>\gamma_{\text{dead-only}} = 1.25</math>  <math>\gamma_{\text{dead}} = 1.1</math>  <math>\gamma_{\text{wind}} = 1.0</math></p>	<p><b>Minimum Beta - 700 Year</b></p>	<p><b>Average Beta - 700 Year</b></p>	<p><b>Required Resistance Ratios (LRFD/ASD)</b></p>

## SECTION 9

## Summary

Judgment must be employed in the calibration regarding the performance of existing structures under the current specifications and setting the target reliability index  $\beta$  for the LRFD-LTS specifications.

The LRFD-LTS specifications were calibrated using the standard ASD-based specifications as a baseline. The variabilities of the loads and resistances were considered in a rigorous manner. The wind loads have higher variabilities than the dead loads. Therefore, a structure with high wind-to-total-load ratio will require higher resistance and associated resistances compared to ASD. This was shown to be on the

order of a 10% increase for high-mast structures. For structures with approximately one-half wind load (e.g., cantilever structures), on average the required resistance will not change significantly. It is important to note that resistance is proportional to section thickness and proportional to the square of the diameter [i.e., a 10% resistance increase may be associated with a 10% increase in thickness (area) or a 5% increase in diameter or area].

The reliability index for the LRFD-LTS specifications is more uniform over the range of load ratios of practical interest than the current ASD-based specifications.

---

# Annex A

**Table A1. Statistical parameters of wind for Central United States.**

		<i>n</i>	Annual			300 Year		700 Year		1,700 Year	
			Mean	Cov	Max	Mean	Cov	Mean	Cov	Mean	Cov
1	Birmingham, Alabama	34	46.6	0.139	62.3	76.0	0.085	80.0	0.082	84.0	0.080
2	Prescott, Arizona	17	52.2	0.169	66.0	92.0	0.096	98.0	0.091	104.0	0.089
3	Tucson, Arizona	30	51.4	0.167	77.7	89.0	0.096	95.0	0.091	101.0	0.089
4	Yuma, Arizona	29	48.9	0.157	65.1	83.0	0.093	88.0	0.089	93.0	0.084
5	Fort Smith, Arkansas	26	46.6	0.150	60.7	78.0	0.091	83.0	0.085	87.0	0.082
6	Little Rock, Arkansas	35	46.7	0.206	72.2	90.0	0.111	96.0	0.106	103.0	0.102
7	Denver, Colorado	27	49.2	0.096	62.3	70.0	0.073	73.0	0.069	76.0	0.066
8	Grand Junction, Colorado	31	52.7	0.102	69.9	76.0	0.073	80.0	0.069	84.0	0.065
9	Pueblo, Colorado	37	62.8	0.118	79.2	95.0	0.079	100.0	0.075	105.0	0.071
10	Hartford, Connecticut	38	45.1	0.151	66.8	75.0	0.090	80.0	0.085	84.0	0.080
11	Washington, D.C.	33	48.3	0.135	66.3	78.0	0.085	82.0	0.082	86.0	0.078
12	Atlanta, Georgia	42	47.4	0.195	75.5	88.0	0.102	94.0	0.097	100.0	0.092
13	Macon, Georgia	28	45.0	0.169	59.7	79.0	0.100	84.0	0.095	89.0	0.088
14	Boise, Idaho	38	47.8	0.111	61.9	71.0	0.078	74.0	0.073	78.0	0.070
15	Pocatello, Idaho	39	53.3	0.128	71.6	84.0	0.079	88.0	0.075	92.0	0.071
16	Chicago, Illinois	35	47.0	0.102	58.6	68.0	0.075	72.0	0.070	75.0	0.066
17	Moline, Illinois	34	54.8	0.141	72.1	89.0	0.086	94.0	0.080	99.0	0.076
18	Peoria, Illinois	35	52.0	0.134	70.2	83.0	0.086	88.0	0.080	92.0	0.076
19	Springfield, Illinois	30	54.2	0.111	70.6	81.0	0.079	85.0	0.075	89.0	0.070
20	Evansville, Indiana	37	46.7	0.130	61.3	74.0	0.079	77.0	0.075	82.0	0.070
21	Fort Wayne, Indiana	36	53.0	0.125	69.0	82.0	0.082	87.0	0.077	91.0	0.074
22	Indianapolis, Indiana	34	55.4	0.200	93.0	103.0	0.105	110.0	0.098	119.0	0.092
23	Burlington, Iowa	23	56.0	0.164	71.9	97.0	0.094	103.0	0.090	110.0	0.085
24	Des Moines, Iowa	27	57.7	0.147	79.9	95.0	0.091	101.0	0.086	107.0	0.081
25	Sioux City, Iowa	36	57.9	0.157	88.1	98.0	0.096	104.0	0.091	111.0	0.085
26	Concordia, Kansas	16	57.6	0.160	73.7	98.0	0.095	104.0	0.092	111.0	0.085
27	Dodge City, Kansas	35	60.6	0.099	71.5	87.0	0.068	91.0	0.064	95.0	0.061
28	Topeka, Kansas	28	54.5	0.150	78.8	91.0	0.095	96.0	0.087	102.0	0.084
29	Wichita, Kansas	37	58.1	0.146	89.5	96.0	0.090	101.0	0.085	107.0	0.080
30	Louisville, Kentucky	32	49.3	0.136	65.7	79.0	0.088	84.0	0.082	88.0	0.078
31	Shreveport, Louisiana	11	44.6	0.121	53.4	69.0	0.078	72.0	0.076	76.0	0.073
32	Baltimore, Maryland	29	55.9	0.123	71.2	87.0	0.080	91.0	0.075	96.0	0.070
33	Detroit, Michigan	44	48.9	0.140	67.6	79.0	0.086	84.0	0.083	89.0	0.078
34	Grand Rapids, Michigan	27	48.3	0.209	66.8	93.0	0.108	99.0	0.102	107.0	0.093
35	Lansing, Michigan	29	53.0	0.125	67.0	83.0	0.082	87.0	0.079	92.0	0.076

(continued on next page)

Table A1. (Continued).

		<i>n</i>	Annual			300 Year		700 Year		1,700 Year	
			Mean	Cov	Max	Mean	Cov	Mean	Cov	Mean	Cov
36	Sault Ste. Marie, Michigan	37	48.4	0.159	67.0	83.0	0.090	87.0	0.086	92.0	0.082
37	Duluth, Minnesota	28	50.9	0.151	69.6	85.0	0.090	90.0	0.087	96.0	0.081
38	Minneapolis, Minnesota	40	49.2	0.185	81.6	90.0	0.099	96.0	0.094	102.0	0.088
39	Columbia, Missouri	28	50.2	0.129	62.4	79.0	0.084	84.0	0.079	88.0	0.075
40	Kansas City, Missouri	44	50.5	0.155	75.2	85.0	0.094	91.0	0.089	96.0	0.085
41	St. Louis, Missouri	19	47.4	0.156	65.7	80.0	0.094	85.0	0.088	90.0	0.084
42	Springfield, Missouri	37	50.1	0.148	71.2	83.0	0.090	88.0	0.085	93.0	0.080
43	Billings, Montana	39	59.4	0.135	84.2	95.0	0.085	100.0	0.083	106.0	0.079
44	Great Falls, Montana	34	59.0	0.110	74.2	88.0	0.075	92.0	0.073	97.0	0.069
45	Havre, Montana	17	58.0	0.159	77.7	99.0	0.095	105.0	0.093	115.0	0.087
46	Helena, Montana	38	55.2	0.118	71.2	84.0	0.078	89.0	0.075	93.0	0.070
47	Missoula, Montana	33	48.3	0.122	70.9	74.0	0.078	79.0	0.075	83.0	0.070
48	North Platte, Nebraska	29	62.0	0.108	74.4	92.0	0.076	96.0	0.073	101.0	0.069
49	Omaha, Nebraska	42	55.0	0.195	104.0	102.0	0.105	109.0	0.100	117.0	0.095
50	Valentine, Nebraska	22	60.6	0.142	74.1	99.0	0.088	105.0	0.083	111.0	0.078
51	Ely, Nevada	39	52.9	0.117	70.1	80.0	0.078	85.0	0.074	89.0	0.070
52	Las Vegas, Nevada	13	54.7	0.128	70.1	85.0	0.083	90.0	0.079	95.0	0.074
53	Reno, Nevada	36	56.5	0.141	76.6	92.0	0.088	97.0	0.082	103.0	0.077
54	Winnemucca, Nevada	28	50.2	0.142	62.6	82.0	0.088	87.0	0.083	92.0	0.078
55	Concord, New Hampshire	37	42.9	0.195	68.5	80.0	0.105	85.0	0.100	92.0	0.094
56	Albuquerque, New Mexico	45	57.2	0.136	84.8	92.0	0.090	97.0	0.085	102.0	0.080
57	Roswell, New Mexico	31	58.2	0.153	81.6	98.0	0.096	104.0	0.088	110.0	0.085
58	Albany, New Mexico	40	47.9	0.140	68.5	77.0	0.085	82.0	0.078	87.0	0.075
59	Binghamton, New York	27	49.2	0.130	63.8	77.0	0.085	82.0	0.078	86.0	0.075
60	Buffalo, New York	34	53.9	0.132	78.6	85.0	0.086	92.0	0.079	96.0	0.076
61	Rochester, New York	37	53.5	0.097	65.4	77.0	0.069	80.0	0.067	84.0	0.063
62	Syracuse, New York	37	50.3	0.121	67.2	77.0	0.082	82.0	0.075	86.0	0.071
63	Charlotte, N. Carolina	27	44.7	0.168	64.6	78.0	0.092	83.0	0.087	88.0	0.082
64	Greensboro, N. Carolina	48	42.3	0.180	66.8	76.0	0.098	81.0	0.092	87.0	0.086
65	Bismarck, North Dakota	38	58.3	0.096	68.9	83.0	0.068	87.0	0.064	91.0	0.062
66	Fargo, North Dakota	36	59.4	0.185	100.5	108.0	0.100	115.0	0.095	123.0	0.090
67	Williston, North Dakota	16	56.5	0.117	69.3	86.0	0.078	90.0	0.074	95.0	0.070
68	Cleveland, Ohio	35	52.7	0.125	68.5	82.0	0.082	86.0	0.078	91.0	0.074
69	Columbus, Ohio	26	49.4	0.133	61.3	78.0	0.085	83.0	0.080	88.0	0.078
70	Dayton, Ohio	35	53.6	0.142	72.0	87.0	0.087	93.0	0.082	98.0	0.078
71	Toledo, Ohio	35	50.8	0.177	82.2	91.0	0.098	97.0	0.092	103.0	0.088
72	Oklahoma City, Oklahoma	26	54.0	0.110	69.3	81.0	0.073	84.0	0.070	88.0	0.067
73	Tulsa, Oklahoma	35	47.9	0.145	68.3	79.0	0.088	84.0	0.082	88.0	0.077
74	Harrisburg, Pennsylvania	39	45.7	0.164	64.4	79.0	0.096	84.0	0.090	89.0	0.085
75	Philadelphia, Pennsylvania	23	49.5	0.115	62.4	75.0	0.078	79.0	0.073	83.0	0.068
76	Pittsburgh, Pennsylvania	18	48.4	0.120	59.6	74.0	0.078	78.0	0.073	82.0	0.068
77	Scranton, Pennsylvania	23	44.6	0.107	54.2	66.0	0.074	69.0	0.070	72.0	0.065
78	Greenville, South Carolina	36	48.5	0.226	71.9	97.0	0.112	105.0	0.108	112.0	0.104
79	Huron, South Dakota	39	61.4	0.132	78.8	98.0	0.085	102.0	0.081	108.0	0.078
80	Rapid City, South Dakota	36	61.0	0.087	70.5	85.0	0.063	88.0	0.061	92.0	0.058
81	Chattanooga, Tennessee	35	47.8	0.218	75.9	94.0	0.114	101.0	0.109	109.0	0.104
82	Knoxville, Tennessee	33	48.8	0.141	65.9	79.0	0.090	84.0	0.085	89.0	0.080
83	Memphis, Tennessee	21	45.4	0.137	60.7	73.0	0.088	77.0	0.082	81.0	0.079
84	Nashville, Tennessee	34	46.8	0.171	70.2	82.0	0.096	87.0	0.091	93.0	0.086
85	Abilene, Texas	34	54.7	0.192	99.9	102.0	0.102	107.0	0.098	116.0	0.092

**Table A1. (Continued).**

		<i>n</i>	Annual			300 Year		700 Year		1,700 Year	
			Mean	Cov	Max	Mean	Cov	Mean	Cov	Mean	Cov
86	Amarillo, Texas	34	61.0	0.117	80.7	93.0	0.079	98.0	0.075	103.0	0.071
87	Dallas, Texas	32	49.1	0.132	66.8	78.0	0.088	82.0	0.084	86.0	0.078
88	El Paso, Texas	32	55.4	0.087	66.7	77.0	0.065	80.0	0.060	83.0	0.056
89	San Antonio, Texas	36	47.0	0.183	79.5	86.0	0.099	91.0	0.094	97.0	0.087
90	Salt Lake City, Utah	36	50.6	0.142	69.0	83.0	0.090	87.0	0.087	92.0	0.082
91	Burlington, Vermont	34	45.7	0.160	66.5	78.0	0.093	83.0	0.090	88.0	0.087
92	Lynchburg, Virginia	34	40.9	0.149	53.4	68.0	0.086	72.0	0.082	76.0	0.078
93	Richmond, Virginia	27	42.2	0.152	61.3	70.0	0.092	75.0	0.085	80.0	0.080
94	Green Bay, Wisconsin	29	56.6	0.212	103.0	110.0	0.112	118.0	0.108	127.0	0.100
95	Madison, Wisconsin	31	55.7	0.190	80.2	102.0	0.105	110.0	0.098	117.0	0.091
96	Milwaukee, Wisconsin	37	53.7	0.121	67.9	82.0	0.082	87.0	0.075	91.0	0.070
97	Cheyenne, Wyoming	42	60.5	0.093	72.6	86.0	0.070	89.0	0.065	93.0	0.060
98	Lander, Wyoming	32	61.2	0.160	80.4	104.0	0.092	111.0	0.086	118.0	0.080
99	Sheridan, Wyoming	37	61.5	0.116	82.0	94.0	0.076	98.0	0.073	103.0	0.071
100	Elkins, West Virginia	10	51.1	0.160	68.5	88.0	0.092	93.0	0.088	98.0	0.084

**Table A2. Statistical parameters of wind for Costal Segment 1.**

		<i>n</i>	Annual			300 Year		700 Year		1,700 Year	
			Mean	Cov	Max	Mean	Cov	Mean	Cov	Mean	Cov
1	Montgomery, Alabama	28	45.3	0.185	76.7	82.0	0.104	88.0	0.095	94.0	0.090
2	Jackson, Mississippi	29	45.9	0.155	64.4	78.0	0.092	82.0	0.087	87.0	0.082
3	Austin, Texas	35	45.1	0.122	58.0	70.0	0.074	73.0	0.071	77.0	0.067
4	Portland, Maine	37	48.5	0.179	72.8	87.0	0.100	92.0	0.096	99.0	0.089

**Table A3. Statistical parameters of wind for Costal Segment 2.**

		<i>n</i>	Annual			300 Year		700 Year		1,700 Year	
			Mean	Cov	Max	Mean	Cov	Mean	Cov	Mean	Cov
1	Boston, Massachusetts	42	56.3	0.172	81.4	100.0	0.098	106.0	0.093	113.0	0.088
2	New York, New York	31	50.3	0.143	61.4	82.0	0.086	87.0	0.079	92.0	0.076
3	Norfolk, Virginia	20	48.9	0.182	68.9	88.0	0.102	94.0	0.097	100.0	0.093

**Table A4. Statistical parameters of wind for Costal Segment 3.**

		<i>n</i>	Annual			300 Year		700 Year		1,700 Year	
			Mean	Cov	Max	Mean	Cov	Mean	Cov	Mean	Cov
1	Jacksonville, Florida	28	48.6	0.206	74.4	93.0	0.112	100.0	0.106	107.0	0.099
2	Tampa, Florida	10	49.6	0.163	65.1	85.0	0.095	90.0	0.090	96.0	0.084
3	Savannah, Georgia	32	47.6	0.202	79.3	90.0	0.108	96.0	0.099	104.0	0.094
4	Block Island, Rhode Island	31	61.4	0.142	86.2	100.0	0.085	106.0	0.081	112.0	0.076

**Table A5. Statistical parameters of wind for Costal Segment 4.**

		<i>n</i>	Annual			300 Year		700 Year		1,700 Year	
			Mean	Cov	Max	Mean	Cov	Mean	Cov	Mean	Cov
1	Nantucket, Massachusetts	23	56.7	0.141	71.3	92.0	0.086	98.0	0.083	103.0	0.078

**Table A6. Statistical parameters of wind for Costal Segment 5.**

		<i>n</i>	Annual			300 Year		700 Year		1,700 Year	
			Mean	Cov	Max	Mean	Cov	Mean	Cov	Mean	Cov
1	Brownsville, Texas	35	43.7	0.185	66.1	80.0	0.098	85.0	0.092	91.0	0.088
2	Corpus Christi, Texas	34	54.5	0.288	127.8	124.0	0.125	134.0	0.118	146.0	0.112
3	Port Arthur, Texas	25	53.1	0.181	81.0	96.0	0.097	102.0	0.092	108.0	0.087
4	Cape Hatteras, N. Carolina	45	58.0	0.214	103.0	113.0	0.110	121.0	0.105	130.0	0.100
5	Wilmington, N. Carolina	26	49.9	0.218	84.3	98.0	0.112	105.0	0.102	113.0	0.096

**Table A7. Statistical parameters of wind for Costal Segment 8.**

		<i>n</i>	Annual			300 Year		700 Year		1,700 Year	
			Mean	Cov	Max	Mean	Cov	Mean	Cov	Mean	Cov
1	Key West, Florida	19	51.0	0.337	89.5	127.0	0.138	140.0	0.125	152.0	0.115

**Table A8. Statistical parameters of wind for the West Coast.**

		<i>n</i>	Annual			300 Year		700 Year		1,700 Year	
			Mean	Cov	Max	Mean	Cov	Mean	Cov	Mean	Cov
1	Fresno, California	37	34.4	0.140	46.5	55.0	0.090	58.0	0.086	62.0	0.080
2	Red Bluff, California	33	52.1	0.141	67.3	85.0	0.089	90.0	0.086	95.0	0.082
3	Sacramento, California	29	46.0	0.223	67.8	92.0	0.112	98.0	0.108	105.0	0.098
4	San Diego, California	38	34.5	0.130	46.6	54.0	0.085	57.0	0.082	60.0	0.080
5	Portland, Oregon	28	52.6	0.196	87.9	99.0	0.104	105.0	0.100	112.0	0.092
6	Roseburg, Oregon	12	35.6	0.169	51.1	62.0	0.095	66.0	0.090	70.0	0.085
7	North Head, Washington	41	71.5	0.141	104.4	116.0	0.088	123.0	0.083	130.0	0.078
8	Quillayute, Washington	11	36.5	0.085	41.9	50.0	0.060	52.0	0.058	54.0	0.056
9	Seattle, Washington	10	41.9	0.080	49.3	57.0	0.060	59.0	0.058	61.0	0.056
10	Spokane, Washington	37	47.8	0.133	64.6	76.0	0.084	80.0	0.077	84.0	0.074
11	Tatoosh Island, Washington	54	66.0	0.106	85.6	97.0	0.073	102.0	0.072	107.0	0.069

# Annex B

**Table B1. Test results (from Stam et al., 2011).**

Connection Detail	$S_r$ [ksi]	No. of Cycles to Failure	$A$ [ksi <sup>3</sup> ]	Category as in ASSHTO-CAFL	No. of Cycles Using Miner's Rule for CAFL
Socket	11.9	249,446	4.2E+08	Ep	2.39E+07
Socket	12	453,948	7.84E+08	Ep	4.46E+07
Socket	6.3	2,072,592	5.18E+08	Ep	2.95E+07
Socket	6.1	2,199,343	4.99E+08	Ep	2.84E+07
Socket	6.1	2,816,706	6.39E+08	Ep	3.64E+07
Socket	11.9	389,428	6.56E+08	Ep	3.73E+07
Socket	11.9	265,540	4.47E+08	Ep	2.55E+07
Socket	11.9	5,144,528	8.67E+09	C	8.67E+06
Socket	11.9	1,683,127	2.84E+09	D	8.27E+06
External Collar	11.9	4,245,460	7.15E+09	C	7.15E+06
External Collar	11.9	2,363,152	3.98E+09	D	1.16E+07
Full Penetration	17.7	422,400	2.34E+09	D	6.83E+06
External Collar	12	2,345,896	4.05E+09	D	1.18E+07
External Collar	12	2,889,260	4.99E+09	C	4.99E+06
External Collar	12	5,755,111	9.94E+09	C	9.94E+06
External Collar	12	3,304,490	5.71E+09	C	5.71E+06
External Collar	12	2,382,309	4.12E+09	D	1.20E+07
Socket	12	235,854	4.08E+08	Ep	2.32E+07
Socket	12	260,700	4.5E+08	Ep	2.56E+07
Socket	12	622,928	1.08E+09	Ep	6.12E+07
External Collar	12	3,939,099	6.81E+09	C	6.81E+06
External Collar	12	6,927,606	1.2E+10	C	1.20E+07
External Collar	12	5,384,143	9.3E+09	C	9.30E+06
External Collar	12	2,863,521	4.95E+09	C	4.95E+06
Full Penetration	12	4,997,925	8.64E+09	C	8.64E+06
Full Penetration	12	7,527,441	1.3E+10	B	3.18E+06
Socket	12	253,657	4.38E+08	Ep	2.49E+07
Socket	12	310,352	5.36E+08	Ep	3.05E+07
Socket	12	792,576	1.37E+09	E	1.50E+07
Socket	12	376,291	6.5E+08	Ep	3.70E+07
Full Penetration	12	6,734,487	1.16E+10	C	1.16E+07
Full Penetration	12	5,219,304	9.02E+09	C	9.02E+06

(continued on next page)

**Table B1. (Continued).**

Connection Detail	$S_r$ [ksi]	No. of Cycles to Failure	$A$ [ksi <sup>3</sup> ]	Category as in ASSHTO-CAFL	No. of Cycles Using Miner's Rule for CAFL
Full Penetration	24	856,122	1.18E+10	C	1.18E+07
Full Penetration	24	747,510	1.03E+10	C	1.03E+07
External Collar	18	512,860	2.99E+09	D	8.72E+06
External Collar	18	653,208	3.81E+09	D	1.11E+07
Full Penetration	18	1,053,554	6.14E+09	C	6.14E+06
Full Penetration	18	880,807	5.14E+09	C	5.14E+06
External Collar	18	468,601	2.73E+09	D	7.97E+06
External Collar	18	337,390	1.97E+09	E	2.16E+07
Full Penetration	24	439,511	6.08E+09	C	6.08E+06
Full Penetration	24	343,175	4.74E+09	C	4.74E+06
Full Penetration	19.07	2,232,742	1.55E+10	B	3.78E+06
Full Penetration	24	490,061	6.77E+09	C	6.77E+06
Full Penetration	21.14	3,516,775	3.32E+10	A	2.40E+06
Full Penetration	24	222,649	3.08E+09	D	8.97E+06
Full Penetration	24	212,891	2.94E+09	D	8.58E+06
Full Penetration	24	1,873,499	2.59E+10	A	1.87E+06
Full Penetration	24	677,763	9.37E+09	C	9.37E+06
Full Penetration	24	633,458	8.76E+09	C	8.76E+06
Full Penetration	28	286,526	6.29E+09	C	6.29E+06
Full Penetration	28	123,072	2.7E+09	D	7.88E+06
Full Penetration	28	129,090	2.83E+09	D	8.26E+06
Full Penetration	12	3,051,996	5.27E+09	C	5.27E+06
External Collar	12	10,652,284	1.84E+10	B	4.49E+06
External Collar	12	10,652,284	1.84E+10	B	4.49E+06
Full Penetration	24	1,272,665	1.76E+10	B	4.30E+06
Full Penetration	24	1,210,499	1.67E+10	B	4.09E+06
External Collar	24	137,220	1.9E+09	E	2.08E+07
External Collar	24	244,763	3.38E+09	D	9.86E+06
Full Penetration	24	292,468	4.04E+09	D	1.18E+07
Full Penetration	24	328,833	4.55E+09	C	4.55E+06
External Collar	24	169,059	2.34E+09	D	6.81E+06
External Collar	24	119,289	1.65E+09	E	1.81E+07

**Table B2. Test results (from Roy et al., 2011).**

Connection Detail	$S_r$ [ksi]	No. of Cycles to Failure	$A$ [ksi <sup>3</sup> ]	Category as in ASSHTO-CAFL	No. of Cycles Using Miner's Rule for Given CAFL
Arm Base	12	1.80E+05	3.11E+08	E	3.41E+06
Hand hole	7	1.78E+06	6.11E+08	B	1.49E+05
Arm Base	12	3.70E+05	6.39E+08	E	7.02E+06
Hand hole	7	1.55E+06	5.32E+08	B	1.30E+05
Hand hole	7	2.10E+06	7.2E+08	B	1.76E+05
Arm Base	12	1.26E+06	2.18E+09	E	2.39E+07
Hand hole	7	2.47E+06	8.47E+08	B	2.07E+05
Arm Base	7	2.30E+06	7.89E+08	E	8.66E+06
Arm Base	7	3.11E+06	1.07E+09	E	1.17E+07

Table B2. (Continued).

Connection Detail	$S_r$ [ksi]	No. of Cycles to Failure	A [ksi <sup>3</sup> ]	Category as in AASHTO-CAFL	No. of Cycles Using Miner's Rule for Given CAFL
Arm Base	11.9	1.61E+06	2.71E+09	D	7.91E+06
Hand hole	7	1.72E+06	5.9E+08	B	1.44E+05
Pole Base	6.9	1.98E+06	6.5E+08	D	1.90E+06
Arm Base	9.9	1.32E+06	1.28E+09	D	3.73E+06
Arm Base	11.9	1.88E+06	3.17E+09	D	9.24E+06
Hand hole	7	2.03E+06	6.96E+08	B	1.70E+05
Arm Base	9.9	1.41E+06	1.37E+09	D	3.99E+06
Hand hole	7	2.21E+06	7.58E+08	B	1.85E+05
Arm Base	9.9	1.17E+06	1.14E+09	D	3.31E+06
Arm Base	11.9	1.81E+06	3.05E+09	D	8.89E+06
Arm Base	9.9	1.29E+06	1.25E+09	D	3.65E+06
Arm Base	9.9	1.49E+06	1.45E+09	D	4.22E+06
Arm Base	11.9	1.55E+06	2.61E+09	D	7.62E+06
Arm Base	12	9.80E+05	1.69E+09	E	1.86E+07
Arm Base	12	1.86E+06	3.21E+09	E	3.53E+07
Arm Base	12	1.25E+06	2.16E+09	E	2.37E+07
Arm Base	10	6.96E+06	6.96E+09	E	7.64E+07
Arm Base	10	9.23E+06	9.23E+09	E	1.01E+08
Arm Base	16	5.84E+06	2.39E+10	E	2.63E+08
Arm Base	16	2.70E+05	1.11E+09	E	1.21E+07
Arm Base	16	4.79E+06	1.96E+10	E	2.15E+08
Arm Base	12	2.80E+05	4.84E+08	ET	2.80E+08
Arm Base	12	2.90E+05	5.01E+08	ET	2.90E+08
Arm Base	7	4.99E+06	1.71E+09	ET	9.90E+08
Pole Base	12	2.70E+05	4.67E+08	E	5.12E+06
Pole Base	12	1.10E+06	1.9E+09	E	2.09E+07
Pole Base	12	1.46E+06	2.52E+09	E	2.77E+07
Arm Sleeve to Pole Connection	7.7	4.51E+06	2.06E+09	E	2.26E+07
Arm Sleeve to Pole Connection	7.7	4.77E+06	2.18E+09	E	2.39E+07
Arm Sleeve to Pole Connection	7.7	5.82E+06	2.66E+09	E	2.92E+07
Arm Sleeve to Pole Connection	7.7	3.61E+06	1.65E+09	E	1.81E+07
Arm Sleeve to Pole Connection	7.7	3.61E+06	1.65E+09	E	1.81E+07
Arm Sleeve to Pole Connection	7.7	4.90E+06	2.24E+09	E	2.45E+07
Arm Sleeve to Pole Connection	7.7	1.11E+07	5.07E+09	E	5.56E+07
Arm Sleeve to Pole Connection	7.7	1.49E+07	6.8E+09	E	7.46E+07
Arm Sleeve to Pole Connection	7.7	1.54E+06	7.03E+08	E	7.72E+06
Arm Sleeve to Pole Connection	7.7	1.54E+06	7.03E+08	E	7.72E+06
Arm Sleeve to Pole Connection	7.7	1.54E+06	7.03E+08	E	7.72E+06
Arm Sleeve to Pole Connection	7.7	1.54E+06	7.03E+08	E	7.72E+06
Arm Sleeve to Pole Connection	16	6.80E+05	2.79E+09	E	3.06E+07
Arm Sleeve to Pole Connection	16	9.40E+05	3.85E+09	E	4.23E+07
Arm Sleeve to Pole Connection	16	6.80E+05	2.79E+09	E	3.06E+07
Arm Sleeve to Pole Connection	12	4.30E+05	7.43E+08	E	8.15E+06

(continued on next page)

Table B2. (Continued).

Connection Detail	$S_r$ [ksi]	No. of Cycles to Failure	A [ksi <sup>3</sup> ]	Category as in ASSHTO-CAFL	No. of Cycles Using Miner's Rule for Given CAFL
Arm Sleeve to Pole Connection	12	6.30E+05	1.09E+09	E	1.19E+07
Arm Sleeve to Pole Connection	12	5.50E+05	9.5E+08	E	1.04E+07
Arm Sleeve to Pole Connection	12	7.50E+05	1.3E+09	E	1.42E+07
Arm Sleeve to Pole Connection	16	1.40E+05	5.73E+08	E	6.29E+06
Arm Sleeve to Pole Connection	16	3.40E+05	1.39E+09	E	1.53E+07
Pole Base	13.1	1.00E+06	2.25E+09	E	2.47E+07
Arm Base	12	4.00E+04	69120000	Ep	3.93E+06
Pole Base	6.6	9.00E+04	25874640	Ep	1.47E+06
Arm Base	12	4.00E+04	69120000	Ep	3.93E+06
Pole Base	6.6	9.00E+04	25874640	Ep	1.47E+06
Arm Base	12	1.00E+04	17280000	Ep	9.83E+05
Pole Base	6.6	1.00E+05	28749600	Ep	1.64E+06
Arm Base	4.5	1.03E+06	93858750	Ep	5.34E+06
Hand hole	26	3.27E+06	5.75E+10	B	1.40E+07
Arm Base	4.5	3.90E+05	35538750	Ep	2.02E+06
Hand hole	2.6	1.25E+07	2.2E+08	B	5.36E+04
Arm Base	2.5	7.00E+04	1093750	Ep	6.22E+04
Stiffener	12	5.90E+05	1.02E+09	Ep	5.80E+07
Stiffener	12	5.90E+05	1.02E+09	Ep	5.80E+07
Stiffener	12	2.70E+05	4.67E+08	Ep	2.65E+07
Stiffener	12	2.70E+05	4.67E+08	Ep	2.65E+07
Stiffener	12	5.10E+05	8.81E+08	Ep	5.01E+07
Stiffener	12	1.07E+06	1.85E+09	Ep	1.05E+08
Stiffener	10	4.50E+05	4.5E+08	Ep	2.56E+07
Stiffener	10	5.20E+05	5.2E+08	Ep	2.96E+07
Stiffener	7	3.08E+06	1.06E+09	Ep	6.01E+07
Stiffener	7	2.57E+06	8.82E+08	Ep	5.02E+07
Stiffener	4.5	2.64E+06	2.41E+08	Ep	1.37E+07
Stiffener	4.5	4.00E+06	3.65E+08	Ep	2.07E+07
Stiffener	16	1.20E+05	4.92E+08	Ep	2.80E+07
Stiffener	16	7.00E+04	2.87E+08	Ep	1.63E+07
Stiffener	16	1.30E+05	5.32E+08	Ep	3.03E+07
Stiffener	16	2.80E+05	1.15E+09	Ep	6.53E+07
Stiffener	16	1.20E+05	4.92E+08	Ep	2.80E+07
Stiffener	16	1.20E+05	4.92E+08	Ep	2.80E+07
Pole Base	8	1.75E+06	8.96E+08	E	9.83E+06
Pole Base	8	6.80E+05	3.48E+08	E	3.82E+06
Pole Base	12	7.50E+05	1.3E+09	D	3.78E+06
Pole Base	11.6	1.13E+06	1.76E+09	D	5.14E+06
Pole Base	12	1.56E+06	2.7E+09	D	7.86E+06
Pole Base	11.6	3.13E+06	4.89E+09	D	1.42E+07
Pole Base	12	3.30E+05	5.7E+08	D	1.66E+06
Pole Base	12	3.30E+05	5.7E+08	D	1.66E+06
Pole Base	11.6	5.90E+05	9.21E+08	D	2.68E+06
Pole Base	14	1.00E+05	2.74E+08	D	8.00E+05
Pole Base	14	1.00E+05	2.74E+08	D	8.00E+05
Pole Base	13.5	3.90E+05	9.6E+08	D	2.80E+06
Pole Base	13.5	4.70E+05	1.16E+09	D	3.37E+06
Pole Base	13.5	4.70E+05	1.16E+09	D	3.37E+06

Table B2. (Continued).

Connection Detail	$S_r$ [ksi]	No. of Cycles to Failure	A [ksi <sup>3</sup> ]	Category as in ASSHTO-CAFL	No. of Cycles Using Miner's Rule for Given CAFL
Pole Base	16	1.40E+05	5.73E+08	D	1.67E+06
Pole Base	16	1.40E+05	5.73E+08	D	1.67E+06
Pole Base	15.4	6.00E+05	2.19E+09	D	6.39E+06
Pole Base	16	6.00E+04	2.46E+08	D	7.17E+05
Pole Base	16	1.50E+05	6.14E+08	D	1.79E+06
Pole Base	15.4	3.40E+05	1.24E+09	D	3.62E+06
Stiffener	12	2.30E+05	3.97E+08	D	1.16E+06
Stiffener	12	5.30E+05	9.16E+08	D	2.67E+06
Pole Base	8.5	3.80E+05	2.33E+08	D	6.80E+05
Stiffener	12	4.00E+05	6.91E+08	D	2.02E+06
Stiffener	12	4.00E+05	6.91E+08	D	2.02E+06
Stiffener	12	5.80E+05	1E+09	D	2.92E+06
Stiffener	7	4.06E+06	1.39E+09	D	4.06E+06
Stiffener	16	1.50E+05	6.14E+08	D	1.79E+06
Stiffener	16	5.00E+04	2.05E+08	D	5.97E+05
Pole Base	11.3	5.00E+04	72144850	D	2.10E+05
Pole Base	11.3	3.00E+05	4.33E+08	D	1.26E+06
Pole Base	11.3	9.00E+04	1.3E+08	D	3.79E+05
Pole Base	11.3	3.00E+05	4.33E+08	D	1.26E+06
Stiffener	16	2.00E+05	8.19E+08	D	2.39E+06
Stiffener	16	3.80E+05	1.56E+09	D	4.54E+06
Stiffener	16	5.00E+04	2.05E+08	D	5.97E+05
Stiffener	16	1.10E+05	4.51E+08	D	1.31E+06
Pole Base	11.3	2.70E+05	3.9E+08	D	1.14E+06

*Abbreviations and acronyms used without definitions in TRB publications:*

A4A	Airlines for America
AAAAE	American Association of Airport Executives
AASHO	American Association of State Highway Officials
AASHTO	American Association of State Highway and Transportation Officials
ACI-NA	Airports Council International-North America
ACRP	Airport Cooperative Research Program
ADA	Americans with Disabilities Act
APTA	American Public Transportation Association
ASCE	American Society of Civil Engineers
ASME	American Society of Mechanical Engineers
ASTM	American Society for Testing and Materials
ATA	American Trucking Associations
CTAA	Community Transportation Association of America
CTBSSP	Commercial Truck and Bus Safety Synthesis Program
DHS	Department of Homeland Security
DOE	Department of Energy
EPA	Environmental Protection Agency
FAA	Federal Aviation Administration
FHWA	Federal Highway Administration
FMCSA	Federal Motor Carrier Safety Administration
FRA	Federal Railroad Administration
FTA	Federal Transit Administration
HMCRRP	Hazardous Materials Cooperative Research Program
IEEE	Institute of Electrical and Electronics Engineers
ISTEA	Intermodal Surface Transportation Efficiency Act of 1991
ITE	Institute of Transportation Engineers
MAP-21	Moving Ahead for Progress in the 21st Century Act (2012)
NASA	National Aeronautics and Space Administration
NASAO	National Association of State Aviation Officials
NCFRP	National Cooperative Freight Research Program
NCHRP	National Cooperative Highway Research Program
NHTSA	National Highway Traffic Safety Administration
NTSB	National Transportation Safety Board
PHMSA	Pipeline and Hazardous Materials Safety Administration
RITA	Research and Innovative Technology Administration
SAE	Society of Automotive Engineers
SAFETEA-LU	Safe, Accountable, Flexible, Efficient Transportation Equity Act: A Legacy for Users (2005)
TCRP	Transit Cooperative Research Program
TEA-21	Transportation Equity Act for the 21st Century (1998)
TRB	Transportation Research Board
TSA	Transportation Security Administration
U.S.DOT	United States Department of Transportation